DEPARTMENT OF OCEANOGRAPHY

UNIVERSITY OF CAPE TOWN

The influence of ocean ridges on the circulation to the south of the Mozambique Channel and Madagascar

ISSUFO FERRÃO MÁRIO HALO

November, 2008

Thesis by dissertation

The influence of ocean ridges on the circulation to the south of the Mozambique Channel and Madagascar

ISSUFO FERRÃO MÁRIO HALO

Supervisors: Dr. Isabelle J. Ansorge

Prof. Johann R. E. Lutjeharms

Dr. Pierrick Penven

November, 2008

Submitted in fulfilment of the requirement for the degree of Master of Science.

ABSTRACT

The Mozambique Channel and the region south of Madagascar are dominated by high variability of the oceanic flow due to the ubiquitous presence of mesoscale eddies. The bottom topography of this region has several shallow ridges.

The water flowing through the Mozambique Channel propagates southwards predominantly as a train of anti-cyclonic eddies, moving towards the Agulhas Current. South of Madagascar, dipolar vortices regularly propagate in a south-westward direction. Their deep extent favours interaction with the shallow bathymetry of the Davie, Mozambique and Madagascar Ridges.

The role of the Madagascar Ridge on the mesoscale circulation is investigated using altimetric observations and model simulations. Two different simulations have been performed: One with no modification of the Madagascar Ridge, the other with the upper 4000 meters of the ridge removed. These simulations suggest that the absence of the Madagascar Ridge results in less retroflection of the East Madagascar Current, and an increase in the mean SSH and its variability in the Agulhas Current region. Such increased variability is associated with eddy intensification and increased strength of the Agulhas Current.

Another objective of this study was to investigate the trajectories taken by eddies across the Mozambique Ridge, in order to determine whether they have a preferred pathway through deep fractures across the ridge. Of a total of twenty anti-cyclonic eddies from the Mozambique Channel not a single one passed through a gateway in the ridge. By contrast, of twenty anti-cyclonic eddies originating from the south of Madagascar, 55 percent passed through a gap in the ridge between 28.5°S - 36.4°E. The pathways taken by cyclonic eddies through the ridge were not statistically significant. Changes on the surface expression of eddy kinetic energy relative to the depth of the sea floor topography during the propagation of these eddies were investigated. No consistent trend is found in the Mozambique Channel, whereas to the south of Madagascar both the cyclonic and the anti-cyclonic eddies show a decreasing profile in the eddy kinetic energy during their propagation.

The interaction between eddies and the Agulhas Current was also investigated. The simulation shows that strong eddies from both the Mozambique Channel and south of Madagascar, interact with the Agulhas Current at about 33°S, enhancing the Agulhas Current's speed over the full depth of the current. Any instability so generated may give rise to the formation of Natal Pulses on the Agulhas Current, as previous studies have already suggested.

KEY WORDS: Eddies, Agulhas Current, Eddy Kinetic Energy, Sea floor topography, Ocean Ridges.

ACKNOWLEDGMENTS

With a warm and cordial feeling of gratitude, I thank all the individuals and institutions that have supported me to carry out this study. Among the people, I specially acknowledge my supervisor Dr Isabelle Ansorge, and the co-supervisors: Professor Johann R. E. Lutjeharms, and Dr Pierrick Penven, for their detailed supervision in all stages of this project. From the grammar of the manuscript, up to the discussions of the results, they have been of great value. I especially acknowledge Dr Pierrick Penven, for his valuable input with a special gift of the book: "How to write and publish a scientific paper", and also his input in terms of modelling skills, that played an important role in the study.

I also acknowledge Professor Frank Shillington, head of the Department of Oceanography at the University of Cape Town (UCT), South Africa, Professor Gerold Siedler, Dr Mathieu Rouault, Dr Nicolas Foucherau and Mr Christo Whittle, for their useful contributions, making themselves promptly available for personal discussions at all times. Thanks also to Dr Pedro Monteiro for introducing me to the scientific community at UCT, and at Council for Scientific and Industrial Research (CSIR), in Stellenbosch. Words of commendations to my colleagues: Messrs Albert Mavume, Atanasio Manhique, Sebastiaan Swart, Neil Swart, Ms Natalie Burls, Jenny Veitch and Veronica Dove, for their help in different matters, in order to improve the quality of this study. A lot of thanks to Mr Emlyn Balarin for the opportunity that he has given me to find out about the scholarships for this project. To him also, and to Mrs Rachmat Harris, and Mrs Helen King thanks for their administrative support. I would like also to thank my family and friends for their enthusiastic support and encouragement.

To the institutions, I mostly acknowledge the University of Cape Town, and the Institut de Recherche pour le Developpement (IRD, Bretagne, France) for allowing me to use their facilities such as offices and computers to run the model simulations. Also I acknowledge the National Research Foundation (NRF), Canon Collin Trust, and the International Post-Graduate Grant at UCT, for their financial assistance.

TABLE OF CONTENTS

LIST OF FIGURES

Figure 5.3.1 – Track of anti-cyclonic eddy2. The red line represents the pathway and the black lines are the bathymetric contours in 1000 m intervals.

Figure 5.3.1.1 – The upper panel shows the changes in sea surface height [red line] with the bathymetry [blue line] and the lower panel shows the change of the eddy kinetic energy with the bathymetry during the course of propagation of anti-cyclonic eddy2.

Figure 5.3.1.2 – Track of anti-cyclonic eddy4. The red line represents the pathway and the black lines are the bathymetric contours in 1000 m intervals.

Figure 5.3.1.2.1 – The upper panel shows the changes of sea surface height [red line] with the bathymetry [blue line] and the lower panel shows the change of the eddy kinetic energy with the bathymetry during the course of propagation of anti-cyclonic eddy4.

Figure 5.3.2.1 – Track of anti-cyclonic eddy5. The red line represents the pathway and the black lines are the bathymetric contours in 1000 m intervals.

Figure 5.3.2.2 – The upper panel shows the variation of the sea surface height profile [red line], and lower panel shows the variation of the eddy kinetic energy profile [red line], with the bathymetric profile [blue line] on both panels during the course of propagation of anti-cyclonic eddy5.

Figure 5.3.2.3 – Track of anti-cyclonic eddy6. The red line represents the pathway and the black lines are the bathymetric contours in 1000 m intervals.

Figure 5.3.2.4 – The upper panel shows the variation of the sea surface height profile [red line], and the lower panel shows the variation of the eddy kinetic energy profile [red line], with the bathymetric profile [blue line] on both panels during the course of propagation of anti-cyclonic eddy6.

Figure 5.3.2.5 – Track of anti-cyclonic eddy7. The red line represents the pathway and the black lines are the bathymetric contours in 1000 m intervals.

Figure 5.3.2.6 – The upper panel shows the variation of the sea surface height profile [red line] and the lower panel shows the variation of the eddy kinetic energy profile [red line], with the bathymetric profile [blue line] on both panels during the course of propagation of anti-cyclonic eddy7.

Figure 5.3.2.7 – Track of anti-cyclonic eddy9. The red line represents the pathway and the black lines are the bathymetric contours in 1000 m intervals.

Figure 5.3.2.8 – The upper panel shows the variation of the sea surface height [red line] and the lower panel shows the variation of the eddy kinetic energy [red line] with the bathymetric profile [blue line] on both panels during the course of propagation of anti-cyclonic eddy9.

Figure 5.3.2.9 – Track of anti-cyclonic eddy16. The red line represents the pathway and the black lines are the bathymetric contours in 1000 m intervals.

Figure 5.3.2.10 – The upper panel shows the variation of the sea surface height [red line] and the lower panel shows the variation of the eddy kinetic energy [red line] with the bathymetric profile [blue line] on both panels during the course of propagation of anti-cyclonic eddy16.

Figure 5.3.3.1 – Track of cyclonic eddy5. The blue line represents the pathway and the black lines are the bathymetric contours in 1000 m intervals.

Figure 5.3.3.2 – The upper panel shows the variation of the sea surface height [red line] and the lower panel shows the variation of the eddy kinetic energy profile [red line], with the bathymetric profile [blue line] on both panels during the course of propagation of cyclonic eddy5.

Figure 5.3.3.3 – Track of cyclonic eddy7. The blue line represents the pathway and the black lines are the bathymetric contours in 1000 m intervals.

Figure 5.3.3.4 – The upper panel shows the variation of the sea surface height [red line] and the lower panel shows the variation of the eddy kinetic energy [red line] with the bathymetric profile [blue line] on both panels during the course of propagation of cyclonic eddy7.

Figure 5.3.3.5 – Track of cyclonic eddy10. The blue line represents the pathway and the black lines are the bathymetric contours in 1000 m intervals.

Figure 5.3.3.6 – The upper panel shows the variation of the sea surface height [red line] and the lower panel shows the variation of the eddy kinetic energy [red line] with the bathymetric profile [blue line] on both panels during the course of propagation of cyclonic eddy10.

Figure 5.3.3.7 – Track of cyclonic eddy11. The blue line represents the pathway and the black lines are the bathymetric contours in 1000 m intervals.

Figure 5.3.3.8 – upper panel shows the variation of the sea surface height [red line] and the lower panel shows the variation of the eddy kinetic energy [red line] with the bathymetric profile [blue line] on both panels during the course of propagation of cyclonic eddy11.

Figure 5.4.1 – Portrayal of the SST [°C] for the month of January of the model year 3. The arrows indicate the position occupied by a mesoscale feature similar to a Natal Pulse. Note the offshore anti-cyclonic eddy with which this perturbation is associated.

Figure 5.4.2 – Portrayal of the SST [°C] for the month of February of the model year 3. The arrows indicate the position occupied by a mesoscale feature similar to a Natal Pulse. Note the offshore anti-cyclonic eddy with which this perturbation is associated.

Figure 5.4.3 – Portrayal of the SST [°C] for the month of March of the model year 3. The arrows indicate the position occupied by a mesoscale feature similar to a Natal Pulse. Note the offshore anti-cyclonic eddy with which this perturbation is associated.

Figure 5.4.4 – Portrayal of the meridional velocities (v [ms^{-1}]) at 33°S for the month of January in model year3. The negative values represent southward motion. This sequence may be compared to that in Figure 5.4.1.

Figure 5.4.5 – Portrayal of the meridional velocities (v [ms^{-1}]) at 33°S for the month of February in model year3. The negative values represent southward motion. This sequence may be compared to that shown in Figure 5.4.2.

Figure 5.4.6 – Portrayal of the meridional velocities (v [ms^{-1}]) at 33°S for the month of March in model year3. The negative values represent southward motion. This sequence may be compared to the contemporaneous one given in Figure 5.4.3.

Figure 5.4.7 – Oku-Weiss [s^{-2}] at 33°S for the month of January, model year3. The negative values represent the rotation and the positives the deformation of the flow. This sequence may be compared to that shown in Figures 5.4.1 and 5.4.4.

LIST OF TABLES

LIST OF ACRONYMS

ACSEX	Agulhas Current Source Experiment
ARGOS	Global array of temperature/salinity profiling floats
AVISO	Archived Validation and Interpretation of Satellites Data for Oceanography
CD	Compact Disc
CNES	National Centre for Spatial Studies
COADS	Comprehensive Ocean Atmospheric Data Set
EACC	East African Coastal Current
ETOPO2	Global Earth Topography at 2 minute degree latitude resolution
EKE	Eddy Kinetic Energy
EMC	East Madagascar Current
FTP	File Transference Protocol
LVS	Live Access Server
MATLAB	Matrix Laboratory
MODIS	Moderate Resolution Imaging Spectroradiometer
MRSU	Marine Remote Sensing Unity
NASA	National Aeronautics and Space Administration
NEMC	North East Madagascar Current
NetCDF	Network Common Data Form
NOAA	National Oceanic and Atmospheric Administration
PSU	Practical Salinity Units
ROMS	Regional Ocean Modelling System
SEC	South Equatorial Current
SSH	Sea Surface Height
SST	Sea Surface Temperature
SWIO	South-West Indian Ocean
UCT	University of Cape Town
WOA	World Ocean Atlas
WOCE	World Ocean Circulation Experiment

1 INTRODUCTION

1.1 The ocean circulation in the South-West Indian Ocean

The ocean circulation in the South-West Indian Ocean is influenced by the input of water masses from the South Equatorial Current. This current is one of the dominant features of the sub-gyre of the South Indian Ocean. The current derives from the northward flows of water from the subtropical gyre, inflow of water from Indonesian Seas and from the North Indian Ocean through the South-West Monsoon Current and Java Current [New et al., 2007; Stramma and Lutjeharms, 1997]. The South Equatorial Current is shallow and flows in a westward direction, lying in a zonal band over the width of the tropical Indian Ocean. It is not a single broad current, rather it consist of several narrow jets that split and coalesce at locations marked by steep topographic formations [Matano et al., 2002].

The path of the South Equatorial Current is very irregular due to the effect of the underlying topography and Rossby waves [Schott and McCreary, 2001], and its zonal position varies seasonally between the North-East Monsoon season and the South-West Monsoon season. Such variability is generated east of 100°E by the annual cycle of the wind stress curl, and propagates westward as a Rossby wave at speeds of 0.1 ms^{-1} [Woodberry et al., 1989]. The total westward volume transport of the current between 10 – 16°S has been calculated as 50 - 55 Sv [New et al., 2007] and its highest volume transport is observed during the South-West Monsoon.

On reaching the east coast of Madagascar at between 17 – 20°S the South Equatorial Current bifurcates into a northward and southward flowing branch [Figure1.2]. Schott and McCreary [2001] termed the northward branch the North-East Madagascar Current [NEMC], and the southward branch the South-East Madagascar Current [SEMC]. The nature of this bifurcation and the influence that the monsoon season has on its zonal position has to date not been accurately resolved. However, these branches are important components to the background ocean circulation of the South-West Indian Ocean region, including the influence on the characteristic of the greater Agulhas Current system.

1.2 The greater Agulhas Current system

The Agulhas Current system lies embedded in the larger scale circulation of the Indian Ocean, and dominates the circulation of the South-West Indian Ocean [Lutjeharms et al., 2001]. The northern part of the system is connected to the inflow waters from the Pacific Ocean [Stammer et al., 2003] through the Indonesian Archipelago [Wyrtki, 1971; 1997; Gordon et al., 1997], and to the south is exposed to water exchange with the Southern Ocean [Lutjeharms and Ansorge, 2001].

The contribution of waters from both the Pacific Ocean and from the Southern Ocean into the upper layers of the greater Agulhas Current system is relatively small [Lutjeharms, 2006]. For this reason, Lutjeharms infers that the Agulhas Current system is largely influenced by aspects of the Indian Ocean that are peculiar to the ocean itself. The system consists of three interdependent components: The Agulhas Current proper; the Agulhas Retroflection; and the Agulhas Return Current [Lutjeharms, 2001]. The Agulhas Current proper is characterized by a northern and southern part. The flow of these parts, northern and southern, present distinctly different characteristics. The northern part is very stable and its flow is tightly coupled to the continental slope [De Ruijter et al., 1999]. By contrast, the path of the southern part is considerably more unstable, comprising large meanders [Gründlingh, 1995; Harris et al., 1978], possibly due to the wider and shallower bathymetry of the Agulhas Bank [Figure 1.2].

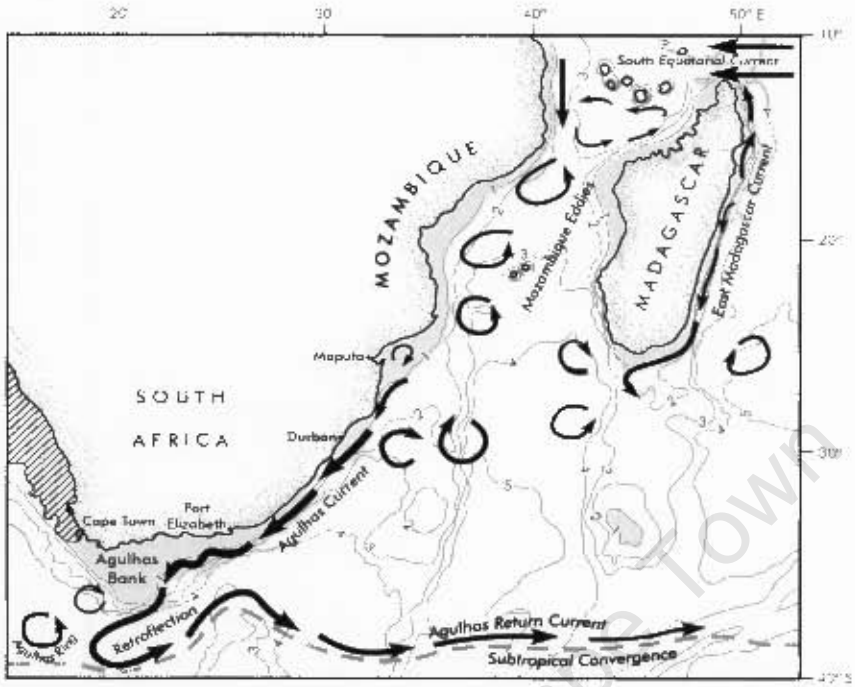

Figure 1.2 - A schematic representation of the ocean circulation in the South-West Indian Ocean. In the figure the black circular features represent the rotating masses of water known as eddies. The clockwise rotations portray cyclonic eddies and the anti-clockwise portray anti-cyclonic eddies. Black arrows represent the oceanic currents. The gray shaded areas represent the bathymetric features with less than 1000 m depth. The numbers represent the depths of the bathymetric contours, intervals in kilometers. The broken line is a representation of the Subtropical Convergence [after Lutjeharms, 2006].

1.2.1 The Agulhas Current proper

The Agulhas Current is a strong western boundary current [Quartly and Srokosz, 2002; 2004; Doglioli et al., 2007]. It forms the western limb of the wind-driven and anti-cyclonic circulation of the South Indian Ocean [Schott and McCreary, 2001]. The exact location where the Agulhas Current starts along the south-eastern African shelf is not fully understood [Lutjeharms et al., 2003], although investigations have identified its northern part starting approximately at the border between Mozambique and South Africa [De Ruijter et al., 1999].

The Agulhas Current is a narrow and fast flowing current, approximately 100 km in width and 2000 m deep [De Ruijter et al., 1999], with surface velocities exceeding 2 ms^{-1} [Lutjeharms, 2007]. The current carries surface layers of warm Indian tropical and subtropical waters

southwards [Biastoch and Krauss, 1999]. The tropical water is characterized by a potential temperature above of 20°C, and salinity ranging between 34.7 – 35.3 psu [practical salinity unity]. The South Indian subtropical water is characterized by a potential temperature above 17°C, and a surface salinity of 35.6 psu [Valentine et al., 1993].

Due to the influence of the Agulhas Current on the global ocean circulation, many researchers have been investigating the volume transport of the current, but this still remains the subject of different opinions. Differences on the estimated volume transport of the current may be related to the different methods applied, or quality of the data used for the calculation, or different geographic locations chosen.

Beal and Bryden [1999], using hydrographic data, estimated a total volume transport of the Agulhas Current of about 70 Sv. Stramma and Lutjeharms [1997] estimated a volume transport of the current in the upper 1000 m of about 65 Sv. Gordon et al. [1987] estimated the transport of the current south of Africa of about 95 Sv. A regional-near synoptic survey of the South-West Indian Ocean carried out from May to July 1995 as a part of the World Ocean Circulation Experiment Hydrographic program, determined the volume transport of the Agulhas Current in the upper 2000 m, through a section at 25°S of about 76 Sv [Donohue and Toole, 2003]. Based on an eddy permitting model Reason et al. [2003] suggest a seasonal variation of the volume transport of the Agulhas Current through to inter-annual scales. The dynamical mechanisms driving the variability of this volume transport remains largely unknown [Fetter et al., 2007]. Through a section at 35°S Reason et al. [2003] estimate a transport of 58 – 59 Sv during summer-autumn and 64 – 65 Sv during the winter-spring seasons.

At about 35°S the Agulhas Current separates from the continental shelf, and at its termination south of Africa the current makes an abrupt turn [Matano et al., 1998] and thus generates another important component of the greater Agulhas Current system known as the Agulhas Retroflection.

1.2.2 The Agulhas Retroflection

The southern component of the Agulhas Current is influenced by the wider shelf associated with the Agulhas Bank [Schouten et al., 2000]. In this region the Agulhas Current undergoes a series of meanders [Harris et al., 1978; Lutjeharms, 1981], with shear eddies and plumes of

warm surface water developing along the shelf edge of the bank. Once the Agulhas Current has passed the southern tip of the African continental shelf, it turns on itself in a tight loop, called the Agulhas Retroflection [Lutjeharms and van Ballegooyen, 1988]. Such a retroflection has been shown to be unstable, and at irregular intervals a loop occludes forming an independent Agulhas ring [Figure 1.2] that moves off into the South Atlantic [Schouten et al., 2000].

The Agulhas rings carry warm and salty Indian Ocean water into the South Atlantic [Gründlingh, 1995] and thus establish a major oceanic connection in the global overturning circulation [De Ruijter et al., 2004]. Such oceanic connection is driven by the Agulhas Current through the Agulhas rings, but also by Agulhas eddies and current filaments at the region of the Agulhas Retroflection [Richardson et al., 2003].

Due to their significant influence on the global thermohaline circulation and climate, the volume transport of Agulhas rings has been of substantial interest. Studies [De Ruijter et al., 1999; 2004] suggest that the annual volume flux due to the shedding of Agulhas rings is about 10 Sv. The rings are characterized by a surface temperature up to 26°C and an average diameter of about 300 – 400 km [Lutjeharms and van Ballegooyen, 1988] and extend through the full water column, moving at a rate of about 5 – 8 km per day [Olson and Evans, 1986]. Based on hydrographic data Gründlingh [1995] estimated an annual volume transport of Agulhas rings of about 2 – 8 Sv. The frequency of these ring shedding events has been estimated by Schouten et al. [2000] to be approx 4 – 5 times per year. Downstream of the Agulhas Current Retroflection the meandering flow back into the Indian Ocean becomes the Agulhas Return Current [Lutjeharms and Ansorge, 2001].

1.2.3 The Agulhas Return Current

The Agulhas Current introduces Indian Ocean water masses into the Retroflection region, though this is limited to water mass less dense than sigma-θ of 27.5, shallower than 1500 or 2000 m [Gordon, 1986]. From this, the Agulhas Return Current is formed and flows along the northern boundary of the Subtropical Convergence [Figure 1.2], at an average latitude of about 39.5°S, increasing to 44°30'S at 60°E [Lutjeharms and Ansorge, 2001]. The Agulhas Return Current meanders between 38 - 40°S in a spatially and temporally continuous fashion and has a core width of approximately 70 km. At the retroflection region the current has a depth of about 4000 m [Schmitz, 1996], and surface speed may exceed 2 ms^{-1}, decreasing eastwards to about 0.75 - 0.13 ms^{-1} [Lutjeharms and Ansorge, 2001], with an associated volume transport of about

44±5 Sv in the upper 1000 m [Boebel et al., 2003]. Based on hydrographic data Lutjeharms and Ansorge [2001] estimated the volume transport of the current to range from 54 Sv in the retroflection region to 15 Sv at 76°E.

The Agulhas Return Current has its strongest kinematics expression on the northern edge of the Agulhas Front in its western part, and is featured with a meandering pattern with three crests and troughs [Boebel et al., 2003]. The meridional gradient property of both the Agulhas Return Current and the Agulhas Front is high and instabilities in the current shear produce a range of mesoscale eddies [Speich et al., 2006], which influence the pattern of the circulation in the greater Agulhas Current system. Besides the Agulhas Return Current, Agulhas Retroflection and the Agulhas Current proper, important components of the greater Agulhas Current system are the sources of the Agulhas Current.

1.2.4 The sources of the Agulhas Current

The Agulhas Current is influenced by a forked pattern of enhanced variability from the Mozambique Channel and from the coast of Madagascar [De Ruijter et al., 2004]. A number of surveys during the World Ocean Circulation Experiment [WOCE] in the 1990s and the Agulhas Current Source Experiment [ACSEX, 2000; 2001] were planned especially with the aim of obtaining a better understanding of the nature of the Agulhas Current, its sources and its role in the South-West Indian Ocean as a whole. These hydrographic surveys, and satellite observations [Ridderinkhof and De Ruijter, 2003; Quartly and Srokosz., 2004; Schouten et al., 2003], and model simulations [Biastoch and Krauss, 1999; Penven et al., 2006; Quartly et al., 2006], strongly suggest that the Agulhas Current receives tributaries of water masses from three different sources: The Mozambique Channel eddies, the southern Madagascar eddies and the recirculation water masses from the sub-tropical gyre of the South-West Indian Ocean [Stramma and Lutjeharms, 1997].

The Mozambique Channel eddies drift southwards along the full length of the channel, and may have an intermittent contribution to the volume transport of the Agulhas Current [Biastoch and Krauss, 1999; Schouten et al., 2002b; 2003; De Ruijter et al., 2002]. Such eddies are probably related to the large scale climate anomalies over the central basin of the equatorial Indian Ocean, near eastern boundary, propagating westward as baroclinic Rossby waves. These climate anomalies reach the northern Mozambique Channel by water mass input from the South Equatorial Current.

At the southernmost tip of the Madagascar land mass the southern branch of the East Madagascar Current separates from the continental shelf, originating a possible retroflection of the current [Lutjeharms and Machu, 2000; Quartly et al., 2006]. Thus such a retroflection may trigger anti-cyclonic ring shedding [De Ruijter et al., 2004]. Such rings may drift south-westwards into the region of the Agulhas Current [Biastoch and Krauss, 1999].

Calculations of the mean dynamic sea surface height from the mean divergence of eddy vorticity fluxes observed from altimetry, in the region close to the eastern African continent in the South-West Indian Ocean, suggest a tight recirculation of water masses [Feron et al., 1998]. These water masses come mainly from the sub-tropical gyre of the South Indian Ocean from east of Madagascar, and from the Agulhas Return Current, and from the Mozambique Channel probably through the Indonesian throughflow [Gordon et al., 1997], via the South Equatorial Current. Thus, the interaction of the water masses from these different sources of the Agulhas Current, specifically the deep eddies [Penven et al., 2006], with the Agulhas Current itself may cause a big meander on the core of the Agulhas Current, known as a Natal Pulse [Lutjeharms and Roberts, 1988].

1.3 The Natal Pulse

One of the most intriguing aspects about the behaviour of the Agulhas Current has been its occasional absence from the near coastal location where it normally is found [Lutjeharms, 2006]. Hydrographic measurements, and satellite observations suggest that the occasional absence of the Agulhas Current is due to the presence of a large cyclonic meander embedded in the northern sector of the current [Figure 1.3], termed the Natal Pulse [Lutjeharms and Roberts, 1988].

The Natal Pulse originates in the Natal Bight, between the South African cities of Durban and Richards Bay [Lutjeharms et al., 2001]. The pulse moves downstream with the Agulhas Current at a rate of about 20 km per day [Lutjeharms, 2006b]. The Pulse causes abrupt directional change in the surface currents along the coast [Lutjeharms and Connell, 1989]. The generation of a Natal Pulse precedes the shedding of an Agulhas ring at the Agulhas Retroflection a half year later [Van Leeuwen et al., 2000]. The Pulse may also generate an upstream retroflection of the Agulhas Current. Such an upstream retroflection prevents Agulhas water from reaching the boundary zone between Atlantic and Indian Ocean water masses [Lutjeharms et al., 2001].

The growing of a Natal Pulse in the Natal Bight is due to barotropic instability of the flow where the continental shelf is less steep [De Ruijter et al., 1999]. De Ruijter et al. [1999] state that at the Natal Bight the stable Agulhas Current becomes marginally stable, so that a slight strengthening or sharpening of the current can make the flow susceptible to barotropic instability. Therefore it is thought [Schouten et al., 2002a] that such a perturbation of the flow is generated by the interaction of large anti-cyclonic eddies, originating in the Mozambique Channel and south of Madagascar, with the Agulhas Current. Figure 1.3 shows a Natal Pulse observed from NOAA-Satellites on 17 June 2006.

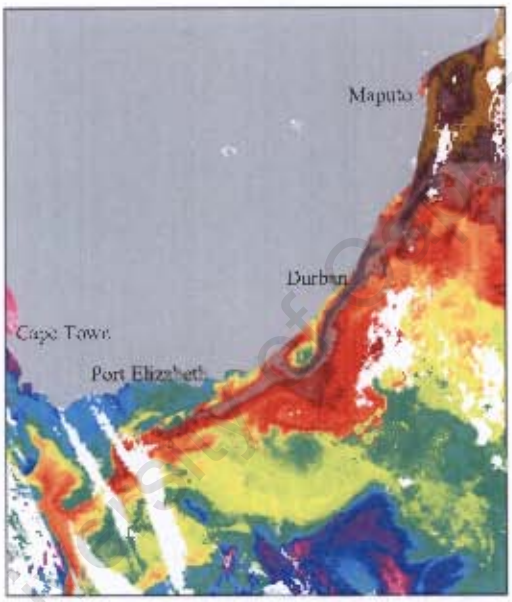

Courtesy: [MRSU]

Figure 1.3 A one day composite of thermal infrared imagery, obtained from the NOAA -17 and NOAA -18 satellites. The Agulhas Current is represented by the continuous red-dark colour off the southern African coast. A well developed Natal Pulse with cold water inside a cyclonic movement in green colour is evident between Durban and Port Elizabeth.

In the greater Agulhas Current system the circulation is strongly controlled by the bathymetric structure of the sea floor [Donohue et al., 1999]. This region has a variety of topographic features such as ocean ridges and ocean basins. The second part of this introduction chapter gives a short description about the bathymetric characteristics of the region.

1.4 The sea floor topography of the South-West Indian Ocean

One of the first order of constraints on the oceanographic environment with regard to how the inter-basin exchange and interaction of water masses occurs is the nature of the sea floor bathymetry [Parson and Evans, 2005]. Recent observations from altimetry indicate that the profile of the bathymetry has a strong influence on ocean circulation [Gille and Sandwell, 2001]. Since the ocean currents cannot pass through barriers such as ridges or seamounts, the currents tend to steer around these barriers and may generate steering flows such as vortices and eddies. In cases of weak currents such interaction may fully break down the flow.

The topography of the Indian Ocean [Figure 1.4] is characterized by a complex pattern of shallow mid-ocean ridges and deep abyssal plains, which in turn may influence the circulation in this region [Donohue and Toole, 2003]. The south-west sector of the Indian Ocean encompasses an array of oceanic ridges such as: South-West Indian Ridge; Mascarene Ridge; Davies Ridge; Mozambique Ridge; and Madagascar Ridge. The region also hosts a number of deep oceanic basins such as: Mascarene Basin; Transkei Basin; Mozambique Basin and Madagascar Basin. These complex bathymetric features are thought [Donohue and Toole, 2003] to impede the flow of deep water masses, although some exchange occurs through the deep fracture zones which transect each ridge system [Figure 1.4].

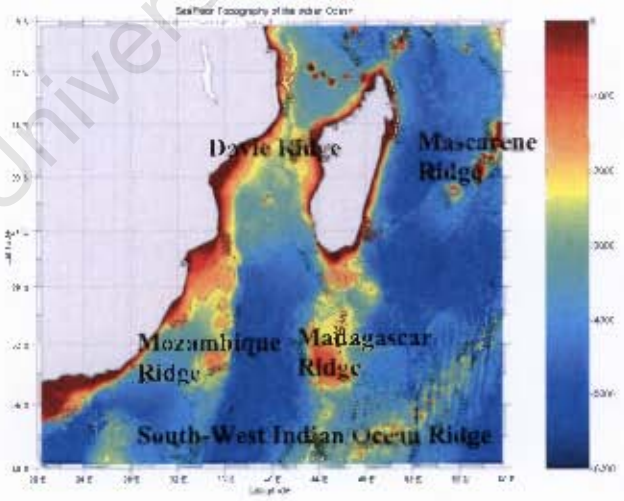

Figure 1.4 – The bathymetry of the South-West Indian Ocean. The shallow bathymetry rises to 2000 m at the Mozambique and Madagascar Ridges, with depths exceeding 5000 m characterizing the abyssal plains [dark-blue colour]. The colour bar gives the varying depth of this region with isobaths contouring spaced at 2000 m intervals. Bathymetric data have been extracted from the global bathymetric dataset of two minutes latitude resolution, ETOPO2 [Smith and Sandwell, 1997].

2 CURRENT KNOWLEDGE

2.1 The ocean circulation and underlying bathymetry in the Mozambique Channel and south of Madagascar

The Mozambique Channel and areas around the southern part of Madagascar lie embedded in the South-West Indian Ocean region, and fall into the domain and influence of the Greater Agulhas Current system. A dominant feature of this region is the mesoscale eddy variability [Figure 1.2] propagating southwards [De Ruijter et al., 2002] along the full length of the Mozambique Channel [Quartly and Srokosz, 2004; De Ruijter et al., 2005]. Previous investigations about the ocean circulation in the Mozambique Channel, based on a limited quantity and quality of hydrographic data, portrayed the flow in the channel as a warm southwards current [Figure 2.1] termed the Mozambique Current [Sætre and Da Silva, 1984; Donguy and Piton, 1991; Richmond, 1997].

With the improvement of the instruments of sea observation such as satellites Altimeters and ocean floats, as well as well designed in-situ observation programs such as [ACSEX], which provided an array of data at useful scales of space and time, and also the development of high resolution ocean models, the water flowing in the Mozambique Channel, and south of Madagascar is now perceived with a new understanding.

The water flowing southward in the Mozambique Channel is now portrayed as an intermittent propagation of mesoscale eddies [Figure 1.2], instead of a steady Mozambique Current [Biastoch and Krauss, 1999; Schouten et al., 2003]. The nature of the formation, behaviour and implication of such mesoscale eddies has been the subject of research among physical and biological oceanographers, but still remains little understood. Nevertheless they all attribute the existence of these eddies to anomalies generated by varying forces over the central basin or in the equatorial regions, propagating westwards as baroclinic Rossby waves, through the South Equatorial Current [De Ruijter et al., 2005]. Studies [Lutjeharms et al., 2001; Chapman et al., 2003] suggest that on approaching the east coast of Madagascar between 17 – 20°S, the South Equatorial Current bifurcates into a northward and southward flowing branch [Quartly and Srokosz, 2004; De Ruijter et al., 2004]. At the northern tip of Madagascar the northward branch is deflected westwards, where on reaching the east coast of Africa at about 11°S this current divides into a northward and southward flowing branches [Schouten et al., 2003].

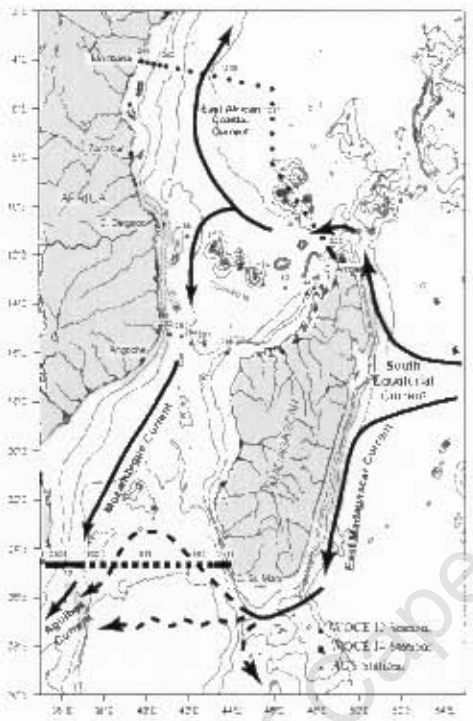

Figure 2.1 - Portrayal of the old concept about the ocean circulation in the Mozambique Channel and around Madagascar. The final destination of the southern branch of the East Madagascar Current after its separation from the continental shelf is presented in broken lines, meaning an issue not well known. The dotted line to the north [12°S] of the Mozambique Channel and the horizontal broken line to the south [24°S] represent the hydrographic stations used by WOCE12 and WOCE14 in-situ observation programme [not used in this study]. The bathymetric contours are in 1000 m intervals, and the solid arrows stand for the oceanic currents with their description labeled [after DiMarco et al., 2002].

The northward branch is termed the East African Coastal Current [Schott and McCreary, 2001] and the southward branch doesn't have a specific name. It breaks up into the train of cyclonic and anti-cyclonic eddies mentioned above, with a frequency of 4 – 5 anti-cyclonic eddies per year [Schouten et al., 2003; Quartly et al., 2006]. These eddies can reach about 400 km in diameter, and they have been observed to extend all the way through the water column to a depth of approximately 2500 m [De Ruijter et al., 2002], and they carry the deep layers water masses including Red Sea Water.

The southward branch of the East Madagascar Current is a narrow current, about 100 km wide and more than 1000 m deep. Its strongest core near the surface is about 50 m deep, moving with a speed exceeding 1 ms^{-1}. This current separates from the continental shelf at the southern tip of Madagascar. Previous research in this region, based on very limited hydrographic data, led to different concepts among the physical oceanographers working in the South-West Indian Ocean about the final destination of the East Madagascar Current after its separation from the continental shelf [Figure 2.1]. Tchernia [1980] supported the possibility that after such separation the East Madagascar Current flows northward along the west coast of Madagascar as a West Madagascar Current, and that it joins the Mozambique Current in the Mozambique Channel. Gründlingh [1988] and Lutjeharms [1988c] suggested a different possibility. Instead of a West Madagascar Current they supported the idea of a net westward flowing crossing the Mozambique Basin and feeding the Agulhas Current. Finally Lutjeharms [1988d] and DiMarco et al. [2000] suggested that the remaining of the waters from the East Madagascar Current couldn't reach the African coast, instead it may retroflect at the vicinity of the Madagascar Ridge [Figure 2.1]. Current investigations based on satellite observations and high resolution models hint at a possible retroflection of the East Madagascar Current in its path after its separation from the continental shelf [Lutjeharms, 1988; Quartly et al., 2006]. Such a retroflection is thought [De Ruijter et al., 2004] to generate a south-westward movement of bipolar vortices and eddies which have been shown from altimetric data and model simulations to propagate into the Agulhas Current region [Schouten et al., 2002]. Recent investigation of the flow to the south of Madagascar, based on hydrographic data (WOCE), and satellite altimeters, add to the current knowledge the existence of a new current on the system of the currents of the South-West Indian Ocean environment: the subtropical South Indian Ocean Countercurrent (SICC)[Siedler et al. 2006]. This current propagates eastwards between 22° and 26° S [Siedler et al. 2006].

Similar to the flow from the East Madagascar Current, the train of eddies from the Mozambique Channel move into the region of the Agulhas Current, and thus, eddies originating from both the Mozambique Channel and the region south of Madagascar contribute intermittently to the volume of the Agulhas Current [Quartly and Srokosz, 2004; Doglioli et al., 2007], and to some extent occasionally affect the behaviour of this current, such as its temporary absence from the continental shelf due the formation of a Natal Pulse, instability and consequent earlier retroflection of the Agulhas Current. De Ruijter et al. [1999] have suggested that an anti-cyclonic eddy interacting with the seaward edge of the Agulhas Current can provide the positive transport anomaly needed to destabilize the Current near Durban, where

the slope is less steep than elsewhere along the South African East coast. These interactions eventually trigger a Natal Pulse. Since such destabilization occurs occasionally [Lutjeharms, 2006] then it seems that the strength and intensity of both the current and eddies, as well as the point of interaction between the eddy and the current may play a crucial role. Such point of interaction may be determined by the route of propagation that an eddy may follow after crossing the Mozambique Ridge, still there is no confirmation of such a hypothesis yet.

2.2 The Mozambique Ridge

The Mozambique Ridge is an elongated feature lying roughly parallel to the south-east coast of Africa [Figure 2.2] between 25 – 35°S and 34 – 36°E, with a north to south orientation [Maia and Recq., 1990]. The ridge is bounded to the east by a deep 3000 m scarp, which descends down to 5000 m into the Mozambique Basin. The western flank of the ridge drops with a smooth slope into the Transkei Basin [Hales and Nation, 1973; Chetty and Green, 1977]. The eastern escarpment of the ridge is linear, and it drops to great depths along its 1300 km length [Fisher and Goodwillie, 1998].

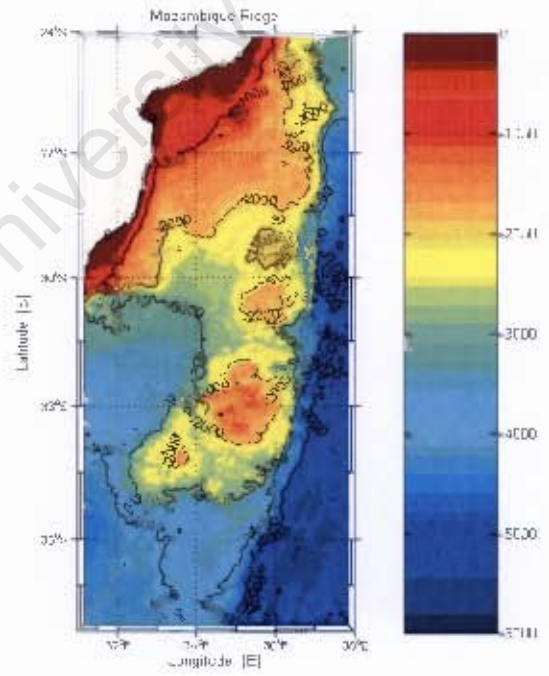

Figure 2.2 – Mozambique Ridge. The colours represent the depths of the ocean and the contours are the isobaths with intervals of 1000 m. The fractures over the ridges allow the deep leakage of chemical physical and biological properties between the Mozambique Basin and the Natal Valley.

The Mozambique Ridge blocks an exchange of zonal flow of the deep and bottom water masses between the Natal Valley and the Mozambique Basin, beneath 2800 – 3000 m respectively [Donohue and Toole, 2003]. The ridge also influences the propagation of cyclonic eddies that move between a west and south-west direction [Quartly and Srokosz, 2002; De Ruijter et al., 2004]. Gründlingh [1987] has suggested that the Mozambique Ridge is responsible for the formation of eddies. Such formation was supposed to be due to an interaction between a transient southward current flowing along the eastern side of the ridge. Dimarco et al. [2002] have suggested that in many cases pairs of eddies at the Mozambique Ridge are formed possibly related to the conservation of potential vorticity as the flow moves into deeper waters. Subsequent studies [Schouten et al., 2003; De Ruijter et al., 2004] disagree fully with such a possibility, and suggest that these eddies are not originated by or at the Mozambican Ridge, instead that they come from the Mozambique Channel and from the east of Madagascar. The latter of these eddies are generated by the interaction between a southward flowing deep jet current to the east of Madagascar with the Madagascar Ridge [Schouten et al., 2003].

2.3 The Madagascar Ridge

The Madagascar Ridge [Figure 2.3] is also an elongated aseismic plateau in the South-West Indian Ocean, which separates two oceanic basins: the Mozambique Basin and the Madagascar Basin. The ridge forms a region of shallow water, between 42 – 47°E, extending 400 km across and southwards from Madagascar for a length of over 1300 km. The depth of the water ranges between 2000 – 3000 m over most of the plateau [Sinha et al., 2008]. The ridge is a broad, and over much of its area, flat-topped feature, covered by 0.5 – 1.0 km of undisturbed sediment [Goslin et al., 1980]. A steep scarp on the western side of the ridge runs down into a 5000 m deep Mozambique Basin, while the slope from the southern half of its eastern flank runs into a 5000 – 6000 m deep Madagascar Basin. To the north, the ridge abuts directly with the island of Madagascar. To the south of the ridge the water depth increases rapidly to more than 3000 m, and beyond this the 4000 m isobaths merge onto the flank of the South-West Indian Ridge [Payet et al.,2004; Sinha et al., 2008].

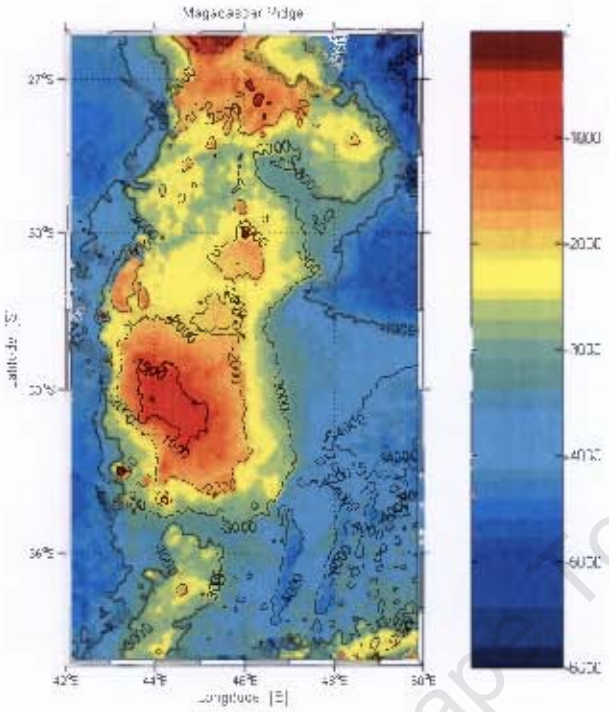

Figure 2.3 - Madagascar Ridge. The colours represent the depth of the ocean, and the contours are the isobaths with 1000 m intervals. The fractures over the ridge set the zonal deep leakage of chemical physical and biological properties between the Madagascar and the Mozambique Basins.

2.4 The Davie Ridge

The Davie Ridge is an important structural feature of the Mozambique Channel [Bassias, 1992]. It runs NNW through the Mozambique Channel west of Madagascar and represents the presumed extinct transform along which Madagascar separated from Somalia between 160 – 117 million years ago, and from India [Dyment, 1991; Kusky et al., 2006]. According to Bassias [1992], it represents the actual configuration of an old fracture zone between Africa and Madagascar along which Madagascar drifted southward during Late Jurassic and Early Cretaceous times. The ridge probably divides the Mozambique Channel into two different domains: the first one, west of the ridge, characterized by a thick crust, and the second one, by a thinner crust, between the Davies Ridge and Malagasy [Recq and Charvis, 2007]. It is thought [Ridderinkhof and De Ruijter, 2003], that this ridge may be responsible for the steering flow and eddy generation in the central part of the Mozambique Channel.

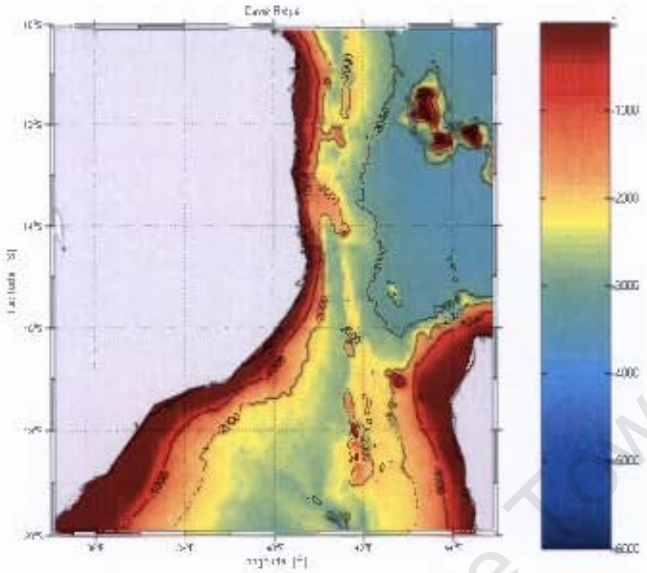

Figure 2.4 - Davie Ridge. The colours represent the depth of the ocean, and the contours are the isobaths with 1000 m intervals. It is thought that this ridge may be responsible for generation of eddies in the central Mozambique Channel.

The region contains many other topographic features which are also important components to understand the regional ocean circulation system. Many of these have a similar physiography to the Mozambique and the Madagascar Ridges. Under the present study, attention is only given to the Mozambique and the Madagascar Ridges. From all the aseismic ridges in the Indian Ocean, the Mozambique and the Madagascar Ridges have the most similar morphology [Sinha et al., 2008]. They have a broad elevated topography especially on the southern half and fall away steeply down into the Mozambique Basin. They are sharply truncated at their southern ends near the latitude 35°S and both Mozambique and Madagascar Ridges extend southward continuously from continental blocks at depths of 1000 – 2000 m.

Similar to the Mozambique Ridge, the Madagascar Ridge also blocks an exchange of a zonal flow of the deep and bottom masses of water between the Madagascar and Mozambique Basins. Investigations of combined satellite and in-situ observations suggest that by conservation of potential vorticity, the bottom topography of the Madagascar Ridge and the beta effect generate anti-cyclonic eddies in the jet current of the East Madagascar Current [De Ruijter et al., 2004]. Hence it stimulates a positive vortex formation which propagates into the region of the Agulhas Current.

Investigations [Quartly and Srokosz, 2004; De Ruijter et al., 2004] on the ocean circulation in the Mozambique Channel and southern part of Madagascar, have suggested that the interaction between eddies in the region with the Agulhas Current, has a strong influence on the pathway of this current and associated mesoscale features [Donohue and Toole, 2003]. Therefore to understand better the contribution of such mesoscale features to the overall circulation of the Agulhas region – the role of bathymetry on this ocean variability must be fully understood.

At the moment, the bathymetric influence of the Mozambique and the Madagascar Ridges on the nature, formation and behaviour of the mesoscale eddies coming from the Mozambique Channel and regions south of Madagascar that propagate into the region of the greater Agulhas Current system is not well understood. Therefore these gaps of knowledge need to be bridged to complement the available knowledge on the understanding of the ocean mesoscale circulation in the region. Therefore, to improve our understanding on bathymetric control and the extent it has in controlling the flow and behaviour of the eddies in the southern part of Mozambique Channel and Madagascar, pertinent questions have been raised to be addressed if the ocean circulation in the region is to be well understood.

3 SCIENTIFIC RESEARCH QUESTIONS

The literature survey on what currently is known about the circulation in the South-West Indian Ocean has shown that there are some scientific questions that still remain unanswered with the present knowledge of this dynamic system. Therefore such open questions tell us that much more scientific research in the region, especially within the Mozambique Channel and southern parts of Madagascar, still needs to be carried out, in order to complement our understanding on the physical processes of the components of the greater Agulhas Current system. Thus the present study will address some of such unknown issues, especially those related to bathymetric influence, since the bathymetry in this region has a strong influence on the dynamics of the overall ocean circulation.

In the greater Agulhas Current system the circulation is strongly controlled by the bathymetric structure of the sea floor [Donohue et al., 1999; Quartly et al., 2006]. Buck [2003] has shown that the ultimate destination of eddies in the East Madagascar Current varies, with some eddies reaching the Agulhas Current, whereas others possibly recirculate in the sub-tropical gyre of the South Indian Ocean. On their paths from the southern part of Madagascar, the propagating eddies cross the Madagascar Ridge with which they may interact in unknown ways, so that the question may be asked:

- How does the bathymetry, especially the shallow Madagascar Ridge influence the mesoscale circulation propagating into the Agulhas Current region?

Studies have shown that once these eddies have survived the interaction with the Madagascar Ridge, they propagate in a south-westerly direction, the cyclonic eddies being more dispersive than the anti-cyclonic eddies and predominantly more drift southwards [De Ruijter et al., 2004]. During the course of their propagation they also interact with a southward flow from the Mozambique Channel, thus they may split or enhance their surface signature [De Ruijter et al., 2004]. On reaching the eastern side of the Mozambique Ridge these eddies undergo further bathymetric interaction, and their path is reoriented. Thus we aim to answer the second research question stated as follow:

- Do these eddies have a preferred routes of propagation through the fracture zones transecting the Mozambique Ridge?

An important aspect to take into account when investigating the mesoscale variability within a system of eddies is to look at their energy expression. Eddy energy may be exported from a region where it is generated by advection by the background flow, or by radiative mechanisms. As already mentioned, the Mozambique Channel and southern parts of Madagascar are regions of enhanced mesoscale variability. Eddies propagating southwards within the Mozambique Channel and south of Madagascar transport considerable amounts of heat.

Schouten et al., [2003], have investigated the variation of the mean sea surface height anomalies of 25 eddies along the Mozambique Channel during the years 1995-2000. The results of such investigation have suggested that the Mozambique Channel eddies increase their expression of the mean sea surface height during the course of their propagation. To complement such investigation with more extensive information about the characteristics of eddies in the region, a cross correlation of variation of sea surface height and eddy kinetic energy with variation of the bathymetric profile during the course of their propagation, in both the Mozambique Channel and the southern parts of Madagascar was investigated under the following research question:

- How does the kinetic energy of these eddies change during the course of their propagation?

It is thought [De Ruijter et al., 1999] that the impact of eddies on the Agulhas Current perturbs the flow of this current. An evident case is the generation of a Natal Pulse, along the southeastern African coast, between Durban and Richards Bay.

Studies have suggested that it is the interaction between large anti-cyclonic eddies originating in the Mozambique Channel and near the southern parts of Madagascar that occasionally causes an instability of the Agulhas Current. Thus the current study also proposes to investigate the physical mechanisms driving such perturbation by addressing the question:

- How do these eddies affect the stability of the Agulhas Current?

4 METHODOLOGY

Due to the lack of hydrographic data within the region of interest, we have used altimetric satellite observations. These provide data with a spatial and temporal covering ideal to address mesoscale studies of the oceans. We also used a regional ocean circulation model termed ROMS in order to simulate ideal situations which are impossible to perform in real life observations, [i.e. removing the bathymetric configuration from the domain of the study]. Such simulations are important because they allow us to understand the processes of the system.

4.1 Satellite Altimeters and data

The era of satellite oceanography have improved the ways in which we interpret the dynamics of the oceans. To study the oceans, satellite Altimeters are designed to measure the sea level by a combination of radar techniques, used to calculate the distance from the satellite to a reflecting surface. This technique allows one to measure a very precise location of the satellite on its orbit, and an accurate variation of the sea surface, with millimeters of precision [CNS, CLS technical report, 1997-2008]. The combination of different satellites observations, enhances higher precision of the altimeters to minimize the constrains of spatial and temporal resolutions, found in an individual satellite measurement. We have used altimetry data, a merged product processed by a reanalysis of altimeter products retrieved by the joint mission satellites: TOPEX-Poseidon + ERS 1, 2; Jason; Envisat. The series is of 10 years duration [1992-2002]. The satellite missions, provide an array of global data categorized in near real time [NRT], and delayed time [DT]. The NRT are mostly used in operational oceanography, and are distributed one week after the date of measurement. The DT are provided two months after the measurement. In our study, we have used the DT gridded data with 1/3X1/3 grid resolution on a Mercator grid. These data are used specially for studies of mesoscale circulation of the oceans, and the climate of the Earth. The data are processed by the French agency: National Center for Spatial Studies [CNES], and are distributed by AVISO, through SSALTO/DUACS. The AVISO proposes several ways of accessing the data, such as FTP – which is a data extracting tool that extracts the data from a global dataset, over a long period, choosing a geographical region, and/or temporal period. Another data server is the LIVE ACCESS SERVER [LVS] – which is a highly configurable Web server, designed to provide flexible access to geo-referenced scientific data; OpenDap – which enables one to access remote data sets through familiar data analysis and visualizations packages; and finally via

media CD and VCD ROMs, free of charge according to the motivated request. Via FTP, the data can be acquired following the link: ftp://ftp.cls.fr/pub/oceano/AVISO .

As already mentioned in this chapter, another tool used in this study was a regional model of ocean circulation. Thus the next section starts by providing a general overview about the model design, and the basic equations on which the model functioning is based.

4.2 ROMS model

4.2.1 History and design of the model

The Regional Ocean Modelling System (ROMS) represents a new generation of ocean circulation model [Shchepetkin and MC-Williams, 2005]. The model was developed in the United States of America (USA), at Rutgers University, and at the University of California Los Angeles (UCLA). The ROMS model stands as a successful improvement of the former Sigma Coordinate Rutgers University Model (SCRUM) [Song and Haidvogel, 1994]. SCRUM, was an improvement of the Semi-spectral Primitive Equation Model (SPEM) [Haidvogel et al., 2000]. ROMS is a free-surface, finite difference model, based on a nonlinear, terrain following curvilinear coordinates [Shchepetkin and MC-Williams, 2005]. The model was designed with important features such as: higher order advection schemes [Shchepetkin and MC-Williams, 1998]; predictor corrector time step algorithm, and parallelization. The first two features allow the model to solve with greater accuracy the dynamics of the coastal processes. The last mentioned feature make it possible to run the model on parallel computers. To date, ROMS has three different versions: ROMS Rutgers, ROMS UCLA, and ROMS (UCLA-IRD). The latter code has been termed by its developers, as, ROMS AGRIF [http://www.brest.ird.fr/Roms_tools/]. The code was developed by a joint effort of modelling researchers from UCLA, and from the Institute de Recherche pour la Development (IRD, France). ROMS AGRIF is a three-dimensional ocean model intended for simulation of currents, ecosystems, biogeochemical cycles and sediment movement in coastal regions, using an AGRIF grid refinement procedure. As already mentioned, ROMS is built as a parallel code, which can be allocated to different processors, in order to run in a shared memory (Open MPI), or in a distributed memory (MPI) machine. Its functioning is based on the primitive equations of the momentum conservation (4.2.1.1 – 4.2.1.2), mass conservation (4.2.1.7), heat and salt

transport (4.2.1.3 – 4.2.1.4), and the equation of state of sea water (4.2.1.5), in an Earth's rotating frame, solved on a Arakawa C grid, under two main approximations: The Boussinesq approximation, and the hydrostatic approximations. The Boussinesq approximation neglects density variations in the momentum equations, except for the gravitational force (or contributions to the buoyancy in the vertical momentum). The hydrostatic approximation, assumes that the vertical gradient of pressure balances the buoyancy. It means that vertical accelerations and Coriolis terms associated with the vertical velocities are neglected. These assumptions require that a typical ocean depth be small compared to a typical ocean length.

4.2.2 The primitive equations of motion

The primitive equations of motion, taking into consideration the Boussinesq approximation, and the hydrostatic approximation (4.2.1.6), can be represented in the Cartesian coordinate system [Hedström, 1997] as follows:

$$\frac{\partial u}{\partial t} = -u\frac{\partial u}{\partial x} - v\frac{\partial u}{\partial y} - w\frac{\partial u}{\partial z} + fv - \frac{\partial \phi}{\partial x} + F_u + D_u \tag{4.2.2.1}$$

$$\frac{\partial v}{\partial t} = -u\frac{\partial v}{\partial x} - v\frac{\partial v}{\partial y} - w\frac{\partial w}{\partial z} - fu - \frac{\partial \phi}{\partial y} + F_v + D_v \tag{4.2.2.2}$$

$$\frac{\partial T}{\partial t} = -u\frac{\partial T}{\partial x} - v\frac{\partial T}{\partial y} - w\frac{\partial T}{\partial z} + F_T + D_T \tag{4.2.2.3}$$

$$\frac{\partial S}{\partial t} = -u\frac{\partial S}{\partial x} - v\frac{\partial S}{\partial y} - w\frac{\partial S}{\partial z} + F_S + D_S \tag{4.2.2.4}$$

$$\rho = \rho(T, S, p) \tag{4.2.2.5}$$

$$\frac{\partial \phi}{\partial z} = -\frac{\rho g}{\rho_0} \tag{4.2.2.6}$$

$$0 = \frac{\partial u}{\partial x} + \frac{\partial v}{\partial y} + \frac{\partial w}{\partial z} \tag{4.2.2.7}$$

In the above equations, (x, y, z) $[m]$ are the Cartesian coordinates, oriented to the east, north, and upward directions respectively; and (u, v, w) [m.s^{-1}] are the corresponding components of the velocity vectors. $f\left[s^{-1}\right]$ is the Coriolis parameter, defined as: $f = 2\Omega\sin(\theta)$; being (θ) the latitude, and $\Omega\left[s^{-1}\right]$ is the Earth's radian rotation frequency. $\phi \quad \left[m^2 s^{-2}\right]$ is the dynamic pressure. $T\left[^0 C\right]$ is the potential temperature of the ocean, $S\left[PSU\right]$ is its salinity, and $p\left[N.m^{-2}\right]$ is the total pressure. F_u, F_v are the forcing terms for the horizontal velocities; and F_T, F_S are the forcing terms for temperature and salinity. D_u, D_v are the dissipating terms for the horizontal velocities, and D_T, D_S are the dissipating terms for temperature and salinity. ρ [kg.m^{-3}] is the density of the sea water, and ρ_0 is the mean density used for the Boussinesq approximation. $g\left[m.s^{-2}\right]$ is the acceleration of gravity.

The numerical solution techniques of the model, obey a vertical and horizontal discretization, functioning in the C grid scheme, as illustrated:

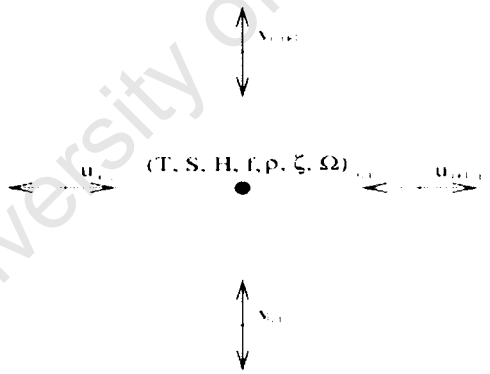

Figure 4.2 – Schematic representation of the variables in the model, into the Arakawa C grid [after Penven, 2000].

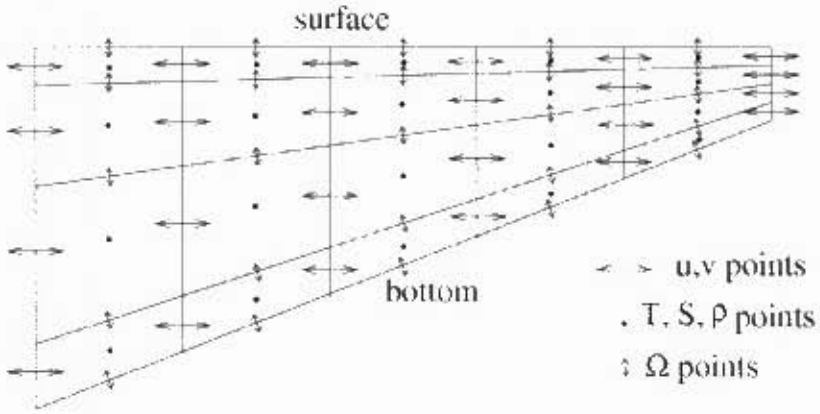

Figure 4.2.1 – Schematic representation of the vertical and horizontal discretization of the model functioning [after Penven, 2000]. Note that the propagation of the variable in each cell is perpendicular to the grid domain, in all directions.

According to [Arakawa and Lamb, 1977], the horizontal arrangement of the variables in the grid is well suited for problems with horizontal resolution, which is fine compared to the first radius of deformation.

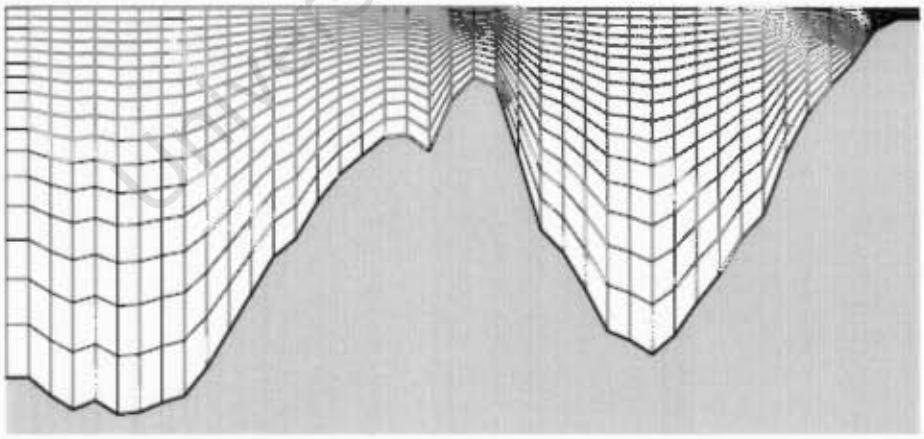

Figure 4.2.2 – Schematic representation of the discretization of the model, following terrain sigma coordinates [after Shchepetkin and MC-Williams, 2005].

4.2.3 The boundary conditions

4.2.3.1 The vertical boundary conditions

The vertical boundary conditions encompass surface and bottom boundaries. The free-surface is delimited by sea level elevation, i.e. $(z = \eta)$. The boundary conditions at the surface are wind stress, heat flux and fresh water fluxes. In our simulation, we have used surface fluxes from a monthly climatology at 0.5° resolution derived from Da Silva et al. [1994].

$[i]$ **- Surface boundaries:**

$$k_M \frac{\partial u}{\partial z} = \tau^x_{surf} \qquad (4.2.3.1.1)$$

$$k_M \frac{\partial v}{\partial z} = \tau^y_{surf} \qquad (4.2.3.1.2)$$

$$k_T \frac{\partial T}{\partial z} = \frac{Q_T}{\rho_0 C_P} \qquad (4.2.3.1.3)$$

$$k_S \frac{\partial S}{\partial z} = \frac{(E - P)S}{\rho_0} \qquad (4.2.3.1.4)$$

Where the terms K_M, K_T, K_S $[m^2 s^{-1}]$ are the coefficients of the vertical turbulent mixing of the momentum, temperature and salinity respectively. τ^x_{surf} and τ^y_{surf} $[m^2 s^{-2}]$ are the zonal and meridional components of the wind stress at the sea surface, Q_T $[W.m^{-2}]$ is the surface heat flux, C_P [J.kg^{-1}.C^{-1}] is the specific heat of the sea water, E $[cm.day^{-1}]$ is evaporation, and P $[cm.day^{-1}]$ is the precipitation. The surface heat flux contains several terms that depends on the sea surface temperature [SST], such as latent heat flux, sensible heat flux, and outgoing infrared radiation. According to Barnier et al. [1998] this feedback process is parameterized in the model as a restoring term at the sea surface. Such a term is obtained by a linearization of the

thermal forcing around a climatological temperature. Thus the total surface heat flux takes the form:

$$Q_T = Q_{net} + \frac{\partial Q}{\partial SST_{c\lim}}\left(SST_{model} - SST_{c\lim}\right) \qquad (4.2.3.1.5)$$

There is not such feedback for the salt flux. But, due to the poor quality of forcing data for precipitation and evaporation, we kept a restoring term, to prevent an inertial drift of the model [Marchesiello et al., 2003]. The salt flux is written as:

$$\text{Salt flux} = \frac{(E-P)SSS_{model}}{\rho_0} + Cff\left(SSS_{model} - SSS_{c\lim}\right) \qquad (4.2.3.1.6)$$

Where SSS_{model} and $SSS_{c\lim}$ are the sea surface salinity in the model and in the climatology. Cff is the inversed time, kept equivalent to the same value of $\frac{dQ}{dSST}$ (~ 30- 40 days).

At the surface $(z = \eta)$, the vertical component of the velocity (w) is defined by:

$$w = \frac{\partial \eta}{\partial t} + u\frac{\partial \eta}{\partial x} + v\frac{\partial \eta}{\partial y} \qquad (4.2.3.1.7)$$

$[ii]$ **- Bottom boundaries:**

At the bottom $(z = -H)$, vertical boundary conditions for the vertical component of the velocity (w), is defined by the form:

$$w = -u\frac{\partial H}{\partial x} - v\frac{\partial H}{\partial y} \qquad (4.2.3.1.8)$$

In our simulation, we have defined this boundary with a global bathymetric dataset at 2 minute resolution: Etopo2 [Smith and Sandwell, 1997]. At the bottom, the frictional effect on bottom currents by the roughness of the seafloor is parameterized as a stress, with the forms

$$k_M \frac{\partial u}{\partial z} = \tau^x_{bottom} \tag{4.2.3.1.9}$$

$$k_M \frac{\partial v}{\partial z} = \tau^y_{bottom} \tag{4.2.3.1.10}$$

Where τ^x_{bottom} and τ^y_{bottom} $\left[m^2 s^{-2}\right]$ are the zonal and meridional components of the bottom stress. The bottom stress is parameterized in a form of linear and quadratic terms of the bottom currents, and is defined as:

$$\tau^x_{bottom} = \left(\gamma_1 + \gamma_2 \sqrt{u^2 + v^2}\right) u \tag{4.2.3.1.11}$$

$$\tau^y_{bottom} = \left(\gamma_1 + \gamma_2 \sqrt{u^2 + v^2}\right) v \tag{4.2.3.1.12}$$

Where $\gamma_1 and \gamma_2$ are coefficients of linear and quadratic bottom stress respectively. Assuming that there is no heat flux, neither salt flux, nor exchange between the water columns and the bottom floor, these fluxes can be prescribed as null and represented with the forms:

$$k_T \frac{\partial T}{\partial z} = 0 \tag{4.2.3.1.13}$$

$$k_S \frac{\partial S}{\partial z} = 0 \tag{4.2.3.1.14}$$

4.2.3.2 The lateral and initial boundary conditions

A satisfactory prescription for open boundary conditions is crucial for the performance of a regional ocean circulation model. As regards outward propagation, Roed and Cooper [1986], have suggested that an open boundary should allow the perturbations generated inside of the computational domain, to leave it without obstruction of the solution inside the model. Marchesiello et al. [2001] have stressed that sometimes there is a competing requirement that

important external information should be conveyed inside of the domain. Otherwise the system may be under-specified. Thus, an active open boundary scheme was developed and implemented in ROMS [Marchesiello et al., 2001]. This algorithm deals successfully with the challenges of open boundary conditions encountered in several ocean circulation models. Such challenges are associated with the incoming information into the model domain and the radiation of the solution (i.e., the outgoing information) from the interior to the exterior of the domain without generating reflections causing deteriorization of the solution inside the system, and guarantee a realistic stable equilibrium state for long periods.

The active, open boundary scheme implemented in ROMS, estimates two horizontal phase velocities, propagating as waves, close to the boundary. The following equations show the derivation of open boundaries:

$$c_x = -\frac{\frac{\partial \varphi}{\partial t}\frac{\partial \varphi}{\partial x}}{\left(\frac{\partial \varphi}{\partial x}\right)^2 + \left(\frac{\partial \varphi}{\partial y}\right)^2} \qquad (4.2.3.2.1)$$

$$c_y = -\frac{\frac{\partial \varphi}{\partial t}\frac{\partial \varphi}{\partial y}}{\left(\frac{\partial \varphi}{\partial x}\right)^2 + \left(\frac{\partial \varphi}{\partial y}\right)^2} \qquad (4.2.3.2.2)$$

Where $c_x \left[m.s^{-1}\right]$ is a normal phase velocity and $c_y \left[m.s^{-1}\right]$ is the tangential phase velocity. φ is any variable in the model, such as (T, S, u, v, η). The propagation of variable φ in the model domain takes a form of the equation below, known as a wave equation:

$$\frac{\partial \varphi}{\partial t} + c_x \frac{\partial \varphi}{\partial x} + c_y \frac{\partial \varphi}{\partial y} = \frac{\varphi_{data} - \varphi}{\tau_{out}} \qquad (4.2.3.2.3)$$

When the propagation of the variable is towards the interior of the model domain, the variable value is nudged towards the data, and the equation, takes the form:

$$\frac{\partial \varphi}{\partial t} = \frac{\varphi_{data} - \varphi}{\tau_{in}} \qquad (4.2.3.2.4)$$

$\tau_{in}, \tau_{out}[s]$ stand for inward and outward nudging time and φ_{data} is a data variable. φ_{data} could be derived from a climatology observation, or from high resolution global models. For the lateral boundaries, (u, v) are computed from WOA temperature and salinity using geostrophy. For the geostrophy calculation we choose a level of no motion $(z_{ref} = -1000[m])$.

The initial conditions for our simulation have been derived from the global monthly climatology dataset at 1° resolution: World Ocean Atlas (WOA, 2001; Conkright et al., 2002). In the model, the initial day of the climatological experiment is set as 1 January of the modeled year 1. The external forcing is repeating a typical climatological year with cycle duration of 360 days [Penven and Tan, 2007].

4.2.4 The Mozambique Channel configuration

To perform our simulation, we have configured the model taking into account the topographic and hydrodynamic features of the region. To preserve a good solution within the region of interest, we extended the size of the domain to (20 - 60°E, 40 - 8°S). The horizontal grid resolution was $\frac{1}{6^0}$ (~17.5 km, at 19.00°S) containing 239x232 grid points on longitude and latitude respectively. For a finer resolution at the surface layers, the sigma coordinates were set to 32 vertical layers. The parameters for the vertical, sigma coordinate stretching, to the surface was set to $theta_s$ =7; to the bottom $theta_b$ = 0; and the minimum depth $h_{\min} = 50[m]$. The transition depth between the horizontal surface level and the bottom terrain- following levels was set to $h_c = 10[m]$. The physical boundaries are open at every side [North, South, East, and West]. The forcing fluxes are derived from monthly climatology at 0.5° resolution (Da Silva [1994]). Our configuration was at first tested for a 30 days run. Afterwards a long-term simulation $(10[years])$ was performed. The model output is averaged and stored every 3 days (a sufficient time scale to resolve mesoscale processes). The time step of the computation is $1800[s]$. A diagnostic analysis revealed a spin up time of the simulation (equilibrium state) after the first 2 years of run. A statistical MatLab toolbox, part of the Romstools, contains different tools to aid the pre-processing of the data, visualization of the model results, and post-processing of the data. It allowed us to perform the basic computation of the mean states (MEAN), standard deviations (STD), and variances (MS) of the main variables. Several

derived variables can be obtained from the simulated variables (see Penven and Tan, [2007], for a wider range of these variables).

4.2.5 The model performance

The ROMS model has been applied successfully in different oceanic regions around the world. In this study, the model was configured and applied to perform the simulation of mesoscale eddies in the Mozambique Channel and south of Madagascar. According to the literature, the flow in the South-West Indian Ocean is predominantly dominated by the presence of the anti-cyclonic eddies. These eddies move southwards through the Mozambique Channel, and south-westwards to the south of Madagascar. The eddies from both regions propagate into the Agulhas Current system. The resulting patterns are reproduced also in our simulation [Fig 4.2.5].

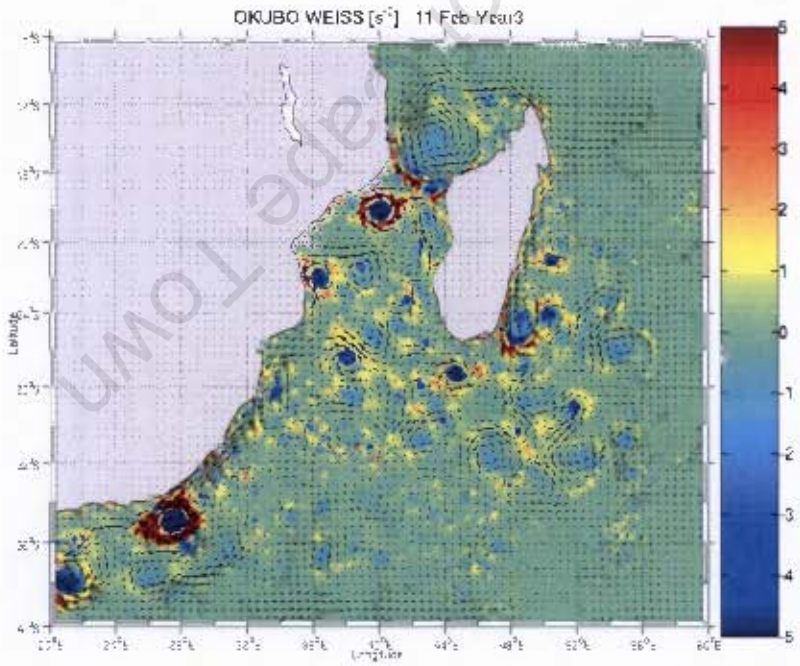

Figure 4.2.5 Snap-shot for 11 February of the modeled year 3. The Okubo-Weiss [s^{-2}] parameter of the flow is used to portray the movement of eddies in the Mozambique Channel and around Madagascar. Predominant anti-cyclonic eddies are shown to move southwards in to the Agulhas region, at a rate and with a trajectory similar to the movement of eddies identified by hydrographic and altimetric data.

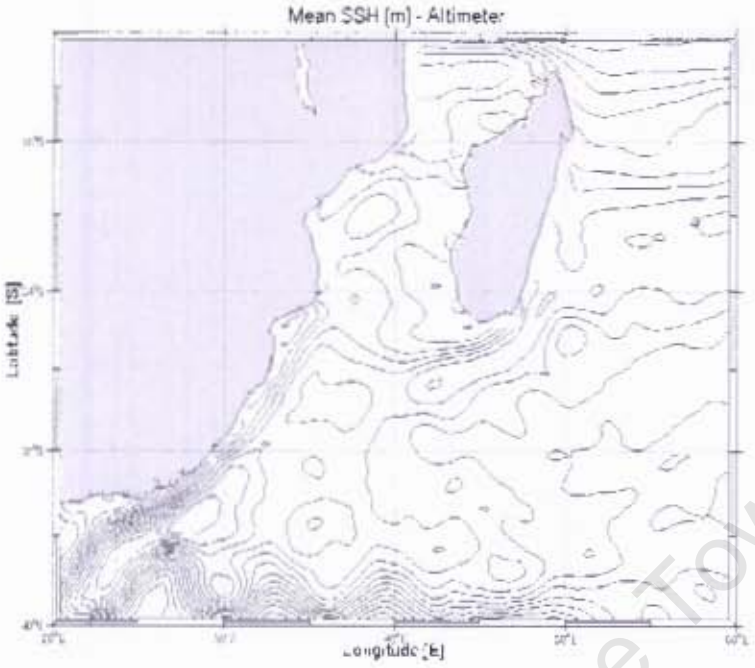

Figure 4.2.5.1[a] - Eight year mean of the sea surface height [m], with a contour interval of 0.1 m calculated from altimeter.

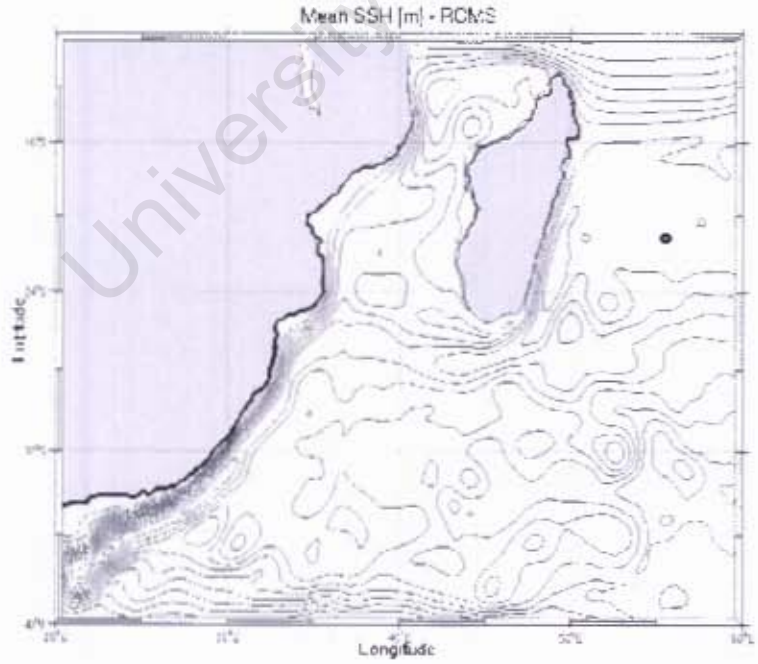

Figure 4.2.5.1[b] - Eight year mean of the sea surface height [m], with a contour interval of 0.1 m calculated with the Model.

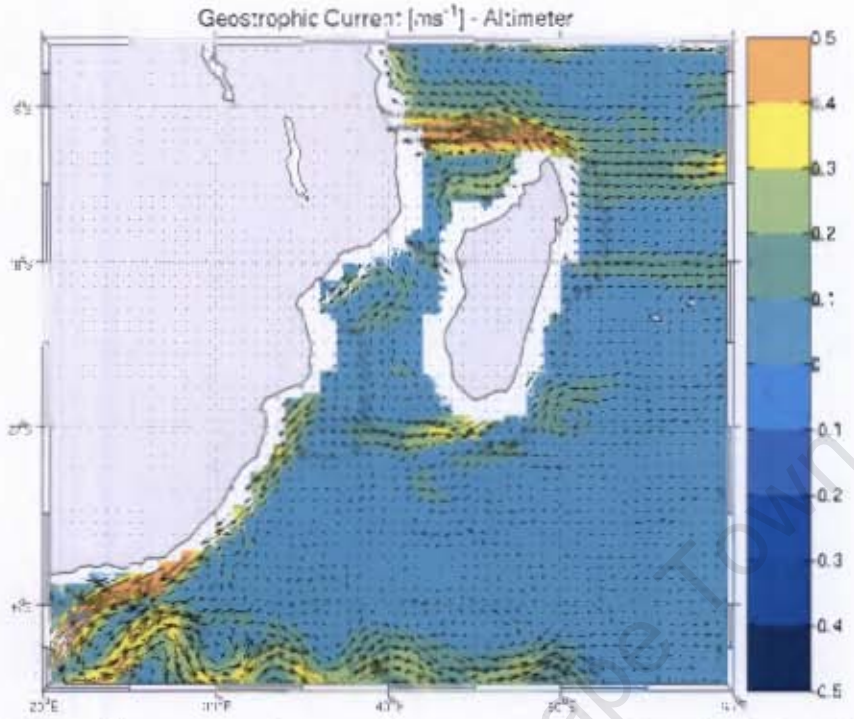

Figure 4.2.5.2[a] – Eight year mean of geostrophic currents (arrows [ms^{-1}]), retrieved from altimeter. The colours indicate the intensity of the velocity field [ms^{-1}].

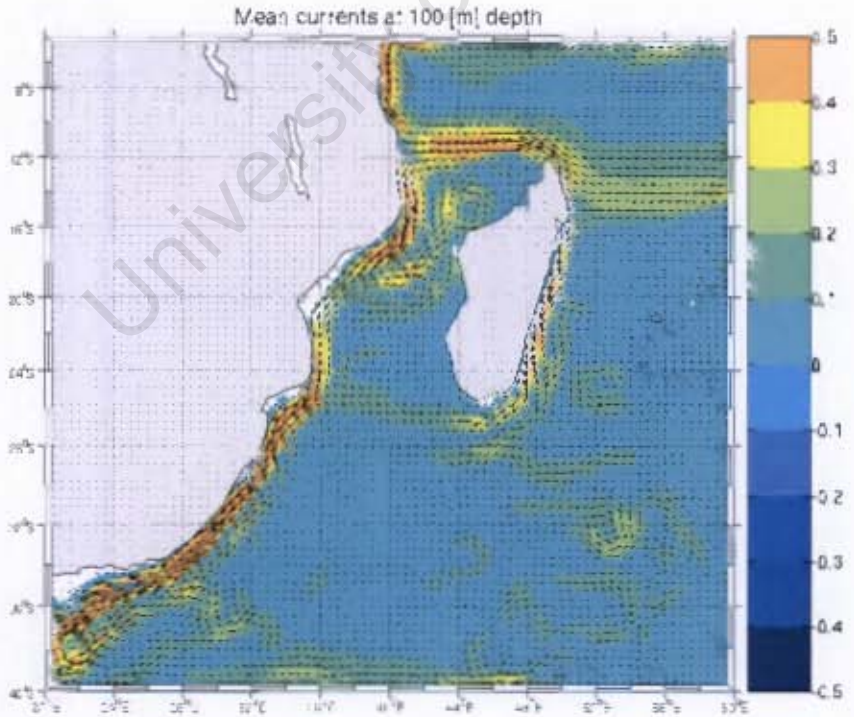

Figure 4.2.5.2[b] – Eight year mean of geostrophic currents (arrows [ms^{-1}]) at 100 [m] depth, simulated with the model. The colours indicate the intensity of the velocity field [ms^{-1}].

As regard to the general ocean circulation in the region (Figures 4.1[b] – 4.2.5.2[b]), the model correctly portrays the westward flow of the South Equatorial Current splitting into two branches on the east coast of Madagascar. The northward flow, after reaching the northern tip of Madagascar, propagates westward to the east coast of the African continent, where it splits into two branches. The northward branch forms the East African Coastal Current and the southward flow propagates into the Mozambique Channel. To the east coast of South-Africa, the flow of the Agulhas Current, and of the Agulhas Return Current are also represented in our simulation.

Also some limitations on the model results are clearly observed. The model did not reproduce the meandering behaviour of the Agulhas Return Current. It could be associated with the position in which the southern open boundary has been placed. In this region a very strong variability of the flow is present. Therefore we would argue that the nudging of the solution at this active boundary may have influenced the behaviour of the current.

There are limitations in comparing altimeter product with our model simulation. Such limitations are due to the incapability of the altimeter to retrieve information close to the coast. Nevertheless, from the available information, we see that the model reproduces the key elements of the circulation patterns of the system.

4.3 Idealized model simulations

Model simulations allow one to perform experiments that are not possible in real life. With such simulations, we may learn more about a target system being investigated. We have performed an idealized simulation to understand the influence of the sea floor topography on the mesoscale circulation south of Madagascar. The idealized simulation consisted in removing the upper 4000 m of the Madagascar Ridge, turning this bathymetric feature into a flat topped topography.

The results of this simulation were compared with the reference model simulation performed without modification of the bathymetry. Notice that both, the real and the idealized simulations run under exactly the same set of configurations. We have termed the reference experiment (Case-1), and the idealized experiment (Case-2). Figures 4.3.1 and 4.3.2 show these two distinct scenarios.

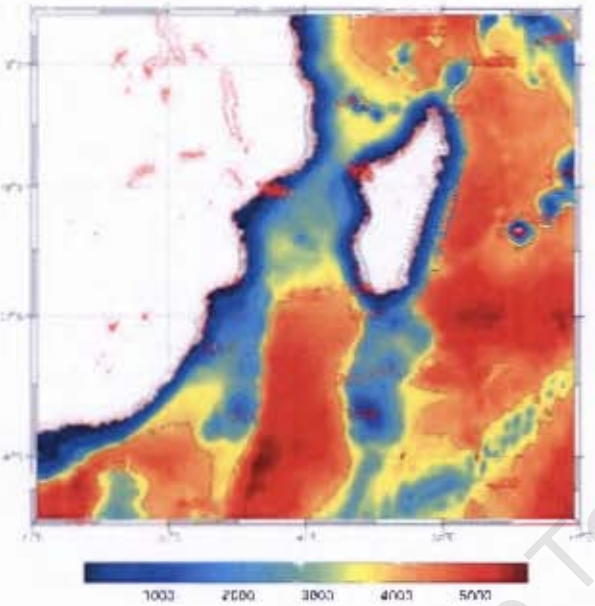

Figure 4.3.1 – ETOPO2 configuration of the South-West Indian Ocean [Case 1]. The colours represent the depths of the ocean with contours in meters.

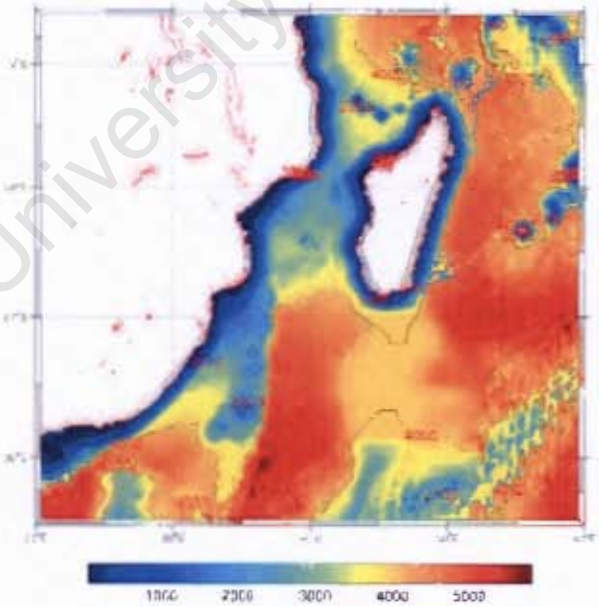

Figure 4.3.2 – ETOPO2 configuration with removal of the Madagascar Ridge [Case 2]. The colours represent the depths of the ocean with contours in meters

Another objective of this study was to verify if the movement of eddies coming from both the Mozambique Channel and south of Madagascar have preferred gateways through the transecting fractures of the Mozambique Ridge. Three such fractures were identified and termed gates as shown in figure 4.3.3 below. For this particular investigation a total of 60 eddies evident in the altimetry were tracked, being 20 cyclonic and 20 anti-cyclonic from south of Madagascar, and 20 anti-cyclonic eddies from the Mozambique Channel.

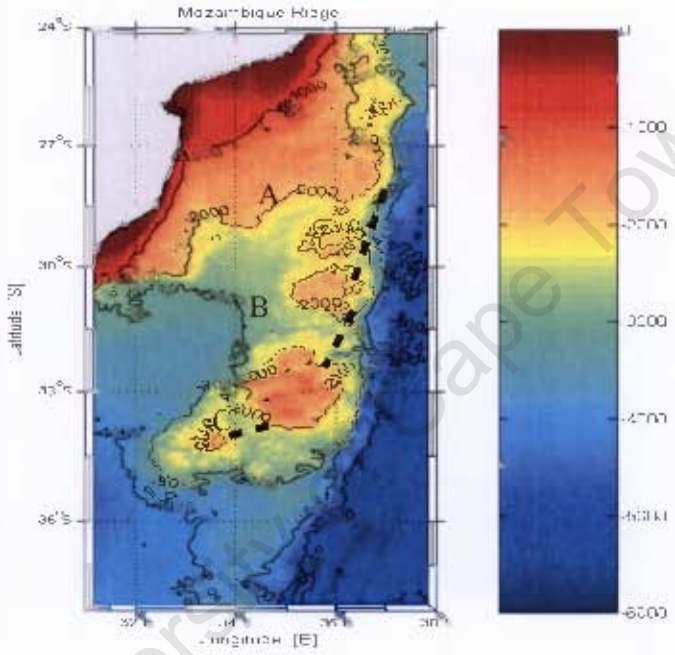

Figure 4.3.3 – The capital letters in the figure represents the main fractures transecting the Mozambique Ridge, termed gates A, B, and C. The colours represent the depths of the ocean in meters, and the black lines are the bathymetric contours in 1000 m intervals.

Fractures	Latitude [°S]	Longitude [°E]	Width [km]
Gate - A	28.5 – 30.9	36.2 – 36.4	270.2
Gate - B	31.0 – 32.5	35.7 – 35.9	166.9
Gate - C	33.3 – 34.2	33.8 – 34.7	128.7

Table 4.3 Summary of the estimated positions and widths of the gates of the Mozambique Ridge.

4.4 Tracking of altimetric eddies

To track eddies from the altimetric data, we have made a few assumptions: first, an eddy could be identified as having a negative height anomaly, greater than 0.1 m, and the anti-cyclonic eddies with a positive height anomaly, greater than + 0.1 m. Second, such features should have a life-time greater than 90 days (3 months). We have superimposed on these the distribution of horizontal components of the geostrophic velocities, to access the clockwise and anti-clockwise rotations of these eddies. A chronologic sequence of these images, animated in a move fashion, provided information related to the propagation of these eddies. Using capabilities of a MatLab function, termed (ginput), we have written a script, which allowed us to extract instantaneous information related to the eddy, such as: the height of the sea level anomalies, the intensity of the horizontal components of geostrophic velocities, its geographical positions (latitude/longitude), and the ocean depth at such a defined position. The depth was obtained by overlaying the bathymetric data on the image at 2 minute resolution, ETOPO2. Our designed script provides the information related at the eddy at each time that a click with the computer mouse is performed within the eddy domain. For each eddy, we have performed 5 clicks. One click in the core of the eddy, two clicks along the meridional direction, to the north and to the south of the core of the eddy. The last two clicks were made along the zonal direction, to the east and to the west of the core of the eddy. The instantaneous speed of the eddy was estimated as a mean of the velocities from every point along the zonal and meridional directions. We have tracked a total of 60 eddies: 20 anti-cyclonic eddies along the Mozambique Channel, 20 anti-cyclonic and 20 cyclonic eddies in the south of Madagascar.

An investigation of several two-dimensional (2-D) plots of the sea surface height (SSH) and eddy kinetic energy (EKE) profiles, both superimposed onto the depth of the seafloor topography has also been performed. Such an investigation allows one to visualize how the changes in both SSH and EKE at the surface of the eddy changes with the bathymetric configuration of the sea floor topography during the course of propagation of an eddy. The EKE was computed as a mean of every points at each time step, and the position of the eddy was determined also as a mean of all the latitude and longitude positions obtained during the extraction of the ''u'' and ''v'' components. The findings of the investigation are presented and discussed in the next chapter 5.

5 RESULTS AND DISCUSSION

5.1 The influence of the Madagascar Ridge on the circulation

This chapter presents and discusses the findings of the current study, which has been motivated by the aforementioned key research questions. Such questions were identified as gaps in the current knowledge about the mesoscale ocean circulation in the Mozambique Channel and south of the Madagascar.

The first key research question of this project is: How does the bathymetry, especially the shallow Madagascar Ridge, influence the propagation of eddies into the Agulhas Current. To address this, we have used an idealized model simulation which allowed us to remove the first upper 4000 m of the Madagascar Ridge. Based on such simulation, we have investigated mean states of the sea surface height (SSH) and its variability (i.e., mean square MS_SSH), mean surface currents (U) and their variability (i.e., eddy kinetic energy, EKE) from the eight years of simulation in order to compare with the reference run, in which no modification of the Madagascar Ridge was made. The results from these simulations are presented in [Figures 5.1.1 – 5.1.8].

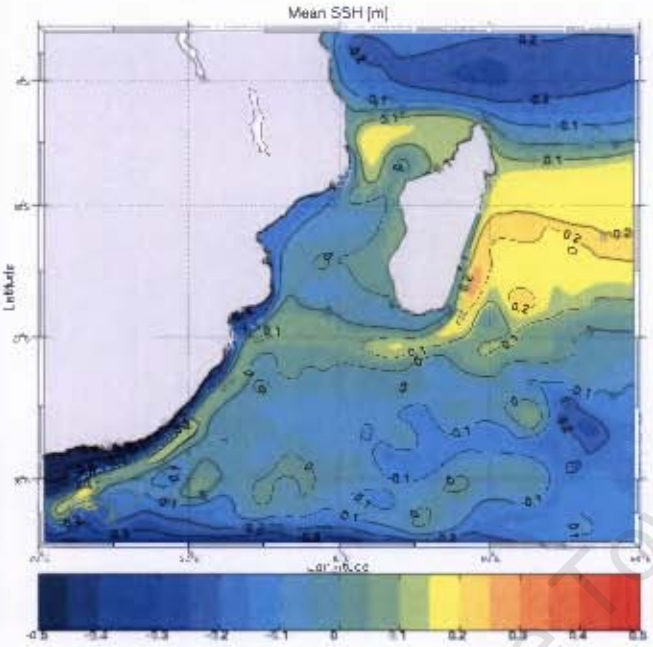

Figure 5.1.1 – Eight year mean of the sea surface height [m], for the simulation in which no modification of the bathymetry was made.

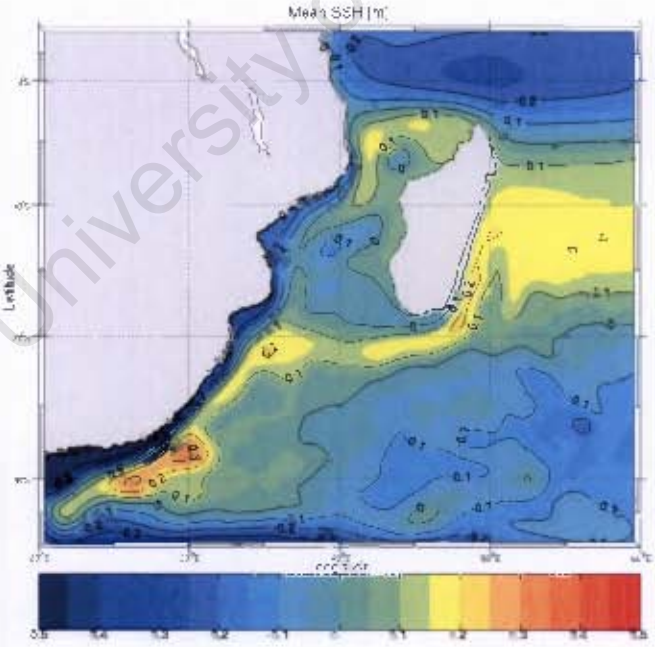

Figure 5.1.2 – Eight year mean of the sea surface height [m], for the simulation in which the upper 4000 [m] of the Madagascar Ridge has been removed.

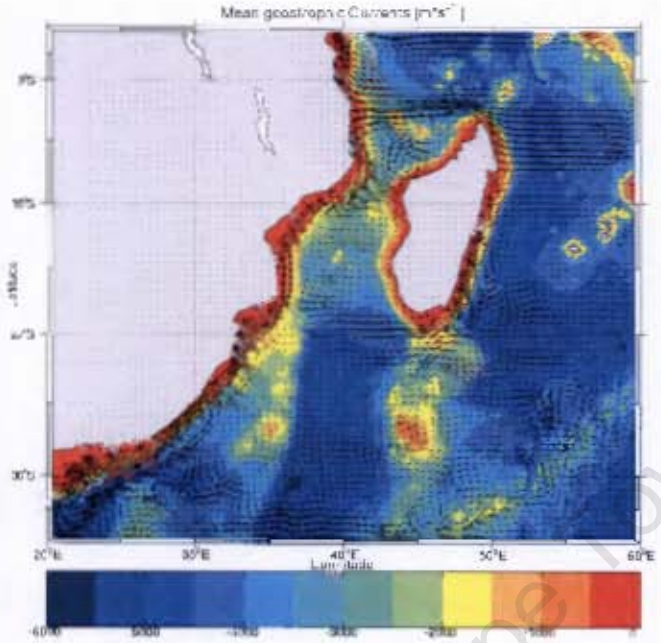

Figure 5.1.3 Eight year mean of geostrophic currents ms^{-1} at 100 [m] depth, for the simulation with no modification of the Madagascar Ridge. The colours represent the depth of the ocean in meters.

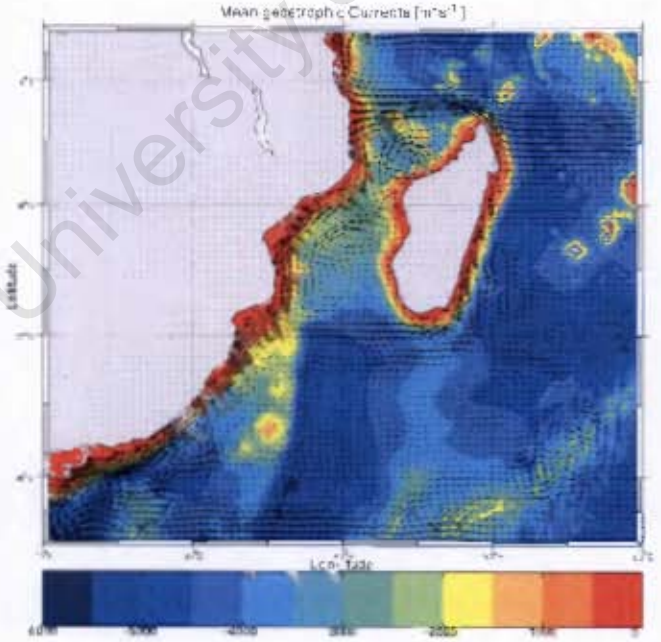

Figure 5.1.4 Eight year mean of geostrophic currents in ms^{-1} at 100 [m] depth, for the simulation in which the Madagascar Ridge has been removed. The colours represent the depth of the ocean in meters.

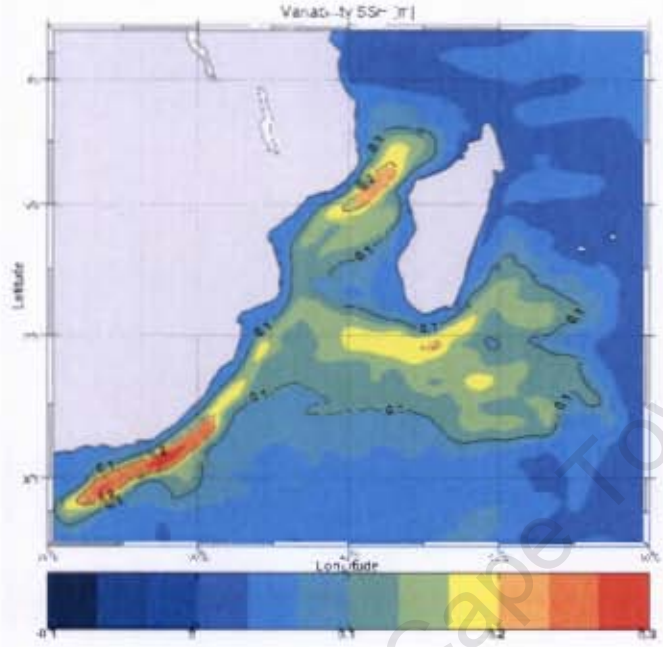

Figure 5.1.5 – MS of the SSH with contours in meters, for the model simulation with no modification of the Madagascar Ridge.

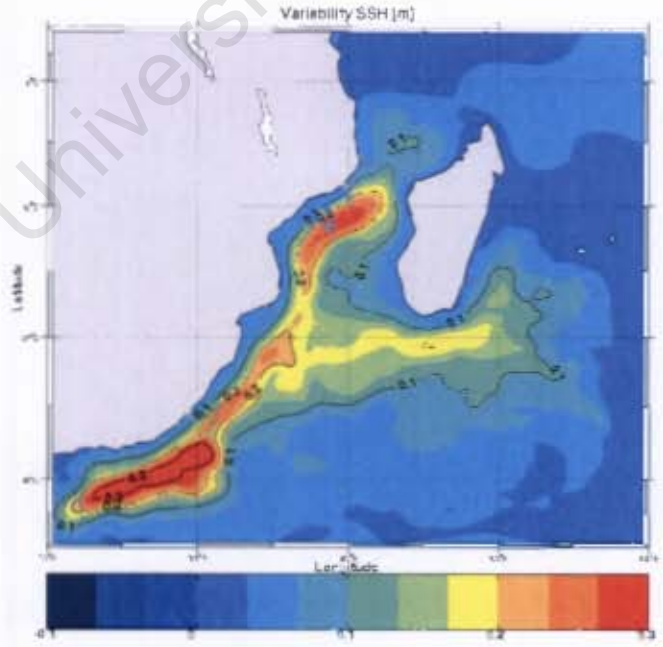

Figure 5.1.6 – MS of the SSH with contours in meters, for the simulation with no Madagascar Ridge.

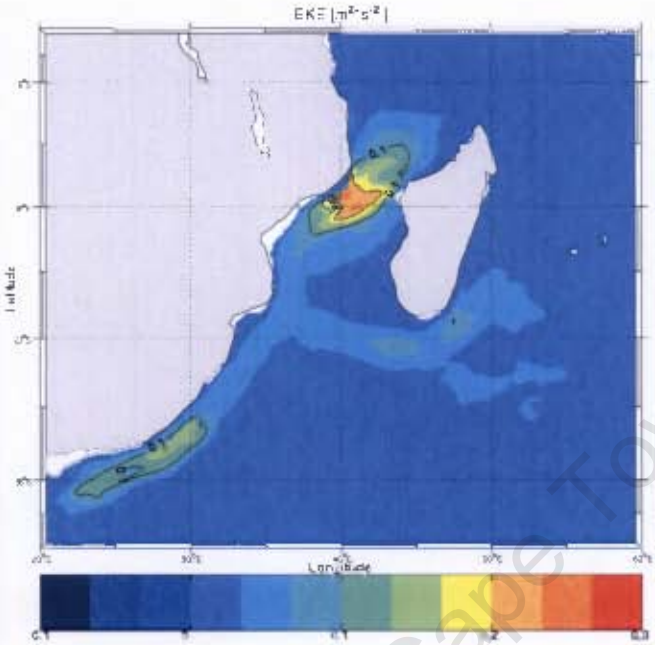

Figure 5.1.7 – Eddy kinetic energy at 100 [m] depth, with contours in m^2s^{-2} for the model simulation with Madagascar Ridge.

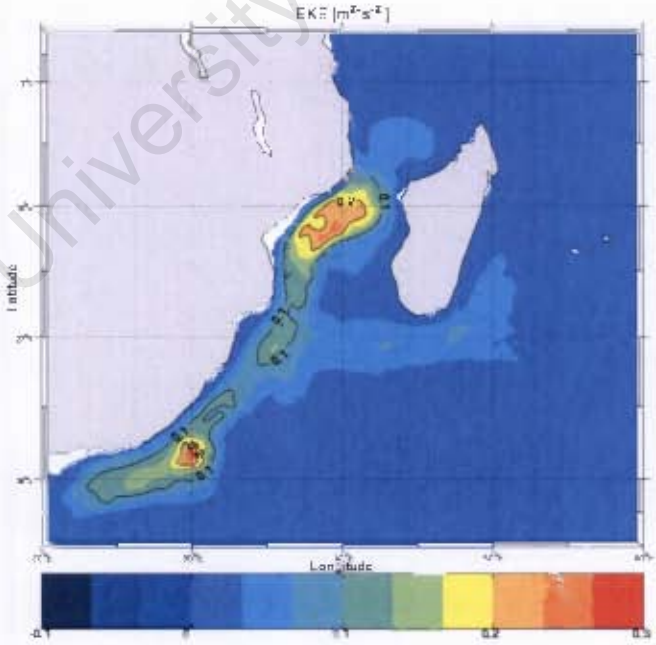

Figure 5.1.8 Eddy kinetic energy at 100 [m] depth, with contours in m^2s^{-2} for the model simulation without Madagascar Ridge.

Comparing the mean patterns of the sea surface height [SSH] and its variability [MS_SSH], the state of the surface currents [U] and the eddy kinetic energy [EKE] from both the simulations some distinctions and some similarities are evident. The simulation in which no modification of the bathymetry was made, is here termed the Reference simulation, and the simulation in which the Madagascar Ridge has been removed, the Idealized simulation.

Looking at the annual mean SSH [Figures 5.1.1- 5.1.2], we notice that at the northern boundary of the domain [i.e. to the north of the Madagascar and in the northern part of the Mozambique Channel], the northern part of the East Madagascar Current [NEMC] and its derived components after reaching the east African coast, all these components were not sensitive to the absence of the Madagascar Ridge [i.e., the mean SSH maintained the same profile in both the simulations] varying between -0.2 and 0.1 m ([Figures 5.1.1-5.1.2], 18 – 5°S, 40 - 60°E). The southern boundary of the domain also was insensible to the absence of the Madagascar Ridge. Here the mean SSH has remained similar in both experiments, ranging between -0.3 to -0.1m [38 – 40°S, 20 - 50°E]. In this domain the mean SSH is possibly related to the eastward flow of the Agulhas Return Current or the Subtropical Convergence that are driven by independent forcing that one would not expect to be influenced strongly by the flow over the Madagascar Ridge.

As a whole, the background mean circulation of the region in the both simulations is similar. Nevertheless, localized differences related to the absence of the Madagascar Ridge can be identified, evident in the distribution of the mean SSH [Figures 5.1.1 - 5.1.2]. For instance, a negative cell of SSH with -0.1 [m] has been observed in the Mozambique Channel [around 18-27°S] in the idealized simulation, and a strong gradient of SSH over the continental shelf compared to the simulation where the Madagascar Ridge had been removed [Figure 5.1.2]. To the east of Madagascar [around 27–18°S, 50-60°E] a weakened recirculation evident in the SSH [Figure 5.1.2] is observed. The SSH signals in this region are more likely related to the westward flow of the South Equatorial Current [SEC]. Along the east coast of Madagascar such signals may be associated with the southward flow of the East Madagascar Current [EMC]. The semi-permanent anti-cyclonic cell of 0.2 m in the SSH south-east of Madagascar [around 23-25°S, 51-53°E], and the cyclonic cell with -0.2 m SSH [at about 35°S and 55°E] that are evident in the reference simulation [Figure 5.1.1], completely vanished in the idealized simulation [Figure 5.1.2]. In the latter simulation, the mean SSH with 0.1 m isolines runs continuously from south of Madagascar, westerly along the 27°S, into the Agulhas Current region. In the reference simulation [Figure 5.1.1], by contrast, the 0.1 m isolines are not

continuous. Thus, the south-westerly link into the Agulhas Current is made by a mean SSH of 0 m isolines. Therefore these differences suggest that in the simulation in which the Madagascar Ridge has been removed [Figure 5.1.2] the volume of water crossing into the Agulhas Current region may be greater than in the reference simulation [Figure 5.1.1]. This may suggest that either an eastward flow, possibly associated with the retroflection of the EMC is limited in the idealized simulation, or that fewer eddies and more mean flow propagate into the Agulhas Current region. To the west [Figure 5.1.2], high mean SSH [at about 27°S, 35°E] is observed in the region of the Mozambique Ridge. At the south-eastern boundary, over the shelf adjacent to the Agulhas Current [at about 37°S, 30°E], the highest mean SSH is observed, reaching 0.3 m further downstream, close to the western boundary of the domain [Figure 5.1.2] which seems to increase the recirculation of the Agulhas Current.

Looking at the Eulerian distribution of the mean surface currents [Figures 5.1.3 and 5.1.4], one can also observe similarities and differences on the mesoscale circulation. The pathways and the nature of the currents to the north-east of Madagascar and to the north of Mozambique Channel remained largely similar [Figures 5.1.3 - 5.1.4]. Nevertheless changes such as the absence of the semi-permanent anti-cyclonic eddy mentioned above, as well as an anti-cyclonic eddy over the shallowest part of the Madagascar Ridge, and another possibly bathymetrically trapped eddy [at about 32°S, 53°E (Figure 5.1.3)] were absent on removal of the Madagascar Ridge [Figure 5.1.4]. In the reference run an anti-cyclonic eddy interacting with the offshore edge of the Agulhas Current [at about 36°S, 30°E] is observed to draw water from the current that then moves to the east [Figure 5.1.3]. In contrast to this idealized simulation, such an anti-cyclonic eddy maintains its anti-clockwise rotation without any water being drawn away to the east when the Madagascar Ridge has been removed [Figure 5.1.4]. These figures also show that there is less expression of the eastward flow south of Madagascar in the simulation in which the Madagascar Ridge has been removed.

Comparing the MS_SSH between [Figures 5.1.5 - 5.1.6 (that represents the flow variability)] one can observe a larger field of variability to the east of the Madagascar Ridge in the simulation with Madagascar [Figure 5.1.5]. When the Madagascar Ridge was removed [Figure 5.1.6], the field of variability was largely moved to the west of the ridge. Strong signals are observed reaching farther west to the region of the Mozambique Ridge, and along the path of the Agulhas Current. A substantial increase is observed at downstream regions of the Agulhas Current.

Both simulations shows that the regions with high values of EKE are concentrated in the Mozambique Channel and adjacent to the continental shelf of south-eastern Africa, along the path of the Agulhas Current, with the strongest signals manifested in the central Mozambique Channel, varying between $0.1 - 0.3\ m^2s^2$.

The mean surface currents from the simulation in which the Madagascar Ridge has been removed [Figure 5.1.4] shows a surprising feature in the mean circulation, located in the central part of the Mozambique Channel [about 23 – 18°S and 40°E]. The absence of the Madagascar Ridge generates a mean cyclonic circulation here which seems responsible for the strong signal of the MS of the SSH observed [Figure 5.1.6], and a low mean SSH [Figure 5.1.2]. For its geographical location [i.e., not being located in a direct downstream region of the Madagascar Ridge], one would not expect changes in the mean circulation here since it would seem far north of the ridge influence, and the dominant flow in the channel is south-westward. Besides that, farther north of this point, the incoming flow from the South Equatorial Current (which on reaching the east African coast at about 11°S splits and generates the southward flow through the Mozambique Channel) remained similar in both simulations. In fact this peculiar result has raised several questions such as the following:

- Are the eddies passing through the Mozambique Channel so variable that they do not affect the calculation of the mean state?

- Is the observed cyclonic feature in the channel and the western boundary current at the Mozambican shelf related to the absence of the Madagascar Ridge, although the ridge is not located upstream of the observed features?

- Does the inflow from the East Madagascar Current and from the South-East Indian Ocean moving into the Agulhas Current region when there is no Madagascar Ridge [Figure 5.1.2] strong enough to block and trap the eddies coming from the Mozambique Channel, forcing them to a cyclonic rotation?

Though these questions are based on the idealized simulation, a closer look at these is important to understand the hydrodynamics of the system. The questions require an answer if the role of Madagascar Ridge on the regional mesoscale circulation is to be fully understood. A proper analysis of other experiments would be needed to address these questions.

The above description of the simulations suggests that the absence of the Madagascar Ridge increases the variability of the mesoscale circulation in downstream regions of the Agulhas Current system and that it also affects the dynamics of the circulation to the south of Madagascar. Thus it raises some other pertinent questions such as: Why is the MS of SSH shifted to the west when the Madagascar Ridge is absent? And why is there an increase of the variability at downstream regions?

As it is already known from the available literature, hydrographic data and satellite observations have to date indicated that the nature of the flow to the south of the Madagascar is characterized by eddy shedding events due to the separation of the southern branch of the EMC from the continental shelf, generating a retroflection of the EMC, and due to the interaction between deep jet currents and Rossby waves from the East Indian Ocean with the topography of the Madagascar Ridge [Schouten et al., 2003].

Thus for the first question we may hypothesise that the large field of SSH variability to the east of the Madagascar Ridge in the reference simulation is a result of the combined effect of the separation of the EMC from the continental shelf and the interaction between currents from the east and Rossby wave features with the Madagascar Ridge which generates local eddies, as some studies already suggest.

Thus, the Madagascar Ridge may trap mesoscale circulation features at its eastside, delaying their propagation westward. In contrast, when the Madagascar Ridge is removed, such mesoscale features may be generated simply as a result of the separation of the EMC from the continental shelf, but not from the interaction between deep jets with the Madagascar Ridge.

For the second question we may explain the higher variability at downstream regions as a result of the absence of the Madagascar Ridge which opens up a free gate for the incoming flow, from the South and East Indian Ocean, allowing a considerable amount of water to have a direct link into the region of the Agulhas Current system. The mesoscale circulating features may cross faster to the west, reaching the African coast. Here eddies interact with the Mozambique Ridge, increasing also the variability [Figure 5.1.6].

5.2 The pathways of eddies through the Mozambique Ridge

To approach the second research question one has to track the pathways of propagation of eddies in the region. This is not the first time that eddies in the Mozambique Channel and South of Madagascar have been tracked. Altimetry studies [De Ruijter et al., 2004] as well as hydrographic measurements [Schouten et al., 2003] and modelling studies [Quartly and Srokosz, 2004] have shown that cyclonic eddies propagate in a southward direction and anti-cyclonic eddies are predominantly propagating in a south-westwards direction.

Here we concentrate on establishing whether eddies formed in both the Mozambique Channel and south of Madagascar move through the gaps or fractures of the Mozambique Ridge [Figure 2.2]. Such information is important to understand better the role of mesoscale eddies on the path and behaviour of the Agulhas Current, such as its temporary absence from the shelf slope by the formation of a Natal Pulse. Occasionally a Natal Pulse is triggered [Schouten et al., 2002a] by the interaction of anti-cyclonic eddies from both the Mozambique Channel and cyclonic and anti-cyclonic eddies from south of Madagascar with the Agulhas Current. This happens only at the Natal Bight. Different pathways of propagation of these eddies through the fractures of the Mozambique Ridge may lead to different points of interaction between such eddies and the Agulhas Current and thus triggering of a Natal Pulse or not. Therefore to establish whether these eddies have such preferred routes three fractures were identified and termed gate-A, gate-B, and gate-C [Figure 4.3.3]. Sixty eddies over a period of ten years were tracked by altimetry. From this collection, twenty anti-cyclonic eddies [red dots] moved the full length of the Mozambique Channel; twenty cyclonic [blue dots] and twenty anti-cyclonic eddies [red dots] moved westward from south of Madagascar [Figure 5.2].

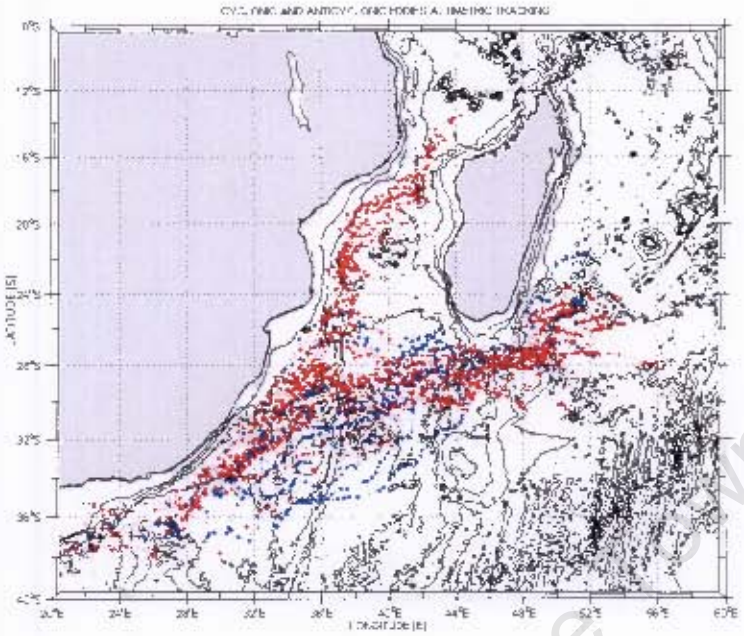

Figure 5.2 – An altimetric tracking of 20 anti-cyclonic eddies [red dots] from Mozambique Channel; 20 cyclonic [blue dots] and 20 anti-cyclonic eddies [red dots] from south of Madagascar. The thin black lines give the bathymetric contours in 1000 m intervals.

An investigation of all the anti-cyclonic eddies coming from the Mozambique Channel shows that none of them passed through the gates of the Mozambique Ridge. Some of these eddies disintegrated at the ridge, possible due to bathymetric interaction, and some were able to survive such interaction. These ones moved poleward into the Agulhas Current region. A study of the anti-cyclonic eddies coming from the south of Madagascar shows that eighteen out of twenty anti-cyclonic eddies survived crossing both the Madagascar and the Mozambique Ridge. The remaining two eddies did not survive. Out of the remaining eighteen, seven [39%] crossed the Mozambique Ridge without passing through the gates, and eleven [61%] passed through gate-A. This suggests a clear preference for these anti-cyclonic eddies to pass through this gate.

Studying the twenty cyclonic eddies coming from the south of Madagascar have shown that thirteen of them [65%] survived crossing both the Madagascar and the Mozambique Ridges. Out of these thirteen, six [46%] crossed the Mozambique Ridge without passing through the gates, and the remaining seven [54%] did pass through the gates. Out of these seven, two went through the gate-A, four went through the gate-B, and 1 went through the gate-C [Table 5.2].

Fractures	Cyclonic eddies	Anti-cyclonic eddies
Gate - A	2	11
Gate - B	4	5
Gate - C	1	4

Table 5.2 – Summary of the altimetrically identified eddies which went through the fractures of the Mozambique Ridge. The position of the gates can be observed in Figure 4.3.3 and Table 4.3

The results of this investigation suggest that anti-cyclonic eddies are more resistant to possible bathymetric interaction than cyclonic eddies. They also have a higher tendency of moving through the gates of the Mozambique Ridge; especially through gate-A, the northernmost fracture of the ridge. Such a tendency could possibly be related to conservation of the angular momentum.

The track of the cyclonic eddies are more south-westward oriented than those of anti-cyclonic eddies. By the conservation of angular momentum on their clockwise rotation, during the course of propagation, these eddies drift to follow through gate-B of the ridge.

Another way to look at the dynamics of the eddy variability is to look at changes in their expression of EKE. We also investigated how such variability might be related to the topographic features of the sea floor bathymetry.

5.3 The variation of the EKE relative to the bottom topography

A series of 2-dimensional plots of the sea surface height of the eddies that crossed bathymetric features combined with the depth of the sea floor topography in the Mozambique Channel and south of Madagascar were used to give answer to the third research question of this study: how does the kinetic energy of these eddies change during the course of their propagation?

We first have started to investigate the relationship between the profiles of the sea surface height and eddy kinetic energy relative to the bottom topography along the pathways of anti-cyclonic eddies moving in the Mozambique Channel. Thereafter, a similar analysis was performed on cyclonic and anti-cyclonic eddies moving from the south of Madagascar into the Agulhas Current region. The results of these investigations are presented below.

5.3.1 EKE of anti-cyclonic in the Mozambique Channel

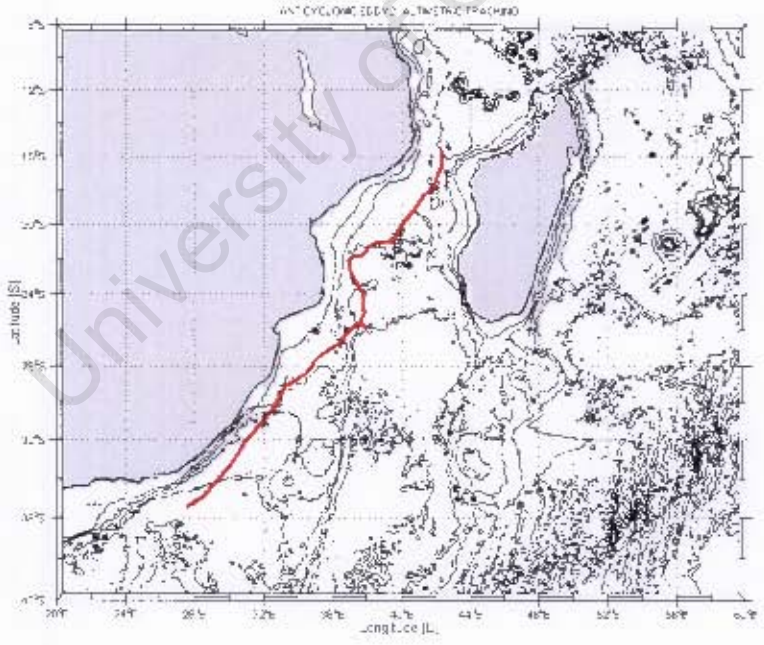

Figure 5.3.1 Track of anti-cyclonic eddy2. The red line represents the pathway and the black lines are the bathymetric contours in 1000 m intervals.

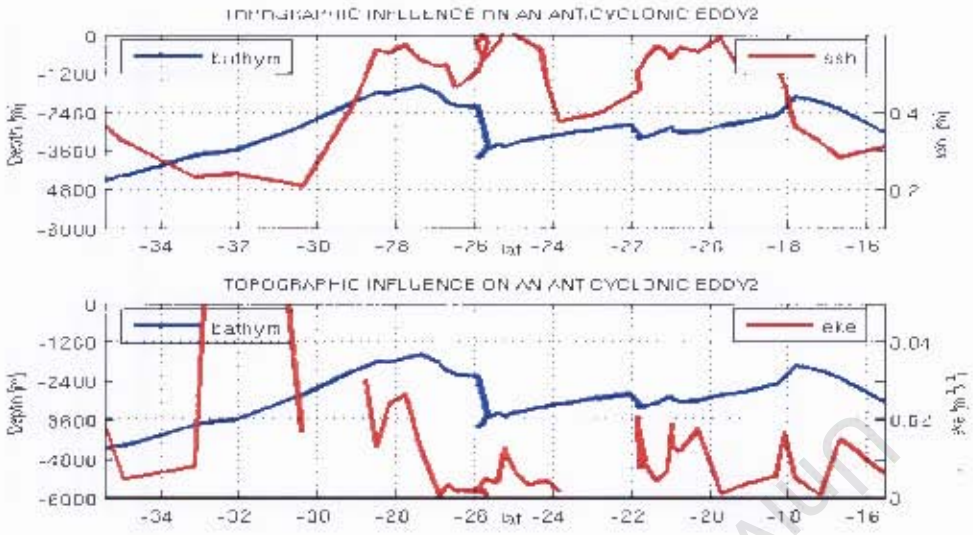

Figure 5.3.1.1 – The upper panel shows the changes in sea surface height [red line] with the bathymetry [blue line] and the lower panel shows the change of the eddy kinetic energy with the bathymetry during the course of propagation of anti-cyclonic eddy2.

The anti-cyclonic eddy2 was first identified in the central part of the Mozambique Channel around 16°S and 42°E on 2 December 1992, and survived for about 10 months. The eddy crossed the full length of the Mozambique Channel southward to the region of the Agulhas Current - in a south-westward direction - and dissipated on 13 October 1993 in the Natal Valley [Figure 5.3.1]. At about 22°S the eddy seems to have followed the 3000 m isobath. After crossing 24°S the eddy drifted back to the shore and travelled parallel to the eastern edge of the Agulhas Current, and its signal was lost at nearly 36°S.

The variations of the sea surface height [SSH] and eddy kinetic energy [EKE] signals with the profile of the bottom topography during the course of its propagation are shown by the curves in Figure 5.3.1.1.

The general profile of the bottom topography [blue line] along the course of propagation of the anti-cyclonic eddy2 shows an increasing depth southward. The SSH of eddy2 is highest over the shallowest part of the bathymetry and the EKE has a peak far to the south [32°S] that seems unrelated to the bottom topography. The discontinuous signal observed is due to the coastal resolution problem the satellite experiences when it tries to capture the horizontal velocities [u, v] when the eddy moved close inshore in the channel between 22 - 24°S and in the Natal Valley between 29 – 30.5°S.

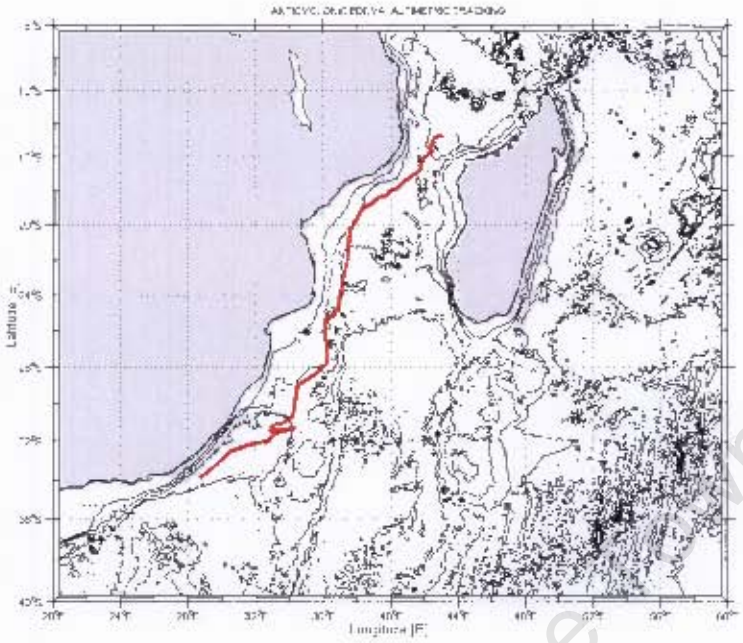

Figure 5.3.1.2 – Track of anti-cyclonic eddy4. The red line represents the pathway and the black lines are the bathymetric contours in 1000 m intervals.

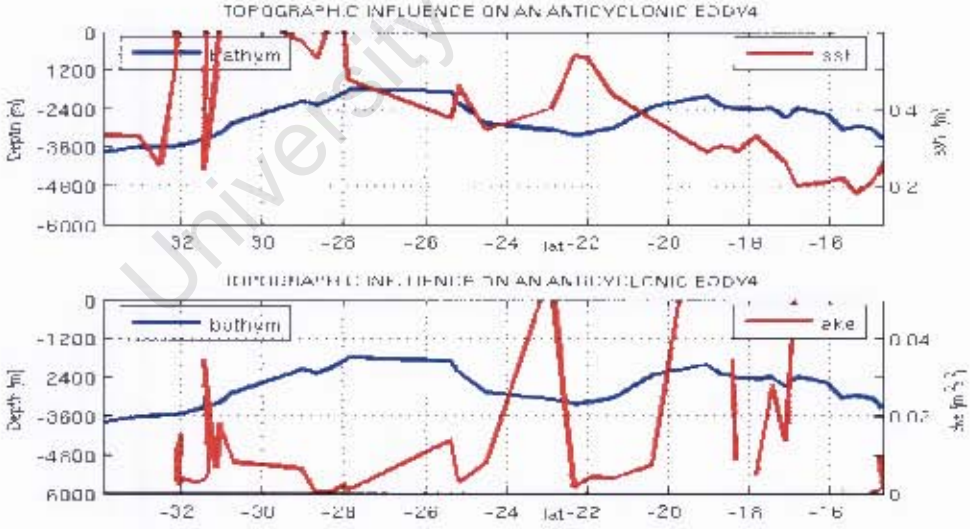

Figure 5.3.1.2.1 – The upper panel shows the changes of sea surface height [red line] with the bathymetry [blue line] and the lower panel shows the change of the eddy kinetic energy with the bathymetry during the course of propagation of anti-cyclonic eddy4.

The anti-cyclonic eddy4 was first identified in the central part of the Mozambique Channel on 28 July 1993 and maintained its integrity for about a year. The eddy crossed the full length of

the Mozambique Channel moved southward into the Agulhas Current region and dissipated on 8 August 1993 in the Natal Valley [Figure 5.3.1.2.2].

The sea surface height [SSH] of anti-cyclonic eddy4 is higher over the deepest parts of the bathymetry and lowest over the northernmost part of the topography to the north [18°S]. The full trend variation of the SSH indicates a southwards increase that seems inversely related to the bottom topography. The highest peak of the eddy kinetic energy [EKE] is observed to the north [24°S] than in its south part. Its full trend indicates a profile that seems unrelated to the bottom topography [Figure 5.3.1.2.1].

Next we present the variation of the eddy kinetic energy of the anti-cyclonic eddies which was corresponded least to the bathymetry during the course of propagation, coming from the region south of Madagascar.

5.3.2 EKE of anti-cyclonic eddies in the south of Madagascar

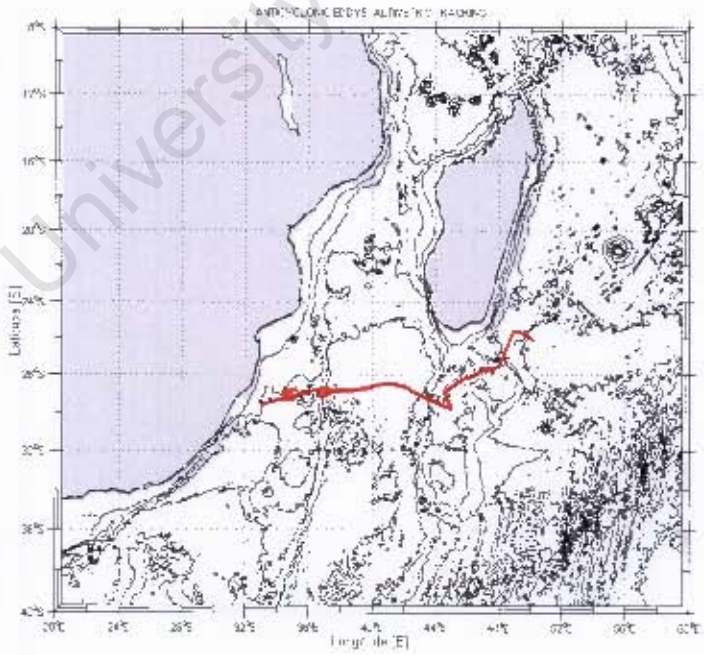

Figure 5.3.2.1 Track of anti-cyclonic eddy5. The red line represents the pathway and the black lines are the bathymetric contours in 1000 m intervals.

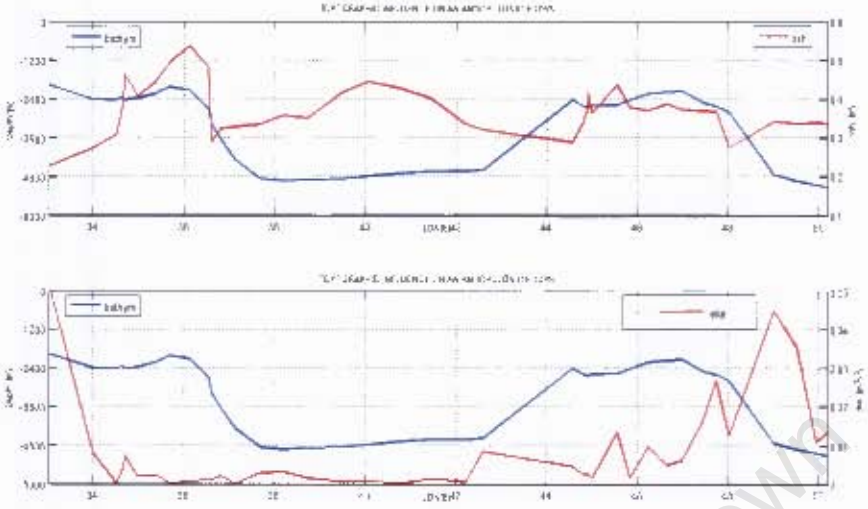

Figure 5.3.2.2 The upper panel shows the variation of the sea surface height profile [red line], and lower panel shows the variation of the eddy kinetic energy profile [red line], with the bathymetric profile [blue line] on both panels during the course of propagation of anti-cyclonic eddy5.

The anti-cyclonic eddy5 was first identified to the east of the Madagascar Ridge on 22 June 1994 and remained intact for about 13 months. The eddy crossed the Madagascar Ridge and the parallel 28°S in a south-westwards direction and then moved westwards along the full width of the Mozambique Basin, and passed through gate-A. After passing the gate it is dissipated in the Natal Valley [Figure 5.3.2.1] on 27 July 1995. The variation of its sea surface height [SSH] and eddy kinetic energy [EKE] with the bottom topography during the propagation is shown in the Figure 5.3.2.2.

The SSH of anti-cyclonic eddy5 was highest over the Mozambique Ridge up to 36°E. Higher values of SSH are also observed over the Madagascar Ridge at about 45°E and in the Mozambique Basin at 40°E [Figure 5.3.2.2]. The lowest value of SSH is observed far to the west 34°E. The full trend suggests an increasing profile that seems unrelated to the profile of the bathymetry. The EKE of the eddy is highest where the SSH is lowest and a higher value is observed to the east of the Madagascar Ridge between 48-50°E [Figure5.3.2.2]. The full trend of the EKE shows a decrease that seems inversely related to the bottom topography just to the east of 42°E.

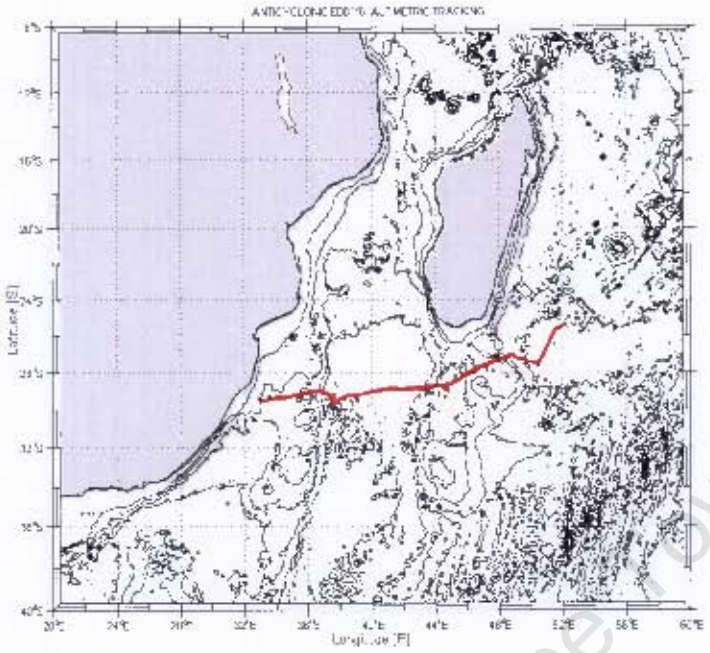

Figure 5.3.2.3 – Track of anti-cyclonic eddy6. The red line represents the pathway and the black lines are the bathymetric contours in 1000 m intervals.

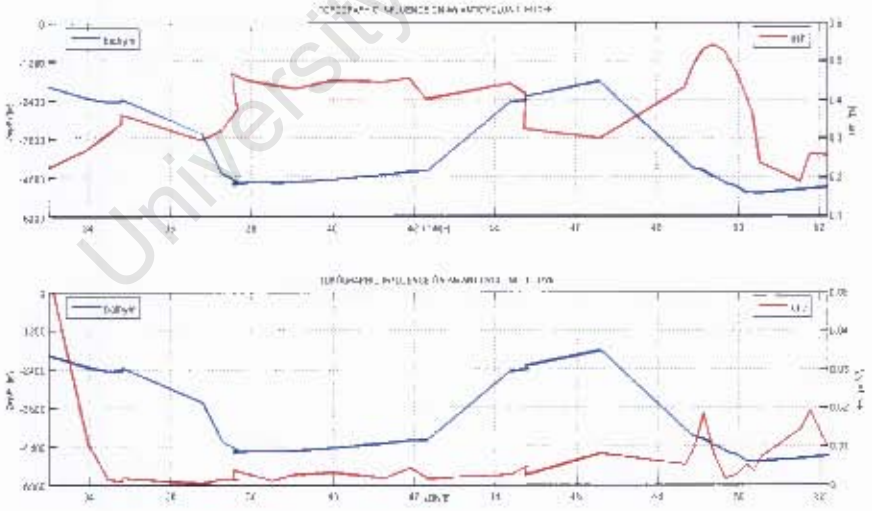

Figure 5.3.2.4 – The upper panel shows the variation of the sea surface height profile [red line], and the lower panel shows the variation of the eddy kinetic energy profile [red line], with the bathymetric profile [blue line] on both panels during the course of propagation of anti-cyclonic eddy6.

The anti-cyclonic eddy6 was observed to the south-east side of Madagascar, in the Madagascar Basin around 52°E on 23 November 1994 and was evident for about 8 months. This eddy crossed the Madagascar Ridge and parallel 28°S in a south-westward direction crossing the Mozambique Basin and passing through the gate-A in the Mozambique Ridge. It dissipated at the 2000 m isobaths around 30°S in the Natal Valley on 12 July 1995 [Figure 5.3.2.3].

The variation of the sea surface height [SSH] (red line on the upper panel) and eddy kinetic energy [EKE] (red line on the lower panel) of anti-cyclonic eddy6 with the bottom topography are shown above [Figure 5.3.2.4]. The SSH is highest around 50°E. Its profile is lower over both the Madagascar and the Mozambique Ridges. The full trend variation suggests a westwards decreasing profile that seems inversely related to the bathymetry.

The EKE is considerably low, except to the far west 34°E where a peak has been observed [Figure 5.3.2.4]. Even though its full trend suggests a westwards decreasing profile that seems unrelated to the bottom topography.

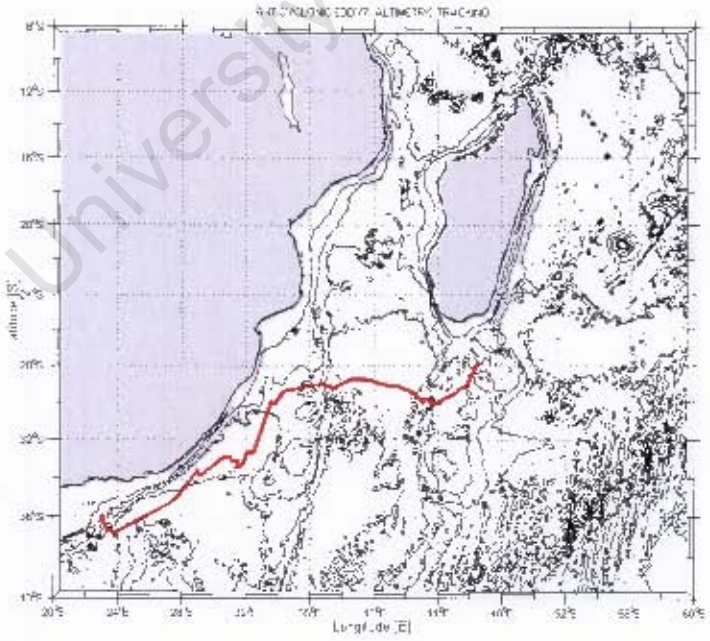

Figure 5.3.2.5 – Track of anti-cyclonic eddy7. The red line represents the pathway and the black lines are the bathymetric contours in 1000 m intervals.

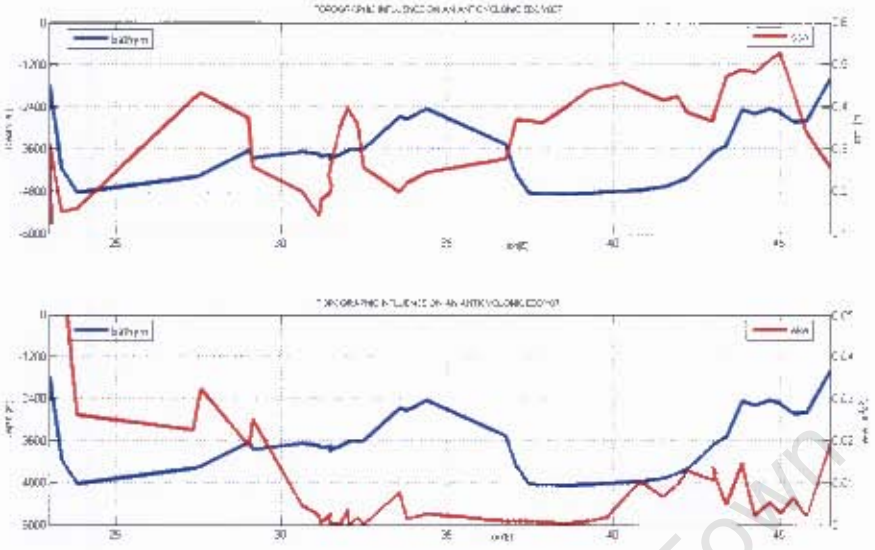

Figure 5.3.2.6 The upper panel shows the variation of the sea surface height profile [red line] and the lower panel shows the variation of the eddy kinetic energy profile [red line], with the bathymetric profile [blue line] on both panels during the course of propagation of anti-cyclonic eddy7.

The anti-cyclonic eddy7 was first identified over the Madagascar Ridge, south of parallel 28°S on 10 May 1995 and continued for about 11 months. Over the ridge the eddy moved south-westwards and it crossed the Mozambique Basin more likely to a north-westwards passing through gate-A of the Mozambique Ridge. Subsequently the eddy moved south-westwards and it dissipated to the east of the Agulhas Bank [Figure 5.3.2.6] on 20 March 1996. The direction of propagation of the anti-cyclonic eddy7 changed considerably from a westward to south-westward after passing the Mozambique Ridge [Figure 5.3.2.5]. Such change seems to be related to the effects of the bathymetry.

The sea surface height [SSH] of anti-cyclonic eddy7 was highest over the Madagascar Ridge 45°E and decreased westwards as it moved downstream into the Agulhas Current region, with a profile that seems to be inversely related to the bottom topography. The eddy kinetic energy [EKE] decreased westwards from 45°E to the east of 35°E. After passing 35°E the EKE increased significantly reaching highest values far west of 30°E [Figure 5.3.2.5].

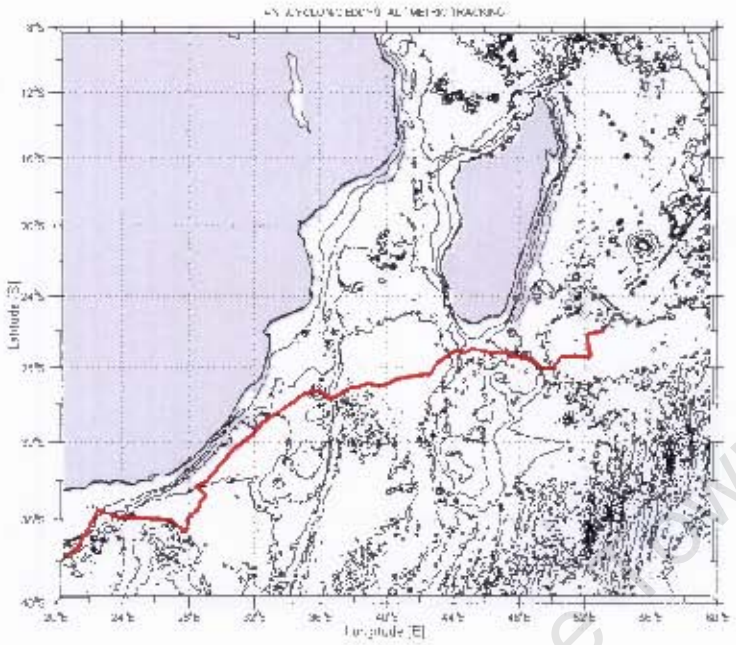

Figure 5.3.2.7 Track of anti-cyclonic eddy9. The red line represents the pathway and the black lines are the bathymetric contours in 1000 m intervals.

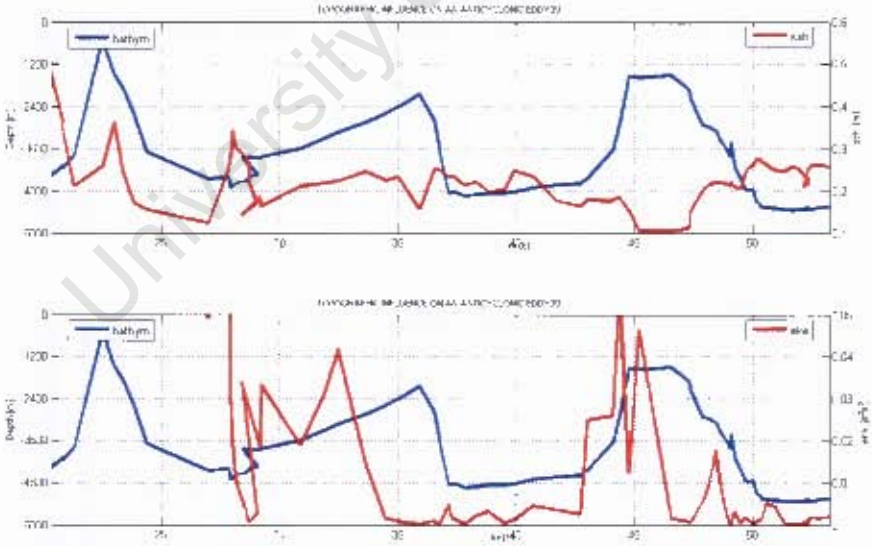

Figure 5.3.2.8 – The upper panel shows the variation of the sea surface height [red line] and the lower panel shows the variation of the eddy kinetic energy [red line] with the bathymetric profile [blue line] on both panels during the course of propagation of anti-cyclonic eddy9.

The anti-cyclonic eddy9 was identified far south-east of Madagascar, in the deepest part of the Madagascar Basin, on 13 September 1995 and could be followed for about 18.5 months. The eddy crossed the Madagascar Ridge north of 28°S in a north-westward direction. After crossing the ridge it moved south-westwards, passing through the gate-A of the Mozambique Ridge, and went out of the domain of study, west of 20°E [Figure 5.3.2.7] on 26 March 1997.

The sea surface height [SSH] of anti-cyclonic eddy9 was lowest over the Madagascar Ridge between 45 – 48°E, and highest far west to 25 E. From the point where the eddy was first identified around 53°E, it moved with its SSH inversely related to the bathymetry until 35°E. After that the variation of the SSH seemed related to the bottom topography, except around 20°E. The eddy kinetic energy [EKE] is highest over both the Madagascar and the Mozambique Ridge, the profile is likely to be related to the bottom topography [Figure 5.3.2.8].

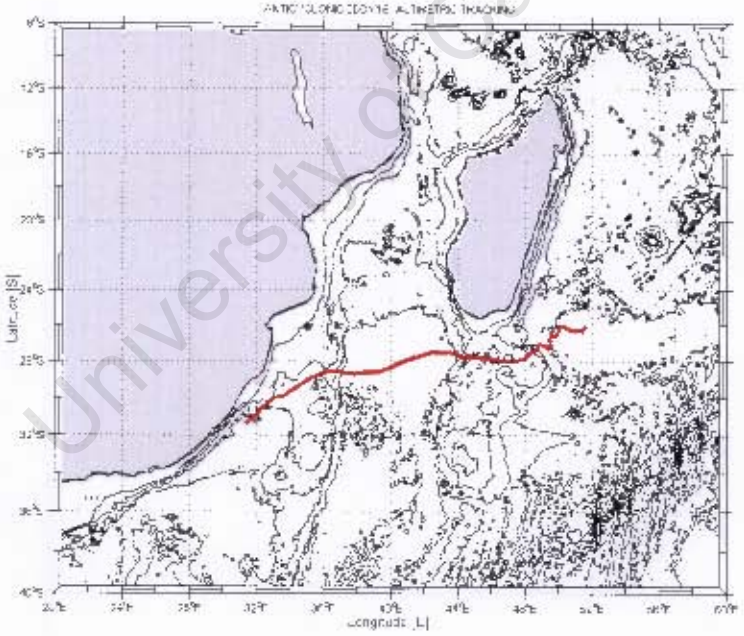

Figure 5.3.2.9 – Track of anti-cyclonic eddy16. The red line represents the pathway and the black lines are the bathymetric contours in 1000 m intervals.

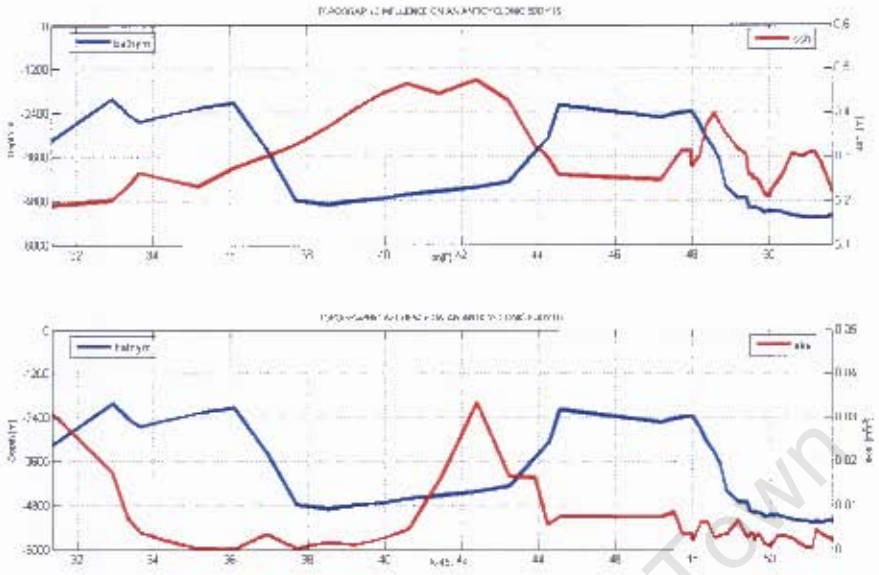

Figure 5.3.2.10 – The upper panel shows the variation of the sea surface height [red line] and the lower panel shows the variation of the eddy kinetic energy [red line] with the bathymetric profile [blue line] on both panels during the course of propagation of anti-cyclonic eddy16.

Anti-cyclonic eddy16 was first identified south-east of Madagascar, in the Madagascar Basin, on 26 August 1998 and remained evident for about a year. The eddy crossed the Madagascar Ridge at about 28°S in a westward direction and moved along the full width of the Mozambique Basin in a south-westward direction. This eddy passed through gate-A of the Mozambique Ridge and disappeared on 11 August 1999 in the Natal Valley [Figure 5.3.2.9].

The sea surface height [SSH] of anti-cyclonic eddy16 was highest in the Mozambique Basin between 40 - 43°E and its profile seems roughly inversely related to the bottom topography. The eddy kinetic energy [EKE] increased westwards to 42°E, and after this point it decreased reaching lowest values over the Mozambique Ridge [34 -38 E]. After passing 34°E, it's EKE has increased rapidly. The trend of the EKE seems totally unrelated to the bathymetry [Figure 5.3.2.10].

5.3.3 EKE of cyclonic eddies south of Madagascar

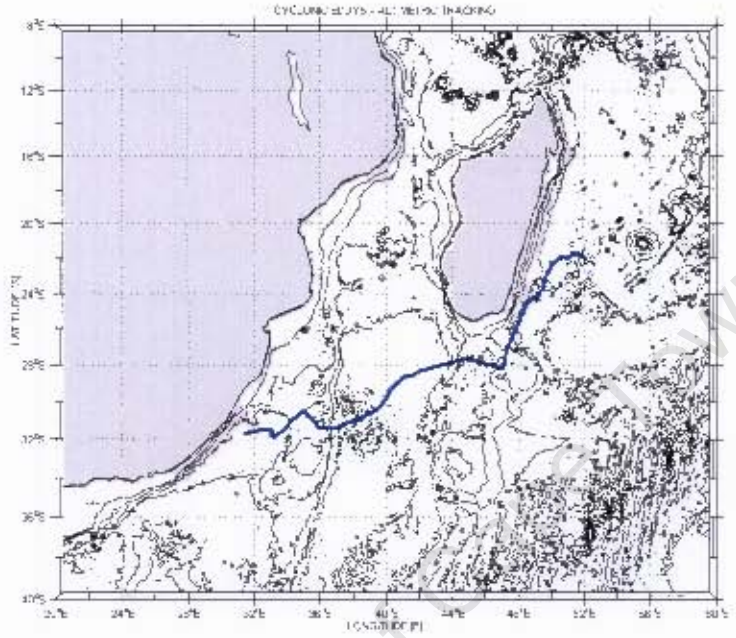

Figure 5.3.3.1 – Track of cyclonic eddy5. The blue line represents the pathway and the black lines are the bathymetric contours in 1000 m intervals.

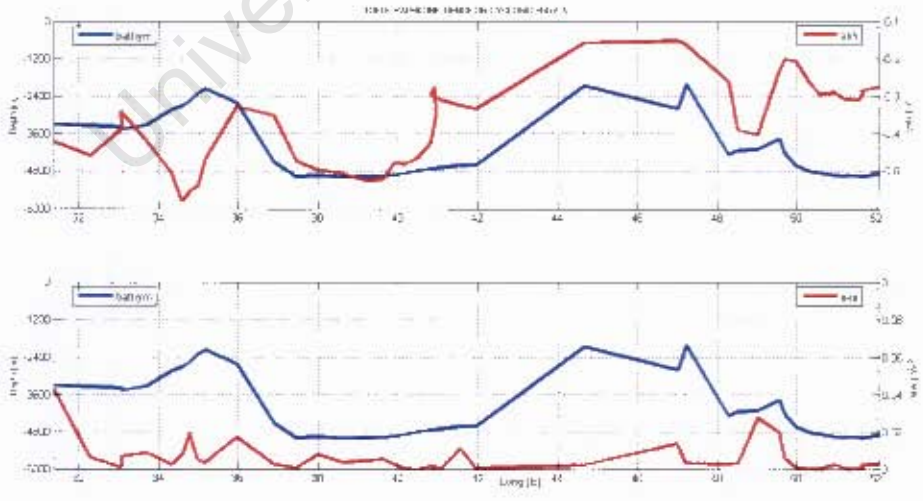

Figure 5.3.3.2 – The upper panel shows the variation of the sea surface height [red line] and the lower panel shows the variation of the eddy kinetic energy profile [red line], with the bathymetric profile [blue line] on both panels during the course of propagation of cyclonic eddy5.

Cyclonic eddy5 was first identified to the east of Madagascar, between the Madagascar main land and Mauritius, at about 52°E and 22°S [Figure 5.3.3.1], on 6 October 1993. The eddy at first moved southwards along the 4000 m isobaths parallel to the east coast of Madagascar, and on reaching 28°S over the Madagascar Ridge the eddy changed its direction, moving westwards. After crossing the Madagascar Ridge it moved south-westwards and passed through gate-B of the Mozambique Ridge, and dissipated in the Natal Valley around 32°S and 32°E.

The sea surface height [SSH] of cyclonic eddy5 was highest over the Madagascar Ridge and lowest over the Mozambique Ridge. The full trend of the SSH shows a decreasing south-westward profile that seems related to the bathymetry. Its eddy kinetic energy [EKE] seems inversely related to the bottom topography [Figure 5.3.3.2]. The full trend of the EKE shows an unclear pattern of variability.

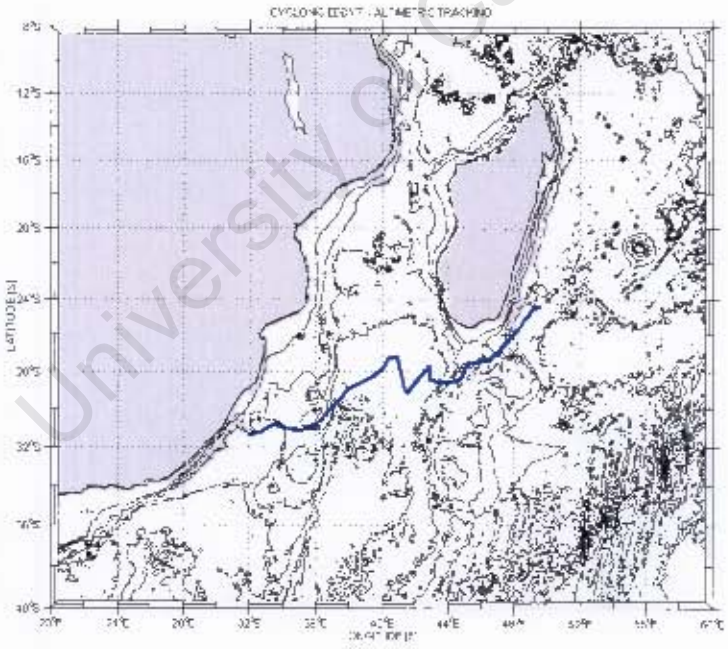

Figure 5.3.3.3 – Track of cyclonic eddy7. The blue line represents the pathway and the black lines are the bathymetric contours in 1000 m intervals.

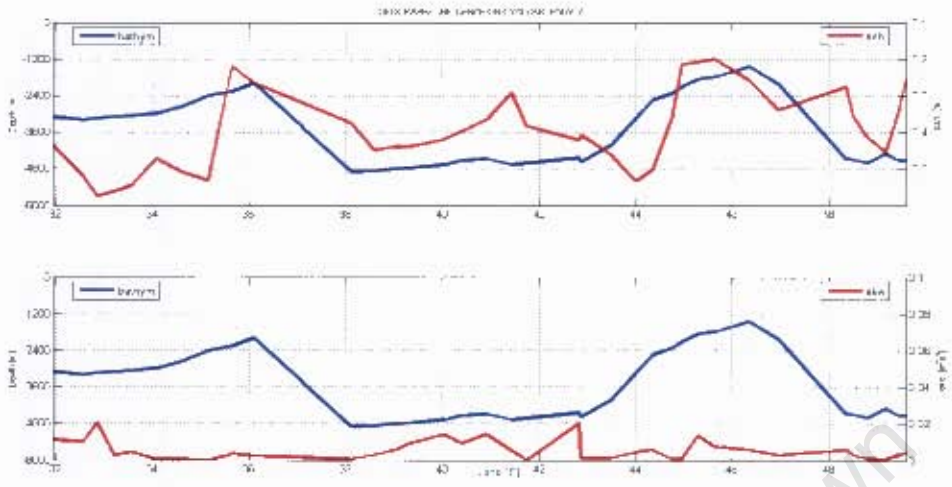

Figure 5.3.3.4 – The upper panel shows the variation of the sea surface height [red line] and the lower panel shows the variation of the eddy kinetic energy [red line] with the bathymetric profile [blue line] on both panels during the course of propagation of cyclonic eddy7.

Cyclonic eddy7 was identified to the south-east of the Madagascar on 01 December 1993 and remained evident in the altimetric signal for about 7.5 months. The eddy moved south-westwards passing through gate-B of the Mozambique Ridge, and dissipated in the Natal Valley [Figure 5.3.3.3] on 15 June 1994.

The sea surface height [SSH] of cyclonic eddy7 was highest over the shallower parts of the bathymetry, the Madagascar [44 – 48 E] and the Mozambique Ridges [35 – 37°E], which therefore seems directly related to the bottom topography. The full trend profile of the SSH is not clear. Its eddy kinetic energy [EKE] became lower during the full course of propagation and seems unrelated to the bathymetry [Figure 5.3.3.4].

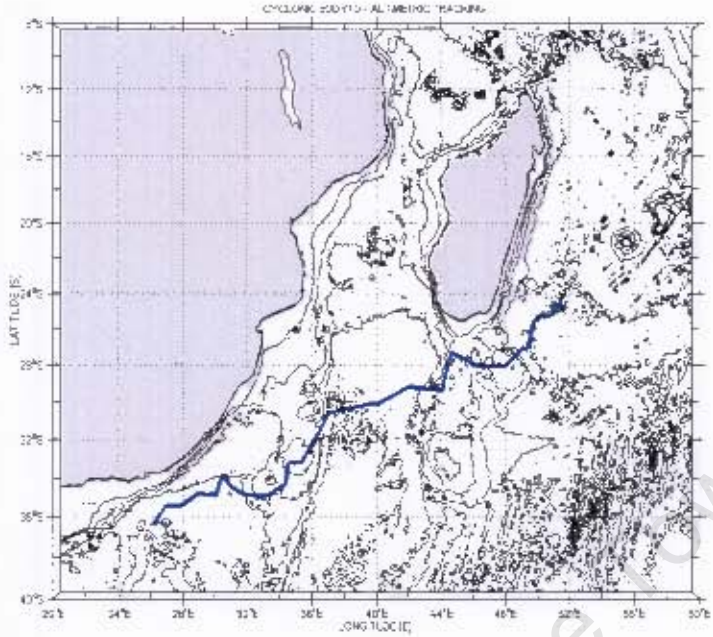

Figure 5.3.3.5 – Track of cyclonic eddy10. The blue line represents the pathway and the black lines are the bathymetric contours in 1000 m intervals.

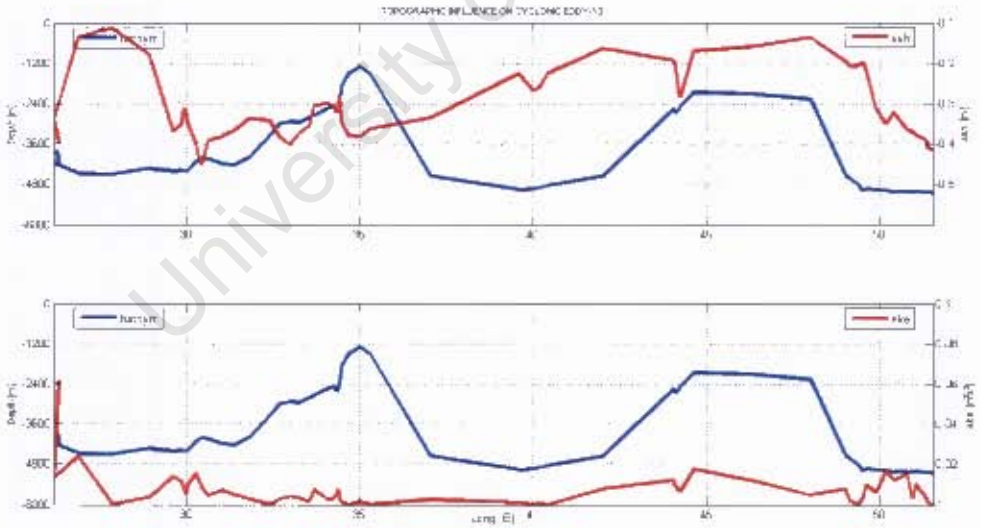

Figure 5.3.3.6 – The upper panel shows the variation of the sea surface height [red line] and the lower panel shows the variation of the eddy kinetic energy [red line] with the bathymetric profile [blue line] on both panels during the course of propagation of cyclonic eddy10.

Cyclonic eddy10 was identified to the south-east of Madagascar, in the Madagascar Basin at about 52°E and 24 °S on 23 August 1995, and could be identified for about 9 months. The pathway shows that cyclonic eddy10 moved south-westwards, crossing over both the

Madagascar and the Mozambique Ridges, and dissipated in the Natal Valley on 15 May 1996. The pathway has a westward direction over the Madagascar Ridge and a south-westward direction over the Madagascar Ridge [Figure 5.3.3.5]. The sea surface height [SSH] of cyclonic eddy10 was highest over the Madagascar Ridge [45 – 50°E] and far west to 30°E in the Natal Valley. The full trend of SSH variation decreased westwards to about 37°E over the eastern slope of the Mozambique Ridge. After this point an increase in the SSH is observed up to the end of the profile. The eddy kinetic energy has a lower variation and seems unrelated to the bottom topography, and its profile relative to the increasing and decreasing trend is unclear [Figure 5.3.3.6].

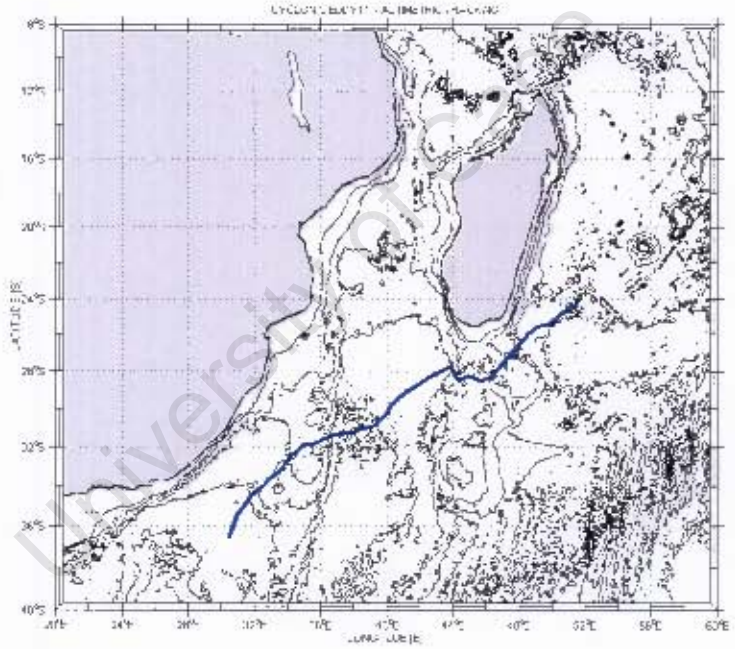

Figure 5.3.3.7 Track of cyclonic eddy11. The blue line represents the pathway and the black lines are the bathymetric contours in 1000 m intervals.

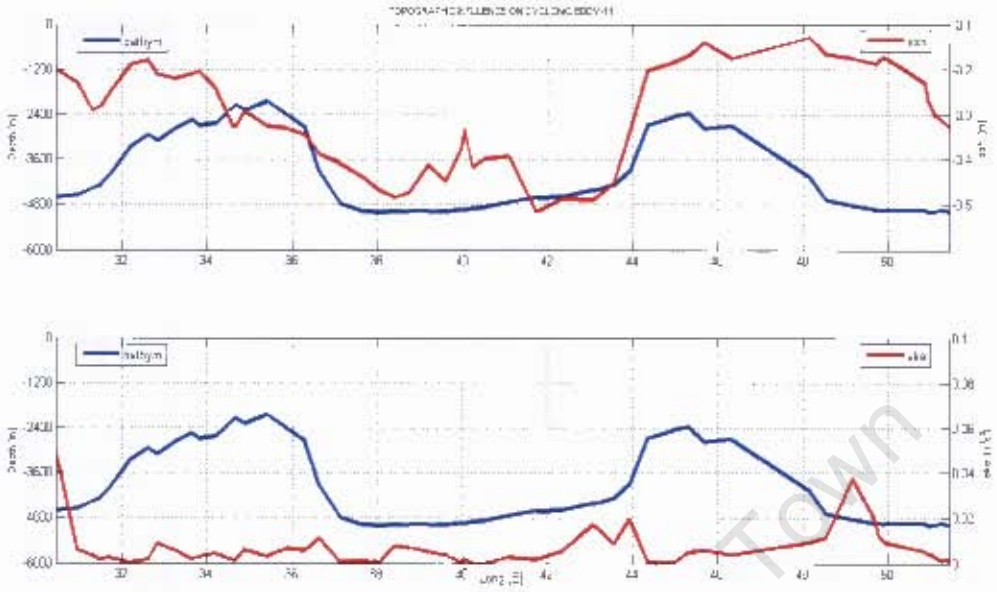

Figure 5.3.3.8 – upper panel shows the variation of the sea surface height [red line] and the lower panel shows the variation of the eddy kinetic energy [red line] with the bathymetric profile [blue line] on both panels during the course of propagation of cyclonic eddy11.

Cyclonic eddy11 was first identified to the south-east of Madagascar, in the Madagascar Basin on 6 November 1996. The pathway shows that the eddy moved in a south-westward direction, crossing both the Madagascar and the Mozambique Ridges. Over the Madagascar Ridge it crossed south of 28°S in a westward direction, and over the Mozambique Ridge it passed through gate-B and finally dissipated in the Natal Valley to the south 36°S and to the west 32° [Figure 5.3.3.7].

The sea surface height of cyclonic eddy11 was highest over both the Mozambique and the Madagascar Ridges, and the lowest SSH was observed over the deepest parts of the bathymetry in the Mozambique Basin [37 – 43°E]. The variation of the SSH seems directly related to the bottom topography [Figure 5.3.3.8]. The eddy kinetic energy [EKE] of cyclonic eddy11 is very low except at small peaks observed between 48 and 50°E and far west to 32°E. Nevertheless, the full trend of EKE shows a westward decrease that seems unrelated to the bottom topography [Figure 5.3.3.8].

The Agulhas Current interacts with several mesoscale features. As described before such an interaction occasionally induces the growth of a Natal Pulse, and thus generates instability in the trajectory of the Agulhas Current. The fourth key research question of this project is: how does the movement of eddies affect the stability of the Agulhas Current? This was investigated and the results are presented and discussed in section 5.4.

5.4 The influence of eddies on the Agulhas Current

To address the above topic with the ROMS we have produced a consecutive series of simulated snap-shots of the sea surface temperature [SST] near the south-eastern region of the African continent; vertical sections of meridional velocities as well as meridional sections of total vorticity and temperature at 33 °S across the Agulhas Current. This has been done to trace the influence of eddies which interact and impact the stability of the Agulhas Current, in order to investigate the physical mechanisms responsible for such an instability of the current.

A thorough investigation of 882 snap-shots for the eight years of simulation of the sea surface temperature [SST] has shown several cases in which the path of the Agulhas Current has been largely perturbed. In a few cases, such a perturbation led to the growth of a mesoscale feature inshore of the Agulhas Current [Figures 5.4.1 – 5.4.3] known as a Natal Pulse [Lutjeharms and Roberts, 1988].

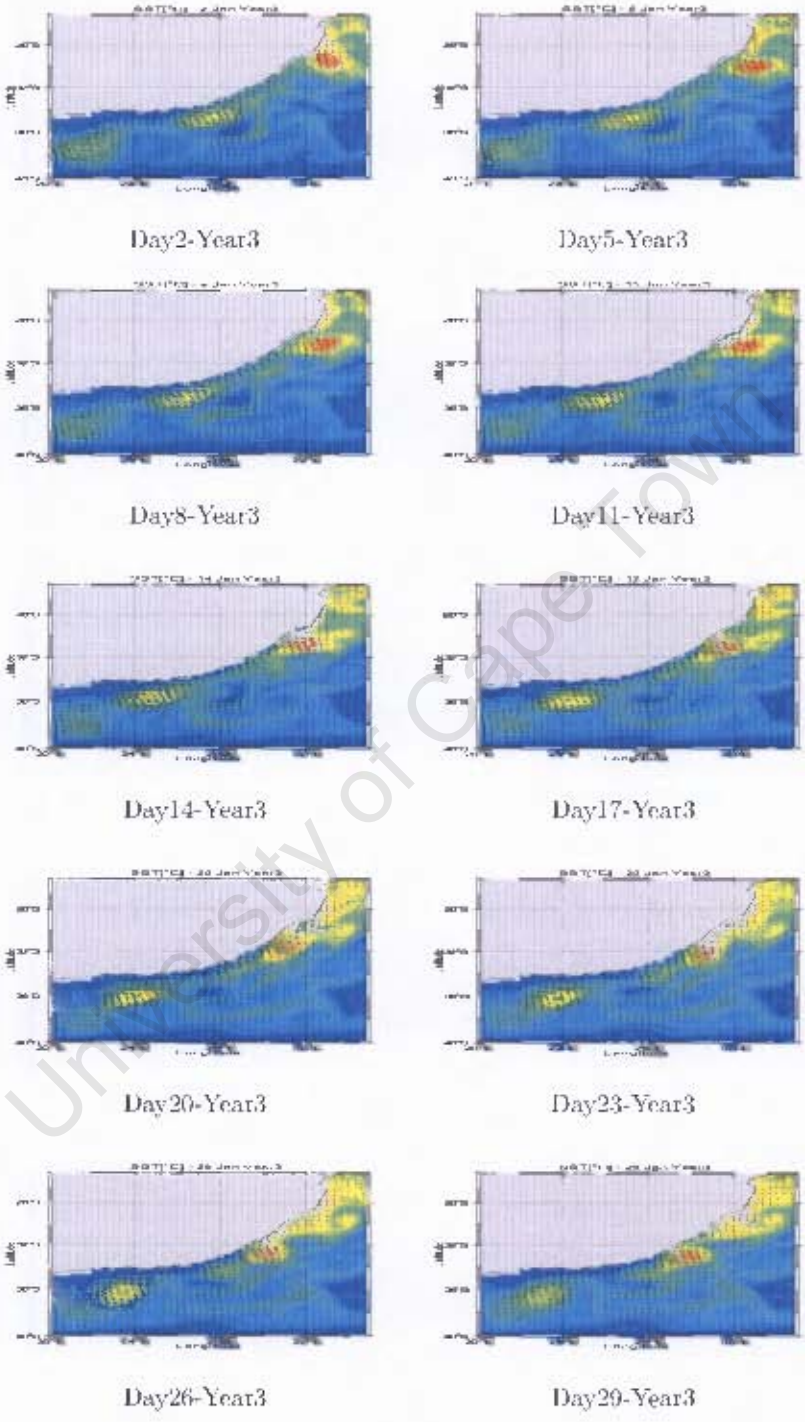

Figure 5.4.1 - Portrayal of horizontal section of temperature [^{o}C] at 50 [m] depth, for the month of January of the model year3. Pertrubation on the path of the Agulhas Current is evident. Note the offshore anti-cyclonic eddy with which this perturbation is associated. The arrows represent geostrophic cuttents.

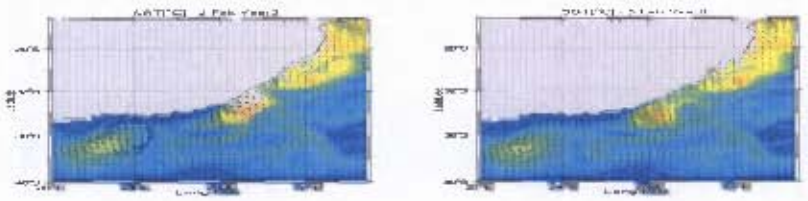

Day2-Year3

Day5-Year3

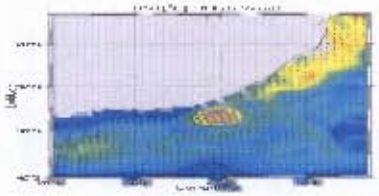

Day8-Year3

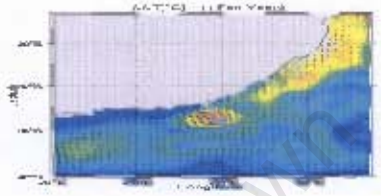

Day11-Year3

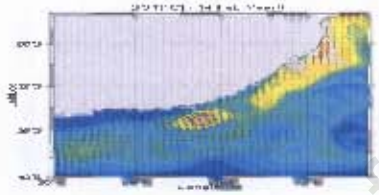

Day14-Year3

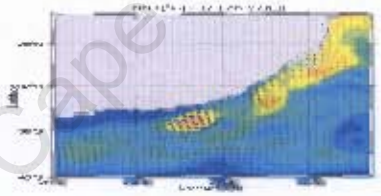

Day17-Year3

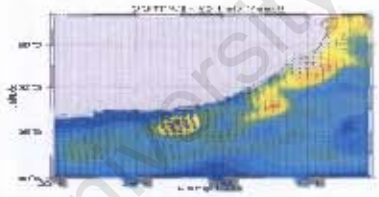

Day20-Year3

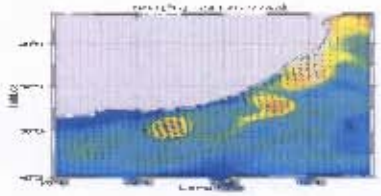

Day23-Year3

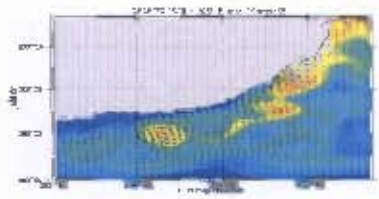

Day26-Year3

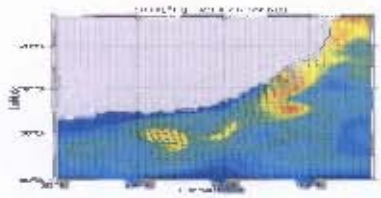

Day29-Year3

Figure 5.4.2 - Portrayal of horizontal section of temperature [^oC] at 50 [m] depth, for the month of February of the model year3. Pertrubation on the path of the Agulhas Current is evident. Note the offshore anti-cyclonic eddy with which this perturbation is associated. The arrows represent geostrophic cuttents.

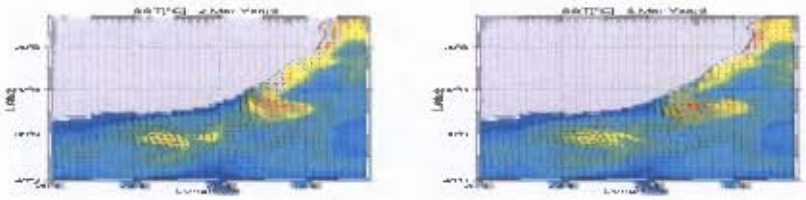

Day2-Year3

Day5-Year3

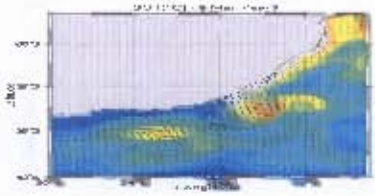

Day8-Year3

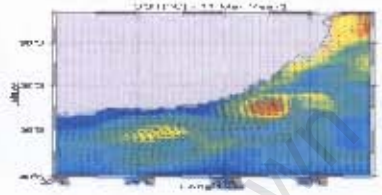

Day11-Year3

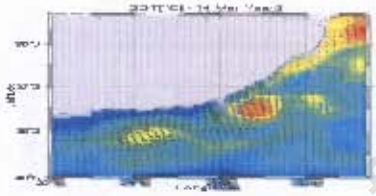

Day14-Year3

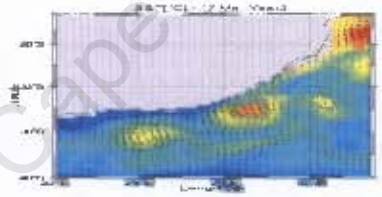

Day17-Year3

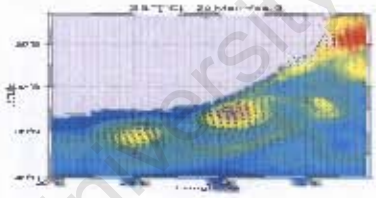

Day20-Year3

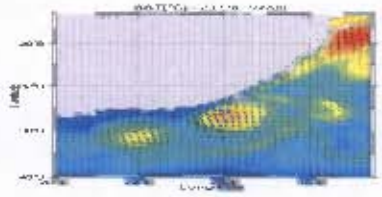

Day23-Year3

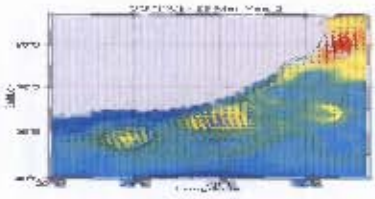

Day26-Year3

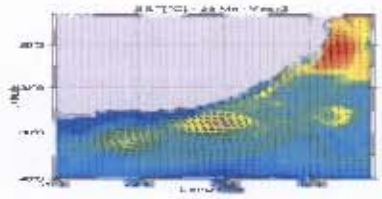

Day29-Year3

Figure 5.4.3 - Portrayal of horizontal section of temperature [°C] at 50 [m] depth, for the month of March of the model year3. Pertrubation on the path of the Agulhas Current is evident. Note the offshore anti-cyclonic eddy with which this perturbation is associated. The arrows represent geostrophic cuttents.

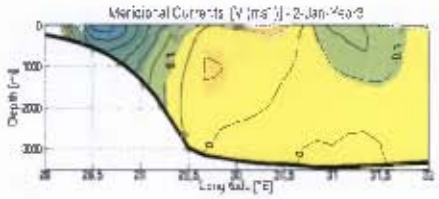

Day2-Year3

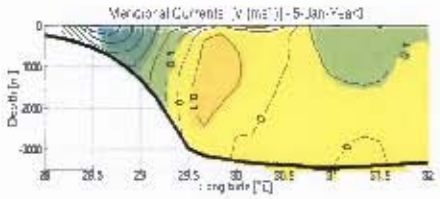

Day5-Year3

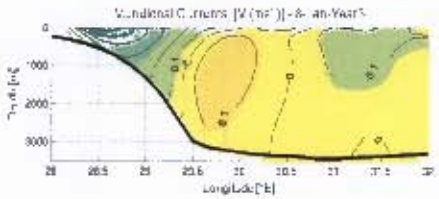

Day8-Year3

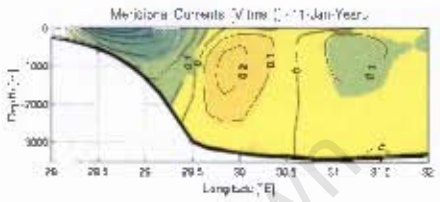

Day11-Year3

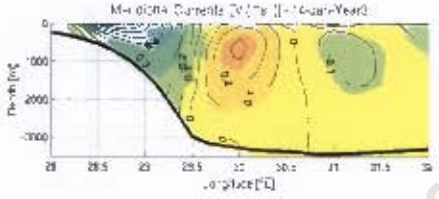

Day14-Year3

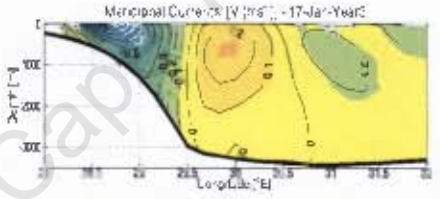

Day17-Year3

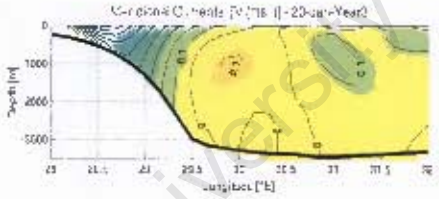

Day20-Year3

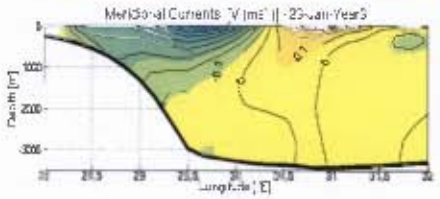

Day23-Year3

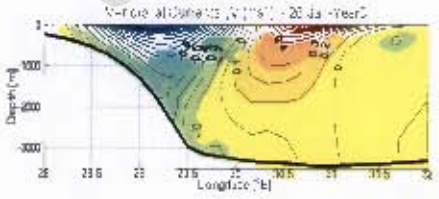

Day26-Year3

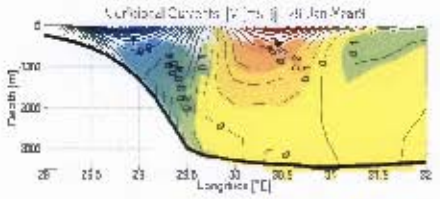

Day29-Year3

Figure 5.4.4 - Meridional currents, at 33°S, South African east coast. Negative values represent a southward velocities, and the positive values represent equatorward velocities. The disposition of the isolines are associated with the pertrubations due to the eddy and Agulhas Current interaction. The section was taken during the month of January of the modeled year 3. The sequence is to be compared with the figure 5.4.1

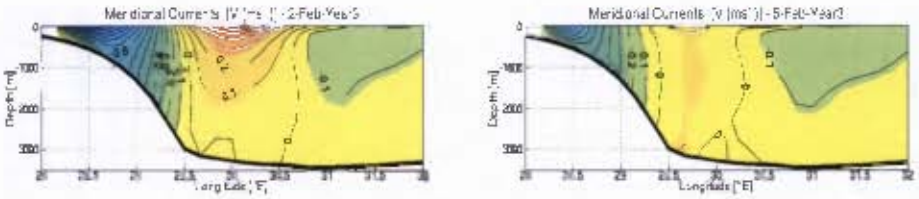

Day2-Year3

Day5-Year3

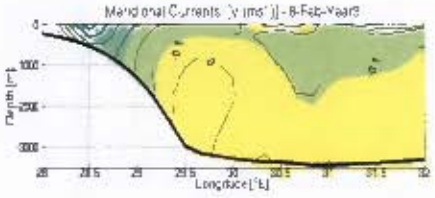

Day8-Year3

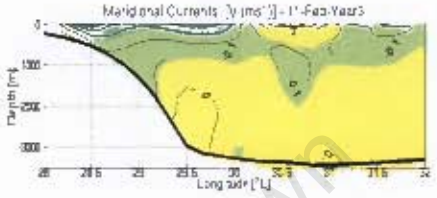

Day11-Year3

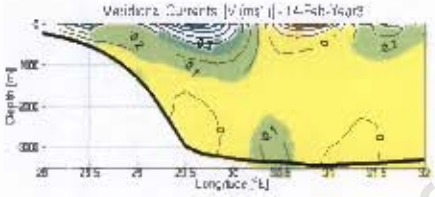

Day14-Year3

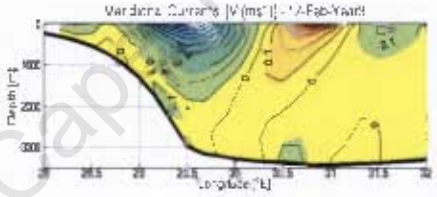

Day17-Year3

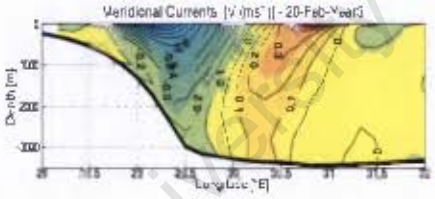

Day20-Year3

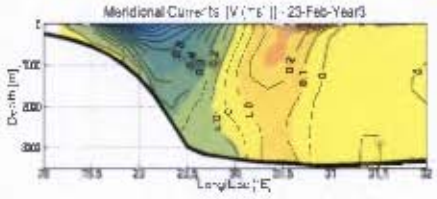

Day23-Year3

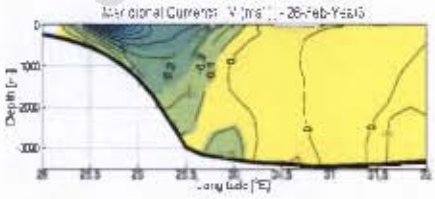

Day26-Year3

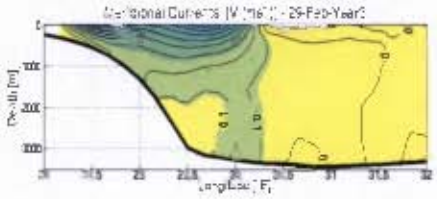

Day29-Year3

Figure 5.4.5 - Meridional currents, at 33°S, South African east coast. Negative values represent a southward velocities, and the positive values represent equatorward velocities. The disposition of the isolines are associated with the perturbations due to the eddy and Agulhas Current interaction. The section was taken during the month of February of the modeled year 3. The sequence is to be compared with the figure 5.4.2

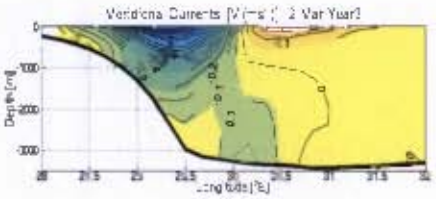

Day2-Year3

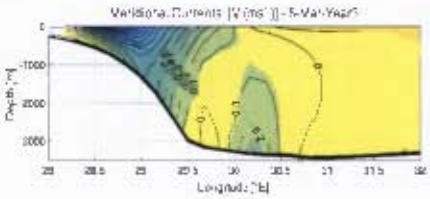

Day5-Year3

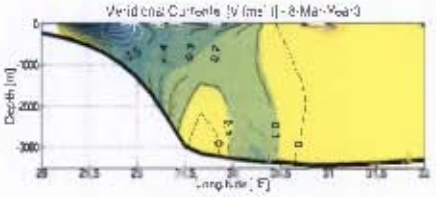

Day8-Year3

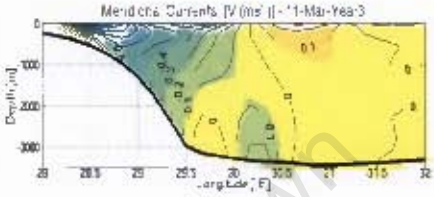

Day11-Year3

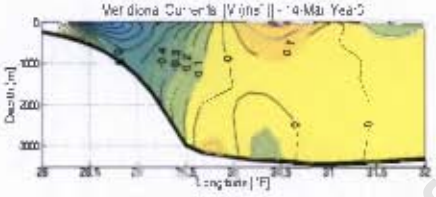

Day14-Year3

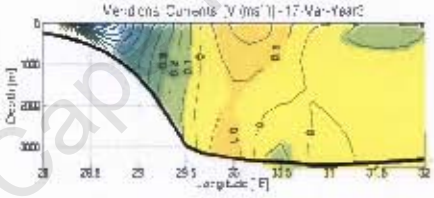

Day17-Year3

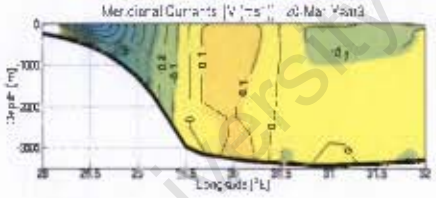

Day20-Year3

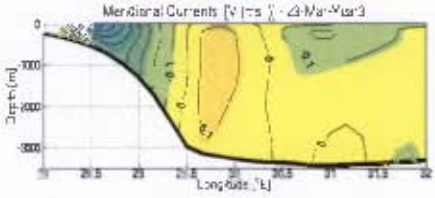

Day23-Year3

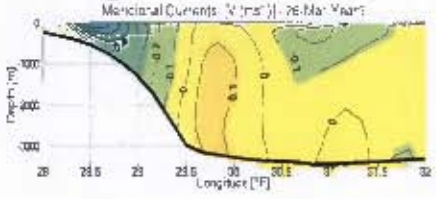

Day26-Year3

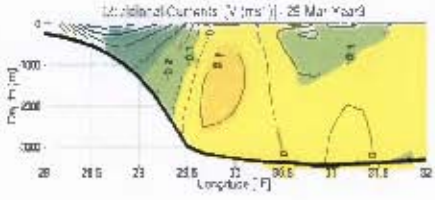

Day29-Year3

Figure 5.4.6 - Meridional currents, at 33°S, South African east coast. Negative values represent a southward velocities, and the positive values represent equatorward velocities. The disposition of the isolines are associated with the pertrubations due to the eddy and Agulhas Current interaction. The section was taken during the month of February of the modeled year 3. The sequence is to be compared with the figure 5.4.3

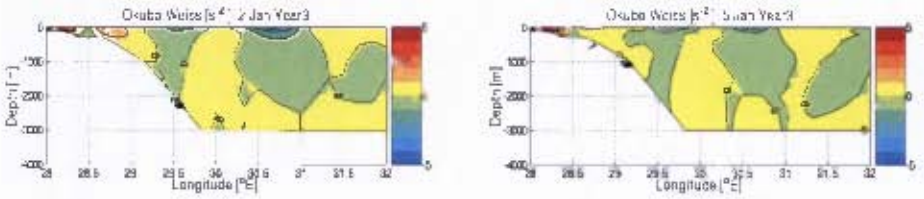

Day2-Year3 Day5-Year3

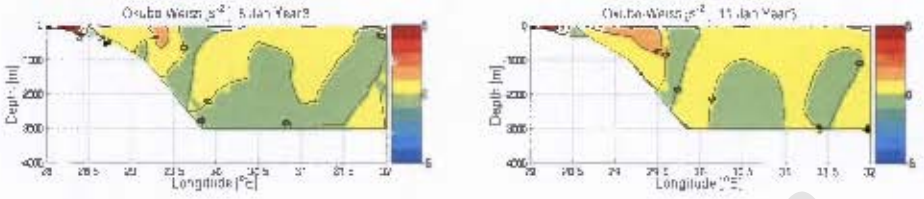

Day8-Year3 Day11-Year3

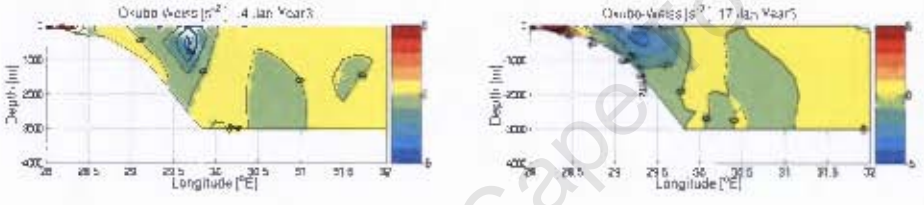

Day14-Year3 Day17-Year3

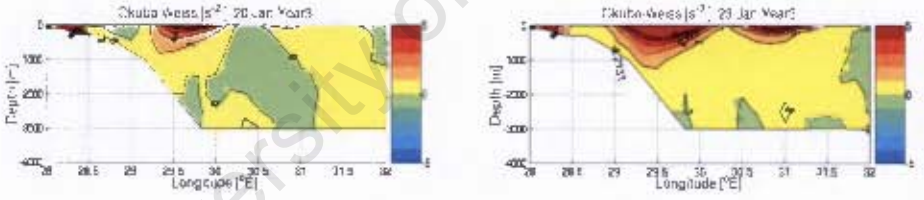

Day20-Year3 Day23-Year3

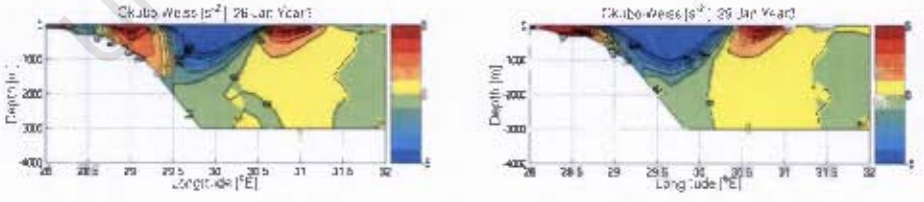

Day26-Year3 Day29-Year3

Figure 5.4.7 - Okubo-Weiss [s^{-2}] at 33°S for the month of January, model year3. The negative values represent the rotation and the positives the deformation of the flow. This sequence may be compared to that shown in figures 5.4.1 and 5.4.4. Okubo-Weiss parameter is a criteria which consist in dividing a turbulent flow into a hyperbolic regions (deformed flow), and rotational regions. The latter part could be used as a proxy to identify eddies. In this work when the rate of rotation dominates the deformation, then we assume to have a presence of an eddy.

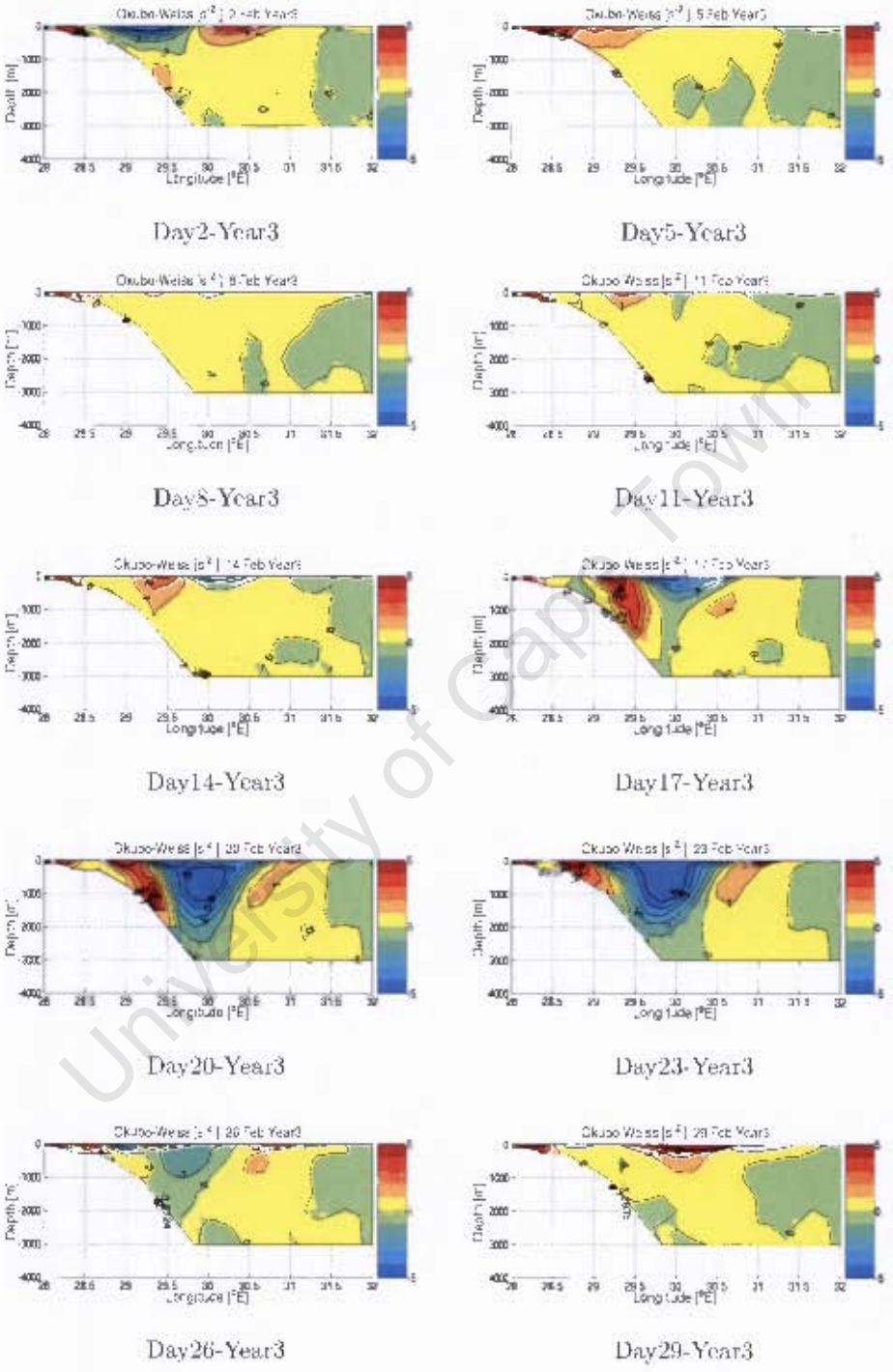

Figure 5.4.8 - Oku-Weiss [s^{-2}] at 33°S, South African east coast, for the month of February, model year3. The negative values represent the rotation and the positives the deformation of the flow. This sequence may be compared to that shown in figures 5.4.2 and 5.4.5

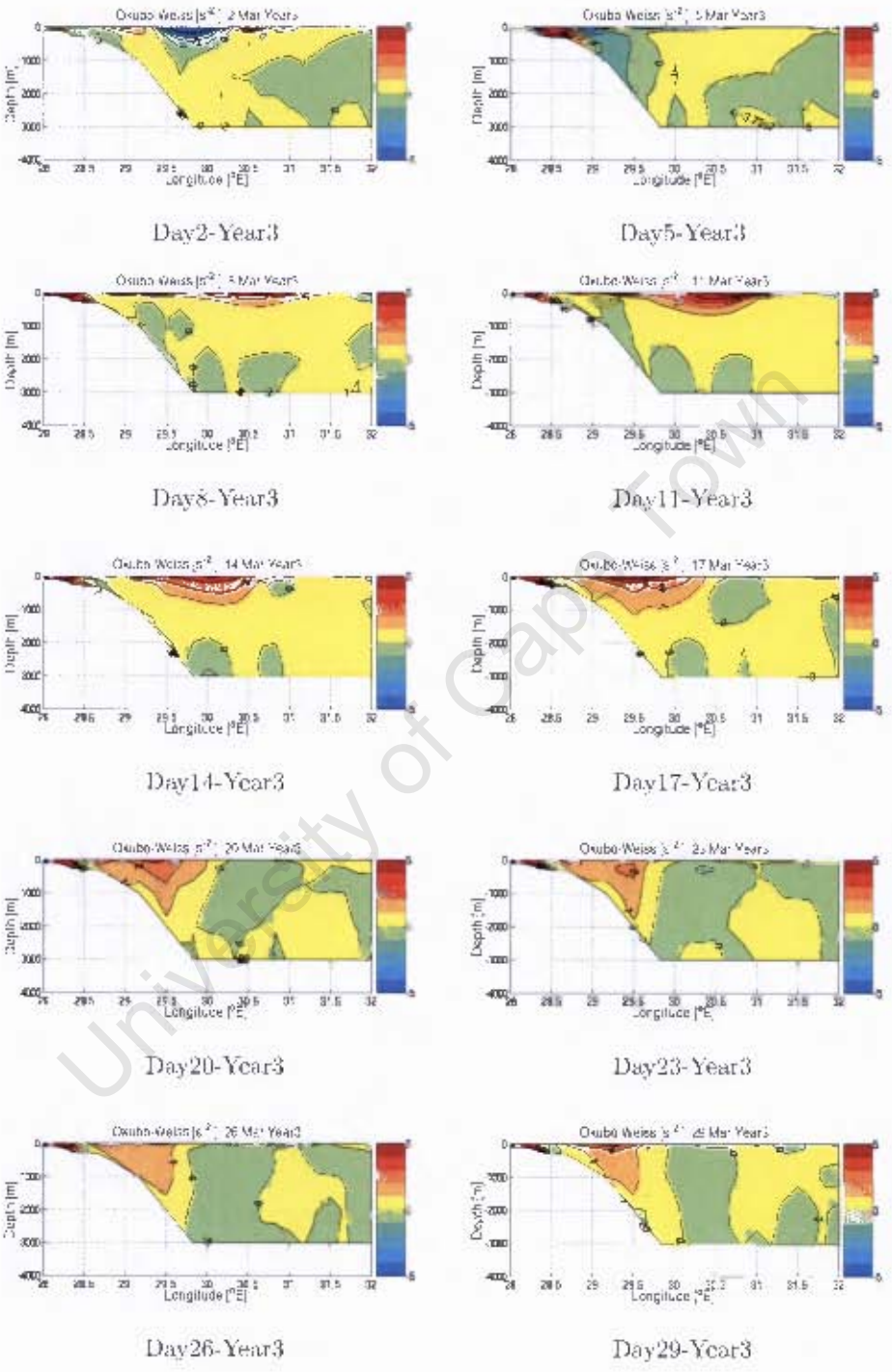

Figure 5.4.9 - Okubo-Weiss s^{-2} at 33°S, South African east coast, for the month of March, model year3. The negative values represent the rotation and the positives the deformation of the flow. This sequence may be compared to that shown in figures 5.4.3 and 5.4.6

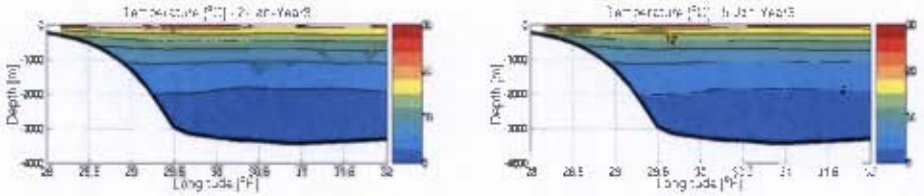

Day2-Year3

Day5-Year3

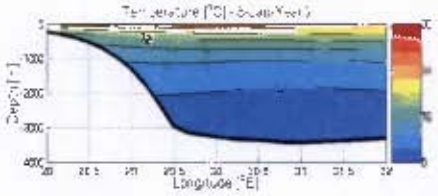

Day8-Year3

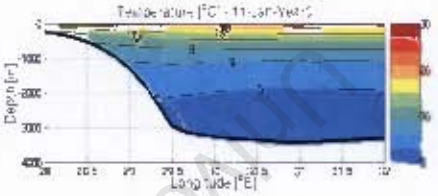

Day11-Year3

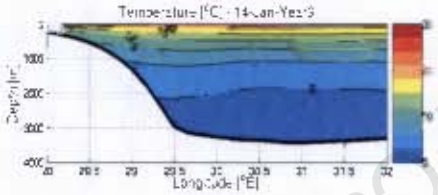

Day14-Year3

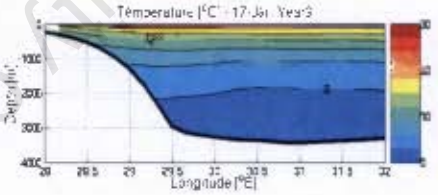

Day17-Year3

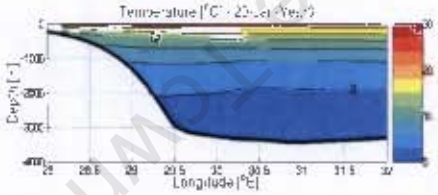

Day20-Year3

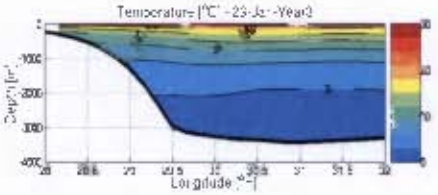

Day23-Year3

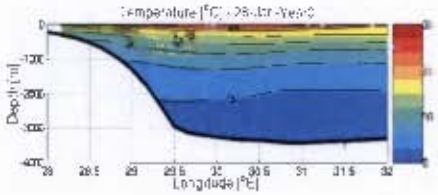

Day26-Year3

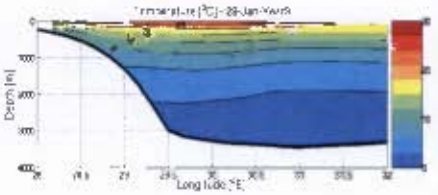

Day29-Year3

Figure 5.4.10 - Portrayal of the temperature in [°C] for the month of January, model year 3. Zonal section at 33°S, South African east coast.

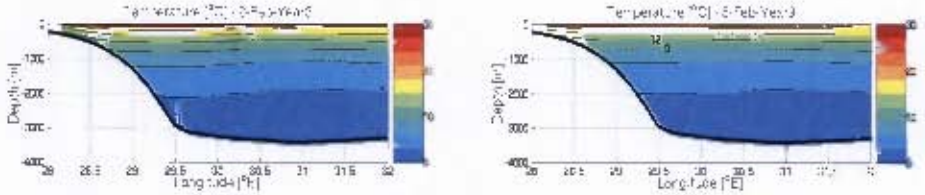

Day2-Year3

Day5-Year3

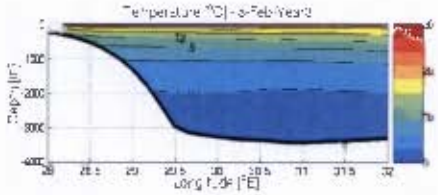

Day8-Year3

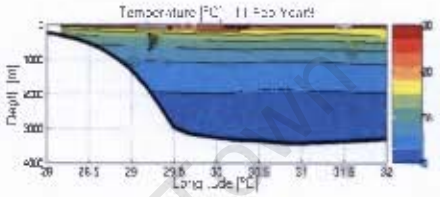

Day11-Year3

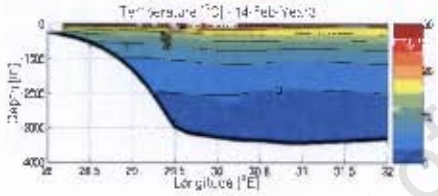

Day14-Year3

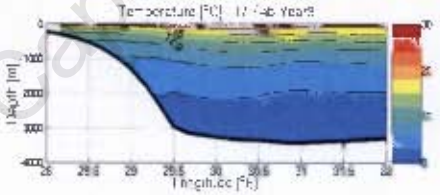

Day17-Year3

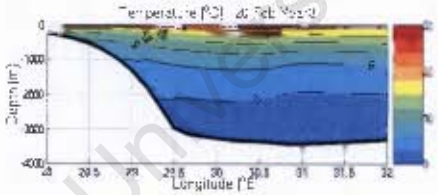

Day20-Year3

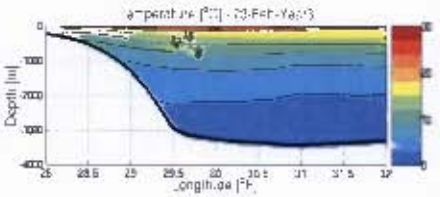

Day23-Year3

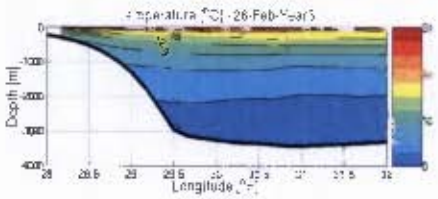

Day26-Year3

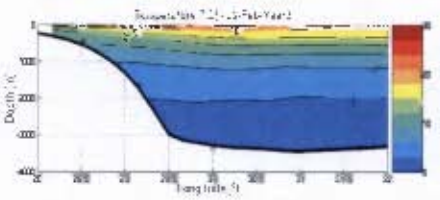

Day29-Year3

Figure 5.4.11 - Cross shelf section of temperature, at 33°S, South African east coast, during the month of February, model year 3.

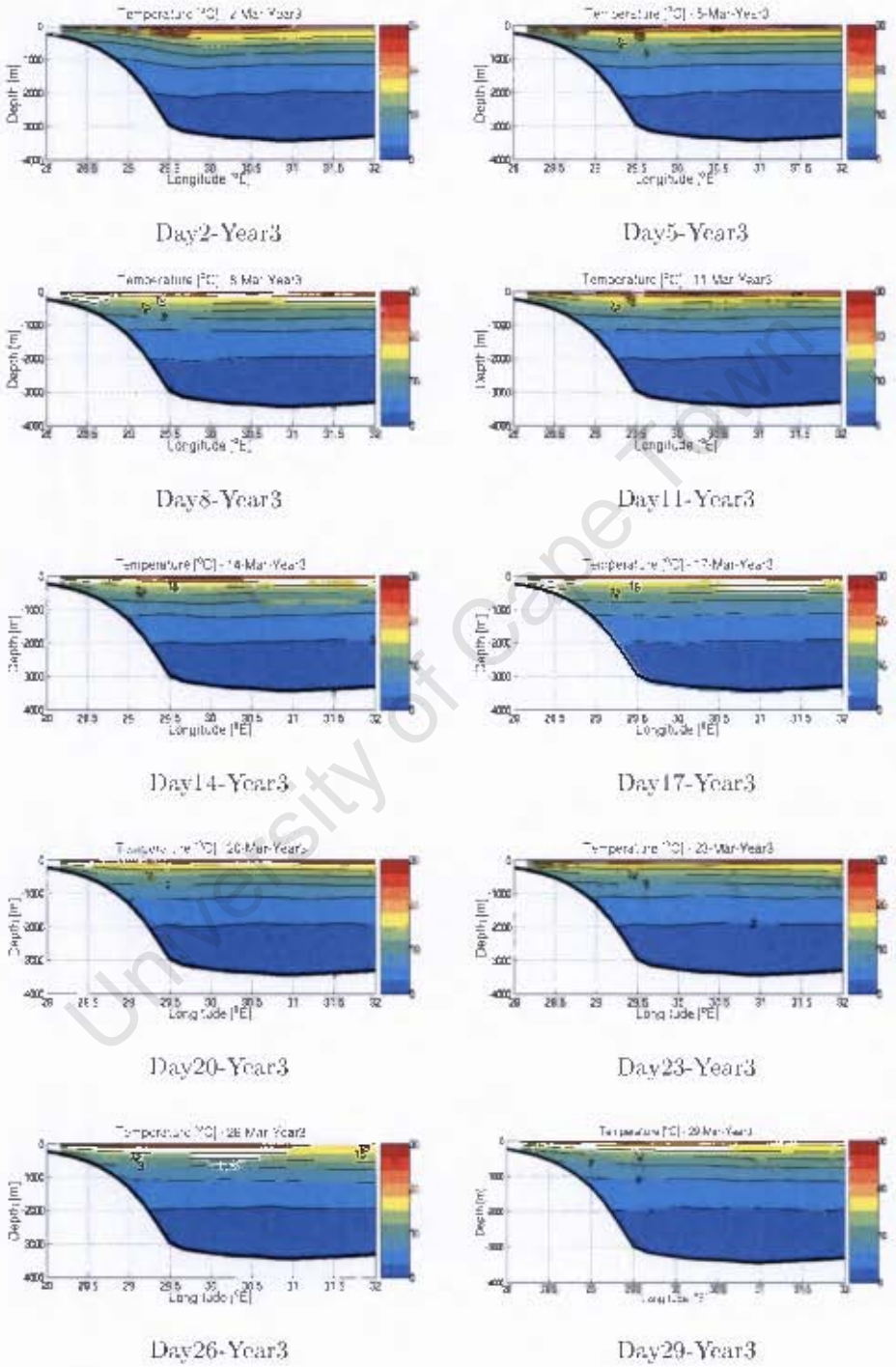

Figure 5.4.12 - Cross shelf section of temperature, at 33°S, South African east coast, during the month of March, model year 3.

The figures presented above [Figure 5.4.1 – Figure 5.4.12] are snapshots and have been selected as the most representatives of the physical mechanisms that lead to the formation of mesoscale Natal Pulses.

Observations of the sea surface temperature [SST] images [Figure 5.4.1 – Figure 5.4.3] show the path of the Agulhas Current along the shelf of south-eastern Africa as a continuous red [warm] strip. The red warm circular features portray anti-cyclonic eddies. Most of these eddies seems to become attached to the eastern edge of the current [vide Schouten et al., 2002a], suggesting that the interaction between anti-cyclonic eddies and the Agulhas Current takes place quite often, and as such is a characteristic feature of the hydrodynamic processes of the Agulhas Current system.

Such interaction is observed on the simulated moving images of the SST [not shown in this text], and is also confirmed by hydrographic data as well as altimetric observations, and they suggest that these eddies mostly come from upstream regions of the Agulhas Current, namely the Mozambique Channel [Schouten et al., 2002a] and south of Madagascar.

Agulhas rings have been observed in SST images as being spawned at the Agulhas Current retroflection [Lutjeharms and van Ballegooyen, 1988]. The occlusion of such rings has been shown [van Leeuwen et al.,2000] to be due to the downstream passage of a Natal Pulse, triggered by the adsorption of offshore eddies onto the Agulhas Current.

The vertical sections of meridional velocities [Figure 5.4.4 – Figure 5.4.6] have been taken across the core of the Agulhas Current at about 33°S. These sections portray the flow of the Agulhas Current along the continental slope [Figure 5.4.4 – 2 January] identified by negative values, portraying a poleward flow. On the eastern edge of the current positive values may be observed representing an equatorward propagation, which portray the presence of anti-cyclonic eddies. The intensity of these eddies varies from 0.1 – 1 ms^{-1} the highest intensities being observed on 26-29 January [Figure 5.4.4].

The path of the northern Agulhas Current is very stable [Schouten et al., 2002a]. In the sections presented above [Figures 5.4.4 – 5.4.6] such a stable regime can be perceived by the structure of the isolines of velocities which set up the meridional velocity field, integrated over the full depth of the water column.

The velocity field of the core of the Agulhas Current is located on the continental slope for most of the time [Figure 5.4.4]. Nevertheless a few cases have been observed where there is a perturbation of this pattern, with a shift of the current from an inshore to an offshore location [Figure 5.4.5]. Thus when such is the case the current becomes marginally stable especially where the bathymetric slope is shallower as suggested by Schouten et al. [2002a]. The perturbation observed on the flow in these images seems related to an offshore movement of the Agulhas Current, from the continental shelf to well east of the shelf slope. The core of the current on these occasions was shifted eastward by almost 1°E.

Observations of the sea surface temperature [SST] images on the same days [Figure 5.4.1 - 23 January and Figure 5.4.2 – 5-14, 29 February], show that days in which the Agulhas Current was displaced were coincident with the presence of an anti-cyclonic eddy on the eastern edge of the current, exactly at or near 33°S.

These intense anti-cyclonic eddies have been held responsible for the occasional offshore movement of the Agulhas Current [Lutjeharms and Roberts, 1988]. The results presented here confirm such a possibility because such a matching also coincide with a surface cooling on the expression of the SST at the inshore sector of the current, similar to the growing of a Natal Pulse – a cyclonic meander of the Agulhas Current [Lutjeharms and Robert, 1988]. Furthermore, the meridional sections of the currents [Figure 5.4.4 – Figure 5.4.6] show that the intensification of the Agulhas Current is observed when the interacting eddies on the eastern edge of the current also increases its intensity [De Ruijter et al., 1999]. Hydrographic studies as well as model simulations such as the one used by A. Biastoch, have shown that when strong eddies interact with the Agulhas Current at the Natal Bight region, then the current is intensified and a Natal Pulse is formed.

The Natal Pulse identified in our simulation was triggered on 23 January and became evident three days later on 26 January [Figure 5.4.1] and lasted to 23 February [Figure 5.4.2]. After this day we couldn't trace the Pulse because it had lost its surface expression. Possibly the Pulse was mixed in the surrounding flow. The presence of this Natal Pulse is also supported by the vertical sections of temperature [Figure 5.4.11 – 8-29 February] which shows an up-lifting of the isotherms on the slope of the continental shelf as a response of the presence of an intense anti-cyclonic eddy on to the east of the current. This eddy pushed the isotherms downwards. To balance the volume relatively cold deep waters moved towards the surface layers – typical situation related to the presence of a Natal Pulse.

Vertical sections of the total vorticity have also been investigated for the three months of the simulation. These are presented in Figures 5.4.7 – 5.4.9. For the period of occurrence of the observed Pulse, it is clearly perceived that positive isolines with high values developed over the bathymetric slope, indicating a strong deformation which seems related to the observed perturbation of the Agulhas Current. To the east strong negative values are observed portraying the rotation of the flow, typical for an anti-cyclonic eddy. These features became more intense [Figure 5.4.8 - 17-23 February] as the Pulse was growing. The isolines of the Okubo-Weiss parameter are very deep, extending to the full depth of the Agulhas Current, suggesting that barotropic instability has been generated on the current due to the interaction with the anti-cyclonic eddies as previous studies also have indicated [De Ruijter et al., 1999].

6 CONCLUSIONS

In this study we have surveyed the published information about the ocean circulation in the South-West Indian Ocean. Thus we have found an array of pertinent issues which needed to be addressed in order to increase our understanding of the hydrodynamic processes of the mesoscale circulation in the Mozambique Channel and the region south of the Madagascar. Therefore from such an array of questions, we have formulated four research questions to address.

In this regard attention was given to the role of the sea floor topography on the ocean circulation in the South-West Indian Ocean. So then, the first key research question of the study was: How does the bathymetry, especially the shallow Madagascar Ridge influence the mesoscale circulation in the region?

According to our methodological approach based on the model simulations, we have found that by removing the Madagascar Ridge from the system, a higher inflow from the East Madagascar Current and from the South-East Indian Ocean seems to propagate into the Agulhas Current region. Such higher inflow in turn increases the variability in the Agulhas Current, as well as an overall strength of the current.

Once they have crossed the Madagascar Ridge, the eddies during the course of their propagation from the south of Madagascar into the vicinity of the Agulhas Current, may undergo a topographic interaction with the Mozambique Ridge. The Mozambique Ridge is a topographic structure with three major fractures, which allows a deep exchange of water between the Mozambique Basin and the Natal Valley. Thus the second research question raised was: Do these eddies have preferred routes of propagation through the fracture zones transecting the Mozambique Ridge?

We have tracked 20 cyclonic and 20 anti-cyclonic eddies coming from the south of Madagascar, and 20 anti-cyclonic eddies from the Mozambique Channel. Not a single one from the Mozambique Channel passed through the gateways of the ridge. Eddies from the south of Madagascar show that the anti-cyclonic ones have a preferred route of propagation through the fractures of the Mozambique Ridge, preferentially passing through the northernmost bathymetric gap. The case for cyclonic eddies was inconclusive [Table 5.2].

Nevertheless, our investigation was limited, based on just 20 cyclonic eddies. Therefore a larger quantity might be required in order that a conclusive result may be achieved.

The third objective of the study was based on the question: How do the eddy kinetic energy [EKE] change during the course of eddy propagation. In this regard the performed correlation of both the sea surface height [SSH] and [EKE] relative to the depth of the sea floor topography, at each position occupied by the eddies, have shown that in the Mozambique Channel the trend of EKE may vary. It can increase or decrease. South of Madagascar, both the cyclonic and the anti-cyclonic eddies have shown a decreasing trend of the EKE moving into the Agulhas Current region. Although the cyclonic profiles were extremely low in kinetic energy, a decreasing trend could still be traced. Eddies crossing the Mozambique Ridge have been observed to propagate onto the edge of the Agulhas Current, interacting and influencing the behaviour and path of the current. From this the fourth research question was formulated: How do eddies affect the stability of the Agulhas Current?

Investigations of the sea surface temperature [SST]; vertical sections of the temperature; sections of meridional currents and Okubo-Weiss parameter, across the Agulhas Current at about 33°S, have shown that, due to the interaction between anti-cyclonic eddies from the upstream regions of the Mozambique Channel and south of Madagascar with the Agulhas Current, at the Natal Bight, the current becomes susceptible to a barotropic instability which leads to the formation of a Natal Pulse.

7 RECOMMENDATIONS

Though the findings of the present study have given answer to the key questions aimed to be addressed, however a lot of unknown issues were found, and such need to be addressed as a future research work. Through the results of the model simulation we ask:

- Are the eddies passing through the Mozambique Channel so variable that they do not affect the calculation of the mean state?

- What would be the volume transport of the flow in the South of Madagscar, when there is no Madagscar Ridge? And what other physical mechanisms have influenced the strong recirculation in the Agulhas Current system in such case?

- In what cases the eddies preserve their energy when passing through the ridges with reduced velocities to preserve their potential vorticity, and where energy is gained possibly through instability processes?

Though these questions are based on the idealized simulation, a closer look at these is important to understand the hydrodynamics of the system. The questions require an answer if the role of Madagascar Ridge on the regional mesoscale circulation is to be fully understood. A proper analysis of other experiments would be needed to address these questions.

7 REFERENCES

Arakawa, A., and V. R. Lamb, 1977: Methods of computational physics. Academic Press. 17, 174–265.

Barnier, B., P. Marchesiello., A. Pimenta de Miranda., J. M. Molines., and M. Coulibaly, 1998: A sigma-coordinate primitive equation model for studying the south Atlantic. Deep-Sea Research I. 45, 543-572.

Bassias, Y, 1992: Petrological and geochemical investigation of rocks from the Davie fracture zone (Mozambique Channel) and some tectonic implications. Journal of African Earth Sciences. 15, 321-339.

Beal, L. M., and H. L. Bryden, 1999: The velocity and vorticity structure of the Agulhas Current at 32°S. Journal of Geophysical Research. 104[C3], 5151-5176.

Biastoch, A., and W. Krauss, 1999: The role of mesoscale eddies in the source regions of the Agulhas Current. Journal of Physical Oceanography. 29[9], 2303-2317.

Boebel, O., T. Rossby., J. R. E. Lutjeharms., W. Zenk., and C. Barron, 2003: Path and variability of the Agulhas Return Current. Deep-Sea Research II. 50[1], 35-56.

Buck, J. J, 2003: Eddies in the East Madagascar Current. MSc Thesis.University of Southampton, Faculty of Science, School of Ocean and Earth Observation, Southampton, 57.

Chapman, P., S. F. DiMarco., R. E. Davis and A. C. Coward, 2003: Flows at intermediate depths around Madagascar based on Alace float trajectories. Deep-Sea Research II. 50[12-13], 1957-1986.

Chetty, P., and R. W. E. Green, 1977: Seismic refraction observations in the Transkei Basin and adjacent areas. Marine Geophysical Researches. 3, 197-208.

Conkright, M. E., and S. Levitus, 2002: World Ocean Database 2001, vol. 1, Introduction [CD-ROM], NOAA Atlas NESDIS, Washington., D. C., 42, 159.

Da Silva, A. M., C. C. Young and S. Levitus, 1994: Atlas of Surface Marine Data 1994, vol1. Algorithms and Procedures, NOAA Atlas NESDIS 6, NOAA, Silver Spring, Md. 74pp.

De Ruijter, W. P. M., H. M. Van Aken., E. J. Beier., J. R. E. Lutjeharms., R. P. Matano and M. W. Schouten, 2004: Eddies and dipoles around south of Madagascar: Formation, pathways and large-scale impact. Deep-Sea Research I. 51[3], 383-400.

De Ruijter, W. P. M., H. Ridderinkhof and M. W. Schouten, 2005: Variability of the South-West Indian Ocean. Philosophical Transactions of the Royal Society. 366, 66-73.

De Ruijter, W. P. M., H. Ridderinkhof., J. R. E. Lutjeharms., M. W. Schouten., and C. Veth, 2002: Observation of the flow in the Mozambique Channel. Geophysical Research Letters. 29[10], 1401-1403.

De Ruijter, W. P. M., J. R. E. Lutjeharms., H. Ridderinkhof, 2000: Observations of the Mozambique Current and East Madagascar Current in the Agulhas Current Source Experiment (ACSEX). WOCE Newsletter 38, 32-34.

De Ruijter, W. P. M., P. J. van Leeuwen and J. R. E. Lutjeharms, 1999: Generation and evolution of Natal Pulses: Solitary meanders in the Agulhas Current. Jounal of Physical Oceanography. 29[12], 3043-3055.

De Ruijter, W. P. M., A. Biastoch., S. S. Drijfhout., J. R. E. Lutjeharms., R. P. Matano., T. Pichevin., P. J. Van Leeuwen and W. Weijer, 1999: Indian-Atlantic inter-ocean exchange: Dynamics, estimation and impact. Journal of Geophysical Research. 104[C9], 20,885-20,910.

DiMarco, S. F., P. Chapman and W. D. Nowlin, 2000: Satellite observations of upwelling on the continental shelf south of Madagascar. Geophysical Research Letters. 27[24], 3965–3968.

DiMarco, S. F., P. Chapman., W. D.Nowlin., P. Hacker., K. Donohue., M. Luther., G. C. Johnson and J. Toole, 2002: Volume transport and property distributions of the Mozambique Channel. Deep-Sea Research I. 49[7-8], 1481-1511.

Doglioli, A. M., B. Blanke., S. Speich and G. Lapeyre, 2007: Tracking coherent structures in a regional ocean model with wavelet analysis: Application to Cape Basin eddies. Journal of Geophysical Research. 112, Art. C05043.

Donohue, K. A., and J. M. Toole, 2003: A near-synoptic survey of the Southwest Indian Ocean. Deep-Sea Research II. 50[12-13], 1893-1931.

Donohue, K. A., F. Eric., B. Lisa, 1999: Comparison of three velocity sections of the Agulhas Current and Agulhas Undercurrent. Journal of Geophysical Research. 105[C12], 28,585-28,593.

Donohue, K. A., G. Hufford and M. Mccartney, 1999: Sources and transport of the deep western boundary current east of the Kerguelen Plateau. Geophysical Research Letters. 26, 851-854.

Donquy, J. R., and B. Piton, 1991: The Mozambique Channel revisited. Oceanologica Acta. 14[6], 549-558.

Dyment. J, 1991: Structure et évolution de la lithosphère océanique dans l'Océan Indien: Apport des données magnétiques. Thèse, universitate, Strasbourg, 374.

Feron, R. C. V., W. P. M. de Ruijter and P. J. van Leeuwen, 1998: A new method to determine the mean sea surface dynamic topography from satellite altimeter observations. Journal of Geo physical Research. 103[C1], 3043-3055.

Fetter, A., J. R. E. Lutjeharms and R. P. Matano, 2007: Atmospheric driving forces of the Agulhas Current in the subtropics. Geophysical Research Letters. 34, L15605, doi: 10/1029/2007GLO30200.

Fischer, R. L., and M. A. Goodwillie, 1998: The physiography of the South-West Indian Ocean. Marine Geophysical Research. 19, 451-455.

Gille, S. T., and D. T. Sandwell, 2001: Gravity, bathymetry, and mesoscale ocean circulation from altimetry, AVISO newsletter 9, 8.

Gordon, A. L, 1986: Inter-ocean exchange of thermocline water. Journal of Geophysical Research. 91[C4], 5037-5046.

Gordon, A. L., J.R.E. Lutjeharms and M.L. Grundlingh, 1987: Select hydrographic sections from the Agulhas research cruises of the research vessels *Knorr* and *Meirinng Naude* 0 1983. Lamont-Doherty Geological Observatory of Columbia University, *Technical report* LDG0-87-1.

Gordon, A. L., D. Olson., P. Hacker., A. Ffield., L. Talley., D. Wilson and M. Barringer, 1997: Advection and diffusion of Indonesian throughflow within the Indian Ocean South Equatorial Current. Journal of Geophysical Research. 24, 2573-2576.

Goslin, J., J. Segoufin., R. Schlich and R. L. Fisher, 1980: Submarine topography and shallow structure of the Madagascar Ridge, western Indian Ocean. Geological Society of America Bulletin. 91, 741–753.

Gründlingh, M. L, 1987: Cyclogenesis in the Mozambique Ridge Current. Deep-Sea Research. 34[1], 89–103.

Gründlingh, M. L, 1988: Altimetry in the South-West Indian Ocean. South African Journal of Science. 84[7], 568–573.

Gründlingh, M. L, 1995: Tracking eddies in the South-East Atlantic and South-West Indian Oceans with Topex-poseidon. Journal of Geophysical Research. 100[C12], 24977-24986.

Haidvogel, D. B., H. Arango., K. Hedstrom., A. Beckmann., P. Rizzoli., A. Shchepetkin, 2000. Model evaluation experiments in the north Atlantic Basin: Simulations in non-linear terrain-following coordinates. Dynamics Atmosphere Oceans. 32, 239-281.

Hales, A. L., and J. B. Nation, 1973: A seismic refraction study in the southern Indian Ocean. Bulletin of the Seismological Society of America. 63, 1951-1966.

Harris, T. F. W., R. Legeckis, D. van Foreest, 1978: Satellite infra-red images in the Agulhas Current System. Deep-Sea Research. 25[6], 543-548.

Hedstrom, K. S, 1997: User's manual for a S-coordinate primitive equation ocean circulation model. SCRUM version 3.0. Institute of Marine and Coastal Sciences, Rutgers University. 116pp. New Brunswick, NJ, USA.

Kusky, T. M., E. Toraman_and T. Raharimahefa, 2006: The great rift valley of Madagascar: An extension of the Africa–Somali diffusive plate boundary? Geological Society. 11, 577-579.

Lutjeharms, J. R. E, 1981: Features of the southern Agulhas Current circulation from satellite remote sensing. South African Journal of Science. 77[5], 231-236.

Lutjeharms, J. R. E, 1988c: On the role of the East Madagascar Current as a source of the Agulhas Current. South African Journal of Science. 84[4], 236-238.

Lutjeharms, J. R. E, 1988d: Remote sensing corroboration of retroflection of the East Madagascar Current as a source of the Agulhas Current. Deep-Sea Research. 35[12], 2045-2050.

Lutjeharms, J. R. E, 2001: The Agulhas Current. In *Encyclopedia of Ocean Science*, editors: J. Steele., S. Thorpe and K. Turekian. Academic Press, London, volume 1, pp. 104-113.

Lutjeharms, J. R. E, 2006: The Agulhas Current. Springer-Verlag. Berlin. 297pp.

Lutjeharms, J. R. E, 2006b: The ocean environment off southeastern Africa – a review. South African Journal of Science. 102, 419.

Lutjeharms, J. R. E, 2007: Three decades of research on the Greater Agulhas Current. Ocean Sciences. 3, 129-147.

Lutjeharms, J. R. E., and A. D. Connell, 1989: The Natal Pulse and inshore counter currents off the South African east coast. South African Journal of Science. 85[8], 533–535.

Lutjeharms, J. R. E., and E. Machu, 2000: An upwelling cell inshore of the East Madagascar Current. Deep-Sea Research I. 47[12], 2405-2411.

Lutjeharms, J. R. E., and I. J. Ansorge, 2001: The Agulhas Return Current. Journal of Marine Systems. 30, 115-138.

Lutjeharms, J. R. E., and R. C. Van Ballegooyen, 1988: The retroflection of the Agulhas Current. Journal of Physical Oceanography. 18[11], 1570-1583.

Lutjeharms, J. R. E., and R. Roberts, 1988: The Natal Pulse: An extreme transient on the Agulhas Current. Journal of Geophysical Research. 93[C1], 631-645.

Lutjeharms, J. R. E., O. Boebel and T. H. Rossby, 2003: Agulhas Cyclones. Deep-Sea Research II. 50, 13-34.

Lutjeharms, J. R. E., O. Boebel., P. C. F van der Vaart., W. P. M. de Ruijter., T. H. Rossby and H. L. Bryden, 2001: Evidence that the Natal Pulse controls the Agulhas Current over its full depth. Geophysical Research Letters. 28, 3449-3452.

Maia, M., and M. Recq, 1990: Isostatic response of the lithosphere beneath the Mozambique Ridge, South-West Indian Ocean and geodynamic implications. Geophysical Journal International. 100, 337-348.

Marchesiello, P., J. MC-Williams and A. F. Shchepetkin, 2001. Open boundary conditions for long terms integrations of oceanic models. Ocean Modelling. 3, 1-20.

Marchesiello, P., A. F. Shchepetkin and J. MC-Williams, 2003. Equilibrium structure and dynamics of the California Current system. Journal of Physical Oceanography. 33, 753-783.

Matano, R. P., C. G. Simionato., W. P. de Ruijter., P. J. van Leeuween (sic)., P. T. Strub., D. B. Chelton and M. G. Schlax, 1998: Seasonal variability in the Agulhas Retroflection region. Geophysical Research Letters. 25[23], 4361-4364.

Matano, R. P., E. J. Beier., P. T. Strub and R. Tokmakian, 2002: Large-scale forcing of the Agulhas variability: The seasonal cycle. Journal of Physical Oceanography. 32[4], 1228-1241.

New, A. L., S. G. Alderson., D. A. Smeed., K. L. Stansfield, 2007: On the circulation of water masses across the Madagascar Plateau in the south Indian Ocean. Deep-Sea Research. 54, 42-47.

Olson, D. B., and R. H. Evans, 1986: Rings of the Agulhas Current. Deep-Sea Research. 33[1], 27-42.

Payet, R. A., N. Soogun., E. Ranaivoson., R. J. Payet and F. Aliabdallah, 2004: Global interna tional waters assessment Indian Ocean Islands, Giwa regional assessment. University of Kalmar, on behalf of United Nations Environment Programme. 45b, 1-73.

Parson, L. M., and A. J. Evans, 2005: Seafloor topography and tectonic elements of the western Indian Ocean. Philosophical Transactions of the Royal Society of London. 363, 15-24.

Penven, P, 2000. Etude Numerique de la circulation dans le sud-Benguela avec une application au recrutement des poissons. These de Doctorat, Laboratoire de Physiques des Oceans, Universite de Bretagne Occidentale, Brest, France. 150.

Penven, P., J. R. E. Lutjeharms and P. Florenchie, 2006: Madagascar: A pacemaker for the Agulhas Current system? Geophysical Research Letters.33, 17609.

Penven, P., and Thi-Anh Tan, 2007: Romstools user's guide. Technical report. Institut de Recherche pour le Developpement Paris, France, 45pp.

Quartly, G. D., and M. A. Srokosz, 2002: SST observation of the Agulhas and East Madagascar Retroflection by the TRMM microwave imager. Journal of Physical Oceanography. 32 [5], 1585 -1592.

Quartly, G. D., and M. A. Srokosz, 2004: Eddies in the southern Mozambique Channel. Deep-Sea Research II. 51[1], 69-83. doi:10.1016/j.dsr2.2003.03.001.

Quartly, G. D., J. J. H. Buck., M. A. Srokosz and A. C. Coward, 2006: Eddies around Madagascar – the retroflection re-considered. Journal of Marine Systems. 63, 115-129.

Reason, C. J. C., J. R. E. Lutjeharms., J. Hermes., A. Biastoch., R. E. Roman, 2003: Inter-ocean fluxes south of Africa in an eddy-permitting model. Deep-Sea Research II. 50[1], 281-298.

Recq, M., and P. Charvis, 2007: A seismic refraction survey in the Kerguelen Isles, southern Indian Ocean. Geophysical Journal International. 84, 529-559.

Richardson, P. L., J. R. E. Lutjeharms and O. Boebel, 2003: Introduction to the inter-ocean exchange around southern Africa. Deep-Sea Research II. 50[1], 1-12.

Richmond, M. D, 1997: A guide to the seashores of eastern Africa and the Western Indian Ocean Islands. Sida. Department for Research Cooperation, SAREC. Zanzibar, Tanzania. 448.

Ridderinkhof, H., and W. P. M. de Ruijter, 2003: Moored current observations in the Mozambique Channel. Deep-Sea Research II. 50, 1933-1955.

Roed, L. P., and C. K. Cooper, 1986: Open boundary conditions in numerical ocean models. Advanced Physical Oceanographic Numerical Modeling, J. J. O'Brien, Ed., D. Reidel Publishing, 411–436.

Sætre, R., and A. J. da Silva, 1984: The circulation of the Mozambique Channel. Deep-Sea Research. 31[5], 485-508.

Schmitz, W. J, 1996: On the eddy field in the Agulhas Retroflection with some global considerations. Journal of Geophysical Research. 101, 16259-16271.

Schott, F. A., and J. P. McCreary, 2001: The monsoon circulation of the Indian Ocean. Progress in Oceanography. 51, 1-123.

Schouten, M. W., W. P. M. de Ruijter., P. J. van Leeuwen, 2002a: Upstream control of Agulhas ring shedding. Journal of Geophysical Research. vol. 107, C8, 3109, doi:10.1029/2001JC000804.

Schouten, M. W., W. P. M. de Ruijter., P. J. van Leeuwen and H. Dijkstra, 2002b: An oceanic teleconection between the equatorial and southern Indian Ocean. Geophysical Research Letters. 29[16], 1812, doi: 10.1029/2001GL014542.

Schouten, M. W., W. P. M. de Ruijter., P. J. van Leeuwen and H. Ridderinkhof, 2003: Eddies and variability in the Mozambique Channel. In *Tropical Studies in Oceanography*, Deep-Sea Research II. 50[12-13], 1987–2003.

Schouten, M. W., W. P. M. de Ruijter., P. J. van Leeuwen and J. R. E. Lutjeharms, 2000: Translation, decay and splitting of Agulhas rings in the south eastern Atlantic Ocean. Journal of Geophysical Research. 105, 21913-21925.

Shchepetkin, A. F., and J. C. McWilliams, 1998: Quasi-monotone advection schemes based on explicity localy adaptive dissipation. Monthly Weather Review. 126, 1541-1580.

Shchepetkin, A. F., and J. C. McWilliams, 2005: The regional oceanic modelling system: A split-explicit, free-surface, topography-following-coordinate ocean model. Ocean Modelling. 9, 347-404.

Siedler, G., M. Rouault and J. R. E. Lutjeharms, 2006: Structure and origin of subtropical South Indian Ocean Countercurrent. Geophysical Research Letters. 33, L24609, doi:10.1029/2006GL027399.

Sinha, C., K. E. Louden and B. Parsons, 2008: The crustal structure of the Madagascar Ridge. Geophysical Journal International. 66, 351-377.

Smith, W. H. F., and D. T. Sandwell, 1997: Global seafloor topography from satellite altimetry and ship depth soundings: Evidence for stochastic reheating of the oceanic lithosphere. Science. 277, 1956-1962.

Song, Y. T., and D. B. Haidvogel, 1994: A semi-implicit ocean circulation model using a generalized topography-following coordinates. Journal of Computational Physics. 115, 228-244.

Speich, S., J. R. E. Lutjeharms., P. Penven and B. Blanke, 2006: Role of bathymetry in Agulhas Current configuration and behaviour. Geophysical Research Letters. 33, L23611, doi: 10.1029/2006GL027157.

SSALTO/DUACS, 2004: Product handbook-MERSEA regional products. Technical report, CLS and CNES, France, 10.

Stammer, D., C. Wunsch., R. Giering., C. Eckert., P. Heimbach., J. Marotzke., A. Adcroft., C. H. Hill and J. Marshall, 2003: Volume, heat, and freshwater transport of the global ocean circulation 1993 – 2000, estimated from a general circulation model constrained by WOCE data. Journal of Geophysical Research. 108, 3007.

Stramma, L., and J. R. E. Lutjeharms, 1997: The flow field of the subtropical gyre of the south Indian Ocean. Journal of Geophysical Research. 102, 5513-5530.

Tchernia, P, 1980: Descriptive Regional Oceanography. Pergamon Press., Oxford. 253pp.

Valentine, H. R., J. R. E. Lutjeharms., G. B. Brundrit, 1993: The water masses and volumetry of the southern Agulhas Current region. Deep-Sea Research I. 40[6], 1285-1305.

Van Leeuwen, P. J., W. P. M. De Ruijter and J. R. E. Lutjeharms, 2000: Natal Pulses and the formation of the Agulhas rings. Journal of Geophysical Research. 105[C3], 6425–6436.

Woodberry, K. E., M. Luther and J. J. O'Brien, 1989: The wind-driven seasonal circulation in the southern tropical Indian Ocean. Journal of Geophysical Research. 94[C12]:17, 985-1802.

Wyrtki, K, 1971: Oceanographic Atlas of the International Indian Ocean Expedition. National Science Foundation. Washington, D.C, 531pp.

Wyrtki, K, 1987: Indonesian throughflow and associated pressure gradient. Journal of Geophysical Research. 92, 941-946.

Annexs:

This chapter provides further information about the influence of eddies on the path of the Agulhas Current, at the South African east coast, during the months of January, February and March, of the model year 3. The images correspond to horizontal and vertical sections of salinity. You may find more informative if you compare this images with the sequence of images on chapter 5, of this thesis, pages 69-80.

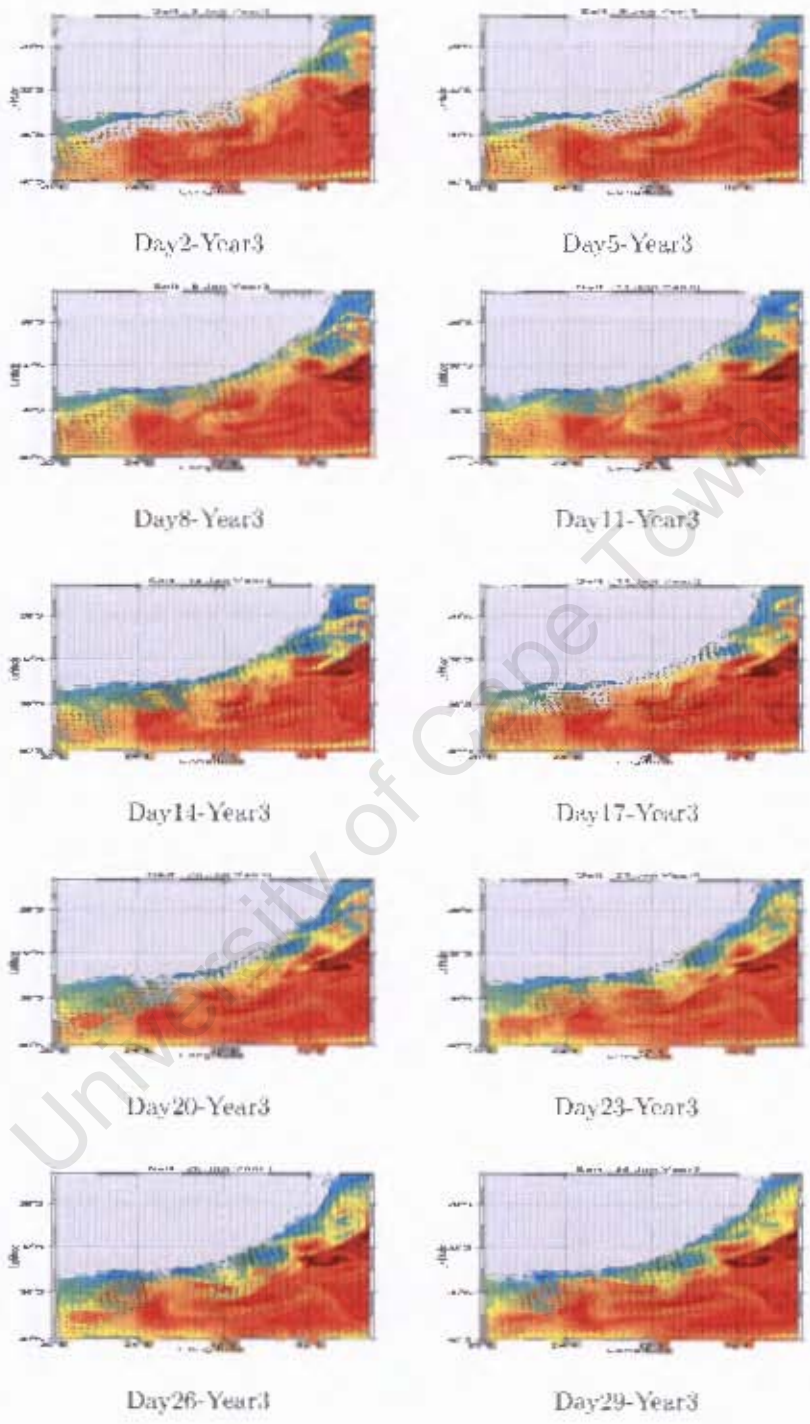

Figure 1: Portrayal of horizontal section of salinity at 50 [m] depth, for the month of January of the model year3. Pertrubation on the path of the Agulhas Current is evident. Note the offshore anti-cyclonic eddy with which this perturbation is associated. The arrows represent geostrophic cuttents.

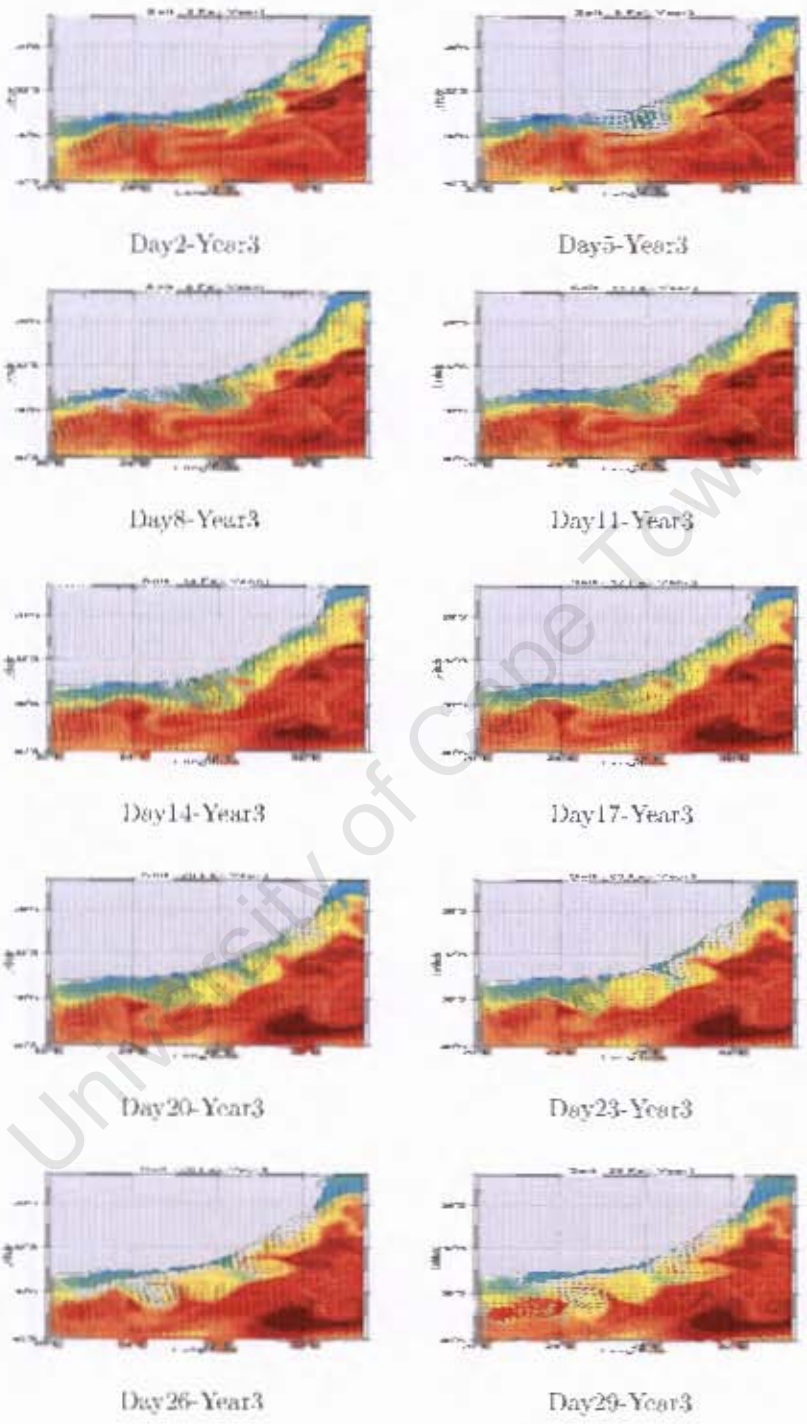

Figure 2: Portrayal of horizontal section of salinity at 50 [m] depth, for the month of February of the model year3. Pertrubation on the path of the Agulhas Current is evident. Note the offshore anti-cyclonic eddy with which this perturbation is associated. The arrows represent geostrophic cuttents.

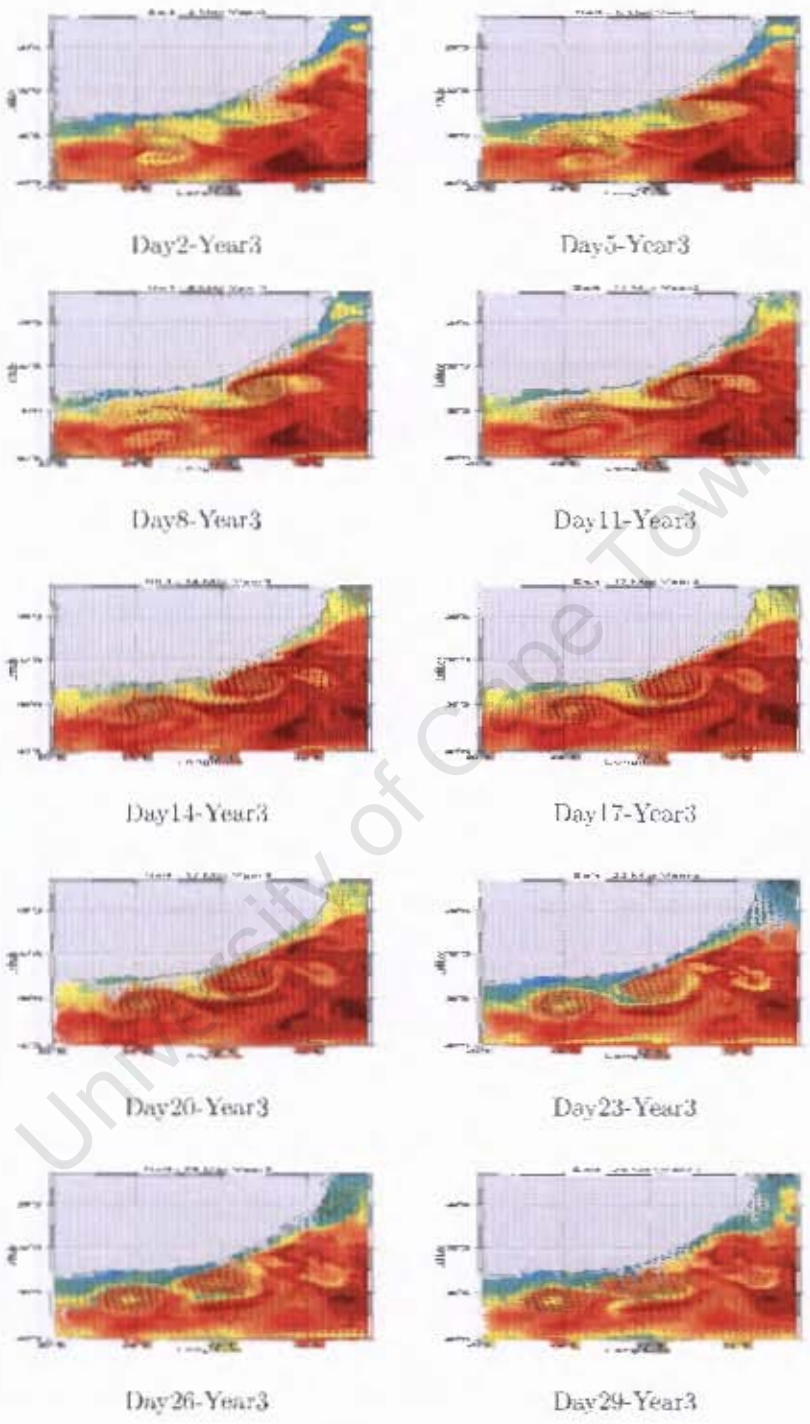

Figure 3: Portrayal of horizontal section of salinity at 50 [m] depth, for the month of March of the model year3. Pertrubation on the path of the Agulhas Current is evident. Note the offshore anti-cyclonic eddy with which this perturbation is associated. The arrows represent geostrophic cuttents.

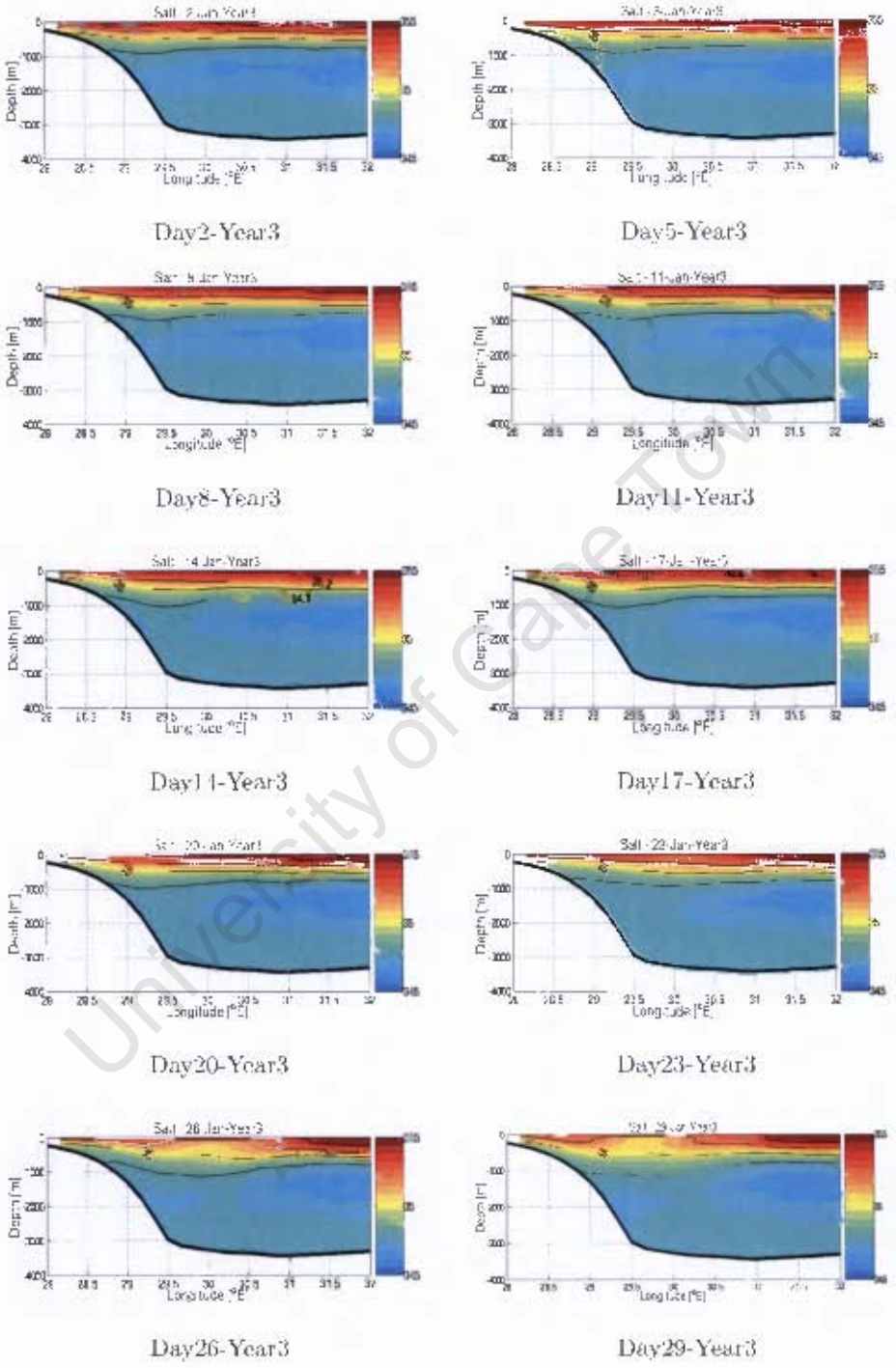

Figure 4: Portrayal of the salinity for the month of January, model year 3. Zonal section at 33°S, South African east coast.

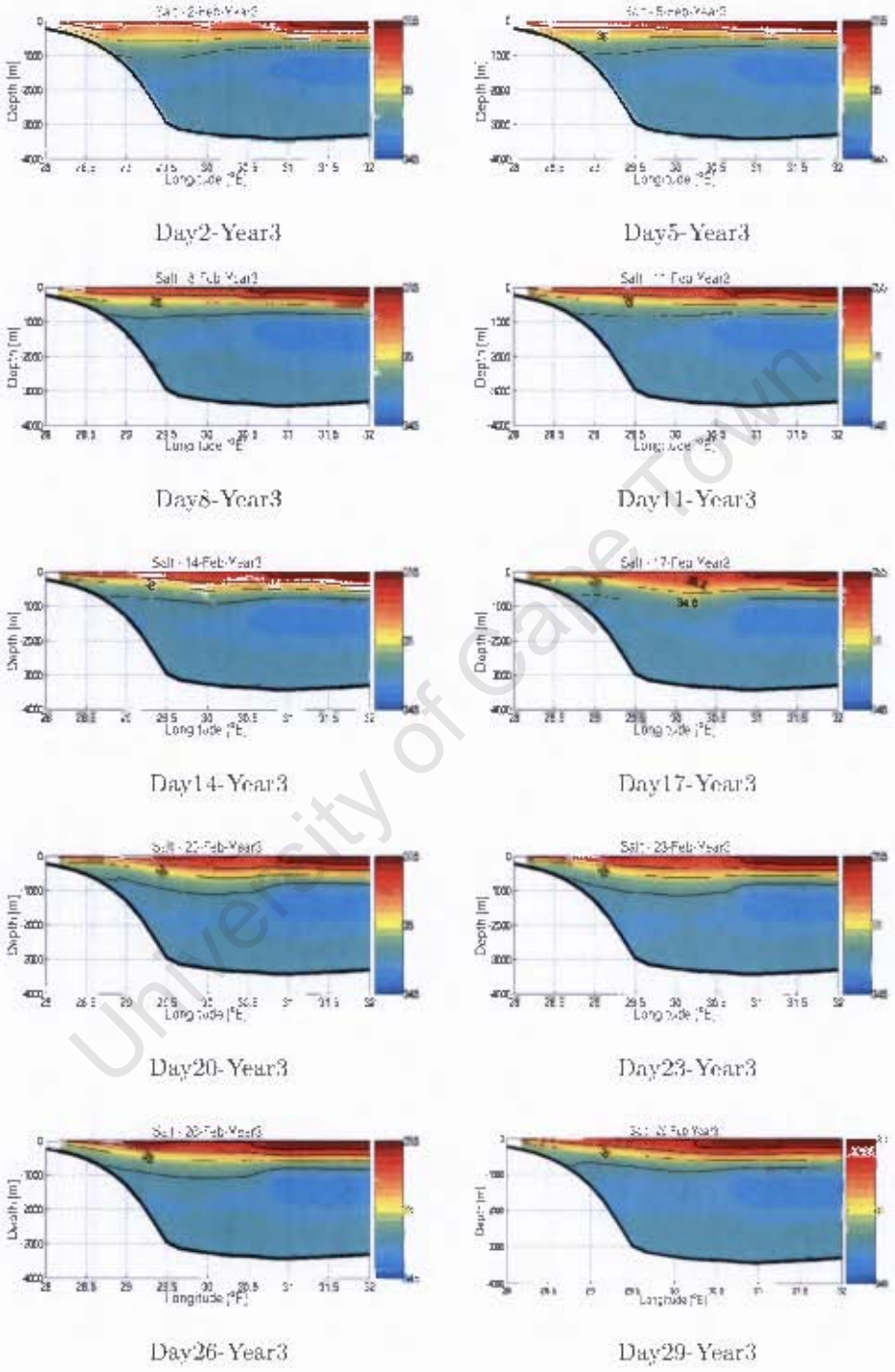

Figure 5: Cross shelf section of salinity, at 33°S, South African east coast, during the month of February, model year 3.

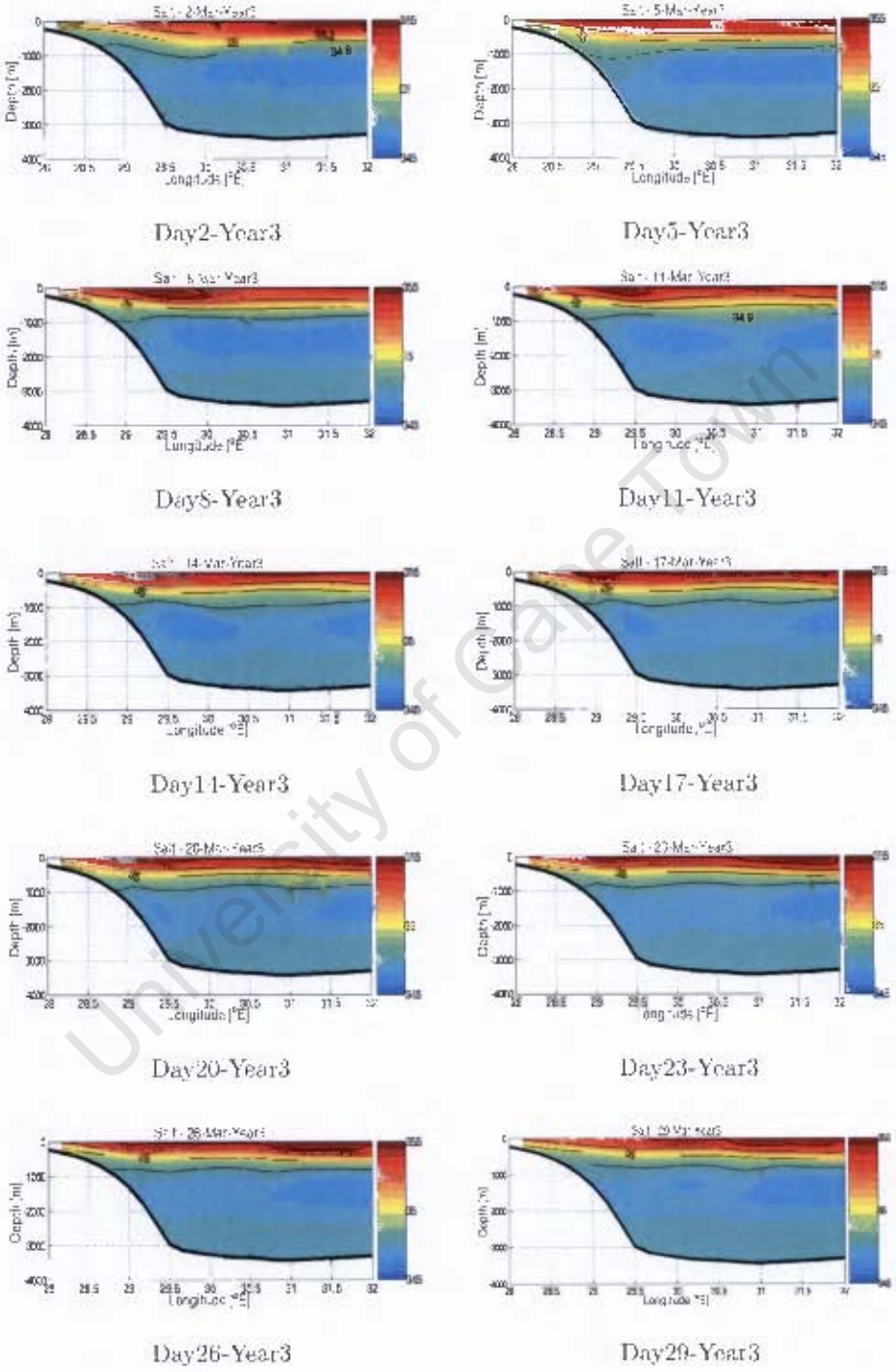

Figure 6: Cross shelf section of salinity, at 33°S, South African east coast, during the month of March, model year 3.